universität wien

MASTERARBEIT / MASTER'S THESIS

Titel der Masterarbeit / Title of the Master's Thesis

„Regulation of inflammatory responses by mRNA decay“

verfasst von / submitted by

Jakob Huemer, BSc

angestrebter akademischer Grad / in partial fulfilment of the requirements for the degree of

Master of Science (MSc)

Wien, 2016 / Vienna 2016

Studienkennzahl lt. Studienblatt / degree programme code as it appears on the student record sheet:	A 066 830
Studienrichtung lt. Studienblatt / degree programme as it appears on the student record sheet:	Masterstudium Molekulare Mikrobiologie, Mikrobielle Ökologie und Immunbiologie
Betreut von / Supervisor:	Univ.-Prof. Mag. Dr. Pavel Kovarik

Acknowledgments

First of all, I want to express my gratitude to Pavel Kovarik for giving me the great opportunity to perform my master thesis in his research group. I am deeply grateful for the numerous discussions, the scientific guidance and all the support, which allowed me to become highly independent, while always being able to account on his professional aid when needed.

Further, I want to thank Vitaly Sedlyarov for always guiding me through several projects and for his help in the laboratory. I am really thankful for him teaching me various techniques and for showing me how to tackle difficult questions conceptually and practically, which enabled me to think outside of the box.

Also, I want to thank all the other members of the Kovarik lab, Florian, Iris, Janos, Kevin, Laura, Lucy, Masha, Terezia and Virginia for useful discussions and general advice. I particularly want to thank my two former fellow students Laura and Kevin – not only for the help provided and intellectual exchange of ideas, but also for the great time we spent together in the lab.

Finally, huge thanks to my family; my parents Herbert and Brigitte and my elder brother Martin and little sister Hanna, and all my dear friends. I am really grateful for your endless support, for enduring my often stressed behavior and for always being there in any situation – this work is dedicated to all of you.

Table of contents

Regulation of inflammatory responses by mRNA decay

Studies of effects of CEBPα overexpression on transdifferentiation of transformed human haploid cells into macrophage-like cells

1. Introduction

1.1. Immunity and gene expression

Throughout life our immune system provides protection against several antigens, comprising of pathogenic prokaryotes, fungi, but also viruses and other harmful substances. At the same time it has to distinguish between pathogens and commensals, such as those in the gut, and elicit tolerance towards beneficial foreign cells[1,2]. The cooperation of the innate with adaptive immunity ensures an adequate immune response with strong dependence on one another[3–5].

Response of the immune system towards a certain pathogen requires initial recognition by pathogen recognition receptors which results in the induction of inflammation. Inflammation needs to be tightly balanced, allowing on the one hand a fast and efficient pathogen clearance followed by tissue repair and on the other hand preventing an exaggerated response which may cause host damage. Therefore, a coordinated gene expression of numerous proteins is required[6]. In contrast to bacteria, where several proteins may be obtained from a single operon, eukaryotic mRNA usually only encodes for one protein. Thus, expression of multiple genes controlling a pathway or a mechanism rather relies in eukaryotes on the presence of regulatory motifs within the DNA and RNA sequence. As such, gene expression can easily be adjusted at each level – from conversion of the genetic information encoded on DNA, over the RNA as intermediate to protein.

Primarily, distinct gene sets become transcribed together upon external stimuli based on the collaborative action of transcription factors and their binding to regulatory DNA sequences, defined inter alia by histone marks and DNA methylation[7]. This is exemplified by $NF_{\kappa}B$, a transcription factor which translocates from the cytoplasm to the nucleus during inflammation and induces transcription of e.g. pro-inflammatory cytokines with shared binding motif in their promoters[8,9].

Although transcription sets the basis for immune gene expression, the involvement of several transcription factors and signaling pathways represents a time-consuming process with a limited dynamics. Yet, for an adequate response to changing environmental conditions, such as the pathogen removal, a quick adaptation in gene expression is demanded. Such dynamic changes can be achieved rapidly at the level of mRNA by post-

transcriptional mechanisms. Modulation of mRNA stability and translation thereby allows altering protein levels more directly, without the delay occurring in transcription[10].

1.2. mRNA – a platform for post-transcriptional regulation in immunity

Messenger RNA of eukaryotes can be generally considered a transient step that links the genetic code from DNA to the final translation of the protein. However, from nuclear pre-mRNA to the mature cytoplasmic mRNA numerous steps occur before translation.

In general, after transcription pre-mRNA is spliced, cleaved at the 3´end and a 5´-methylguanosine cap as well as the 3' poly-A tail are clinched forming the mature mRNA[11]. During this process and prior release into the cytoplasm the nuclear mRNA already forms a complex with RNA-binding proteins (RBPs) and non-coding RNAs (ncRNAs). These complexes are often referred as messenger ribonuclein binding particles (mRBPs) or riboclusters[11,12]. As such nuclear mRNAs commonly display binding of PABPN1 to the poly-A tail, CBC20/80 binding to the 5´cap, as well as exon-junction complexes among several other factors[11]. Depending on the transcript, some mRNAs are immediately translated once they enter the cytoplasm, whereas others are reserved in a translationally silent state until a certain event or relocation to subcellular compartment. Typically, the pioneer round of translation serves as a surveillance mechanism to ensure the sequence correctness and simultaneously allows the exchange of aforementioned nuclear RBPs by eIF4F, eIF4G at the cap and PABPCs at the poly-A tail[13]. In the end that leads to circularization of the mRNA, which is considered to inhibit its decay, render it more translationally active and allows access to 3´UTR[14]. This flux from factors concomitant with the mechanistic consequences, although a common principle is representative for the malleable regulation at post-transcriptional level, which can occur at each stage indicated.

As such post-transcriptional regulation in immunity can take place by alternative splicing, alternative polyadenylation, RNA editing, but also affect translation and mRNA decay[12,15]. Alternative splicing is assisted by heterogeneous nuclear RNPs (hnRNP) and serine-arginine RBPs[16,17]. The thereof altered nucleotide content can lead to a truncated version of the protein, but may as well change function/localization by the loss a certain domain. Alternative splicing and polyadenylation has been described in immune cells already, like for Toll-like receptors (TLRs) in phagocytes[18,19]. Of note, these truncations were also shown to affect 3´UTRs and thus in turn may prevent regulation of miRNA or RBPs further on. Also

restricted to the nucleus is RNA editing, for example by ADARs which induced the change from adenine to inosine[20].

Within the cytoplasm mRNAs can be either translated, stalled in stress granules or degraded within processing bodies (P-bodies)[12]. The relevance of this process is given by mRNA half-lives differing from 15 minutes to more than one day, resulting in no less than 1000-fold difference among mRNA levels[21,22]. In this case, upstream signaling cascades triggered by stress, such as viral dsDNA, interferons or heme deprivation can prevent transcription initiation by phosphorylation of eIF2[12,23]. Importantly, transcripts of many cytokines and chemokines harbor cis-regulatory sequences in their 3´UTR, which can be tightly regulated by different classes of trans-acting RBPs.[6,10,12,15] That way, for instance binding of TTP to AU-rich elements (AREs) as well as miRNA/RISC induced silencing shortens the half-lives by initiation of mRNA degradation, whereas others such as HuR binding to AREs and U-rich elements generally stabilize transcripts. A detailed description for those three factors is given below.

In that regard mRNA degradation does not only remove aberrant transcripts recognized during mRNA maturation, such as those bearing defects in splicing or folding, but also allows to timely target transcripts specifically to determine their life-span[11,24]. In principle, mRNA turnover can be achieved by endonucleases, but also with 3´and 5´exonuclease cutting internally or starting degrading from the 3´or 5´ end[24]. The major mechanism for decay of mature cytoplasmic mRNA in eukaryotes starts with deadenylation of the poly-A tail by Caf1/CCR4/Not1 or PARN[25–29]. This renders the mRNA vulnerable for further processing accomplished by Dcp1/Dcp2-mediated removal of the 5´cap and followed by Xrn1 5´-3´exonucleolytic decay or degradation from the 3´end induced by the exosome **(Fig. 1)**[24,30–32].

Hence, dependent on the cellular requirements upon extra- and intra-cellular cues, transcripts of inflammatory mediators, such as from TNF, are then either rapidly decayed or stabilized and used for translation. Due to this adaptability immune responses cannot only be switched off or on, but also allows controlling its length and intensity[12,22].

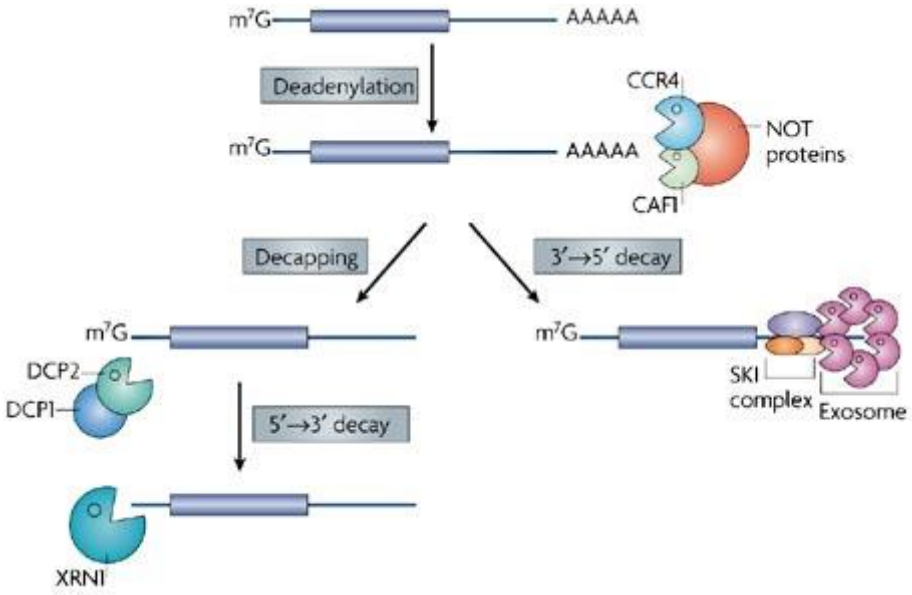

Figure 1| Main mechanism of mature mRNA decay. The picture was taken from reference [33].

1.3. Trans-acting factors in mRNA decay in inflammation

As mentioned earlier RNA-binding proteins have a crucial role in post-transcriptional regulation, this is highlighted by their sheer number exceeding 1500 encoded genes in humans[34,35]. In general they can elicit their function as trans-acting factors binding to cis-regulatory sequences or motifs in the untranslated regions (UTRs) at the 5´and 3´end of mRNAs[15]. These motifs are normally present as a certain array of nucleotides, but can also be secondary structures like stem loop[7,10,12,15].

This is particularly important in immune responses and inflammation. Here, different RBPs bind predominantly to their confined regulatory sequences within the 3´UTR of inflammatory mediators as cytokines and chemokines, but also enzymes as iNOS, promoting dynamic changes in mRNA stability in a time-resolved manner[10,36]. Hence, they promote changes lasting either in mRNA degradation or mRNA stabilization and must be highly regulated to maintain immune homeostasis. This was highlighted by the observations made by Hao and Baltimore[37]. They could show that the immediate, early and resolution phase of TNF-induced inflammation relies on the expression kinetics of 3 groups of inflammatory transcripts. The precise timing of their expression was shown to be mainly given due to different mRNA decay rates. As such group I transcripts (immediate) were degraded rapidly, whereas group II (early) remained longer and group III (late) persisted. Furthermore, this correlated with the number of destabilizing adenine and uridine-rich elements (AU-rich

elements; AREs) present in the 3´UTR, with class I harboring the most, which gradually decreases towards class III transcripts.

Although this indicates a simple and linear mechanism by which mRNA stability can be easily regulated based on one specific cis-regulatory element which can be bound by one trans-acting factor, mRNA decay seems to be far more complex. First, there is a variety of regulatory sequences within the 3´UTR of inflammatory transcripts other than AREs[7,10,12,15]. These include GU-rich elements (GREs), U-rich elements (UREs) as well as stem-loop structures, such as the constitutive decay element (CDE). Those structures can be bound by many different RNA-binding proteins, including mRNA destabilizers as Tristetraprolin (TTP), AU-binding factor 1 (AUF1), KH-type splicing regulatory protein (KSRP), Roquin 1 and Roquin 2, CELF1 (CUGBP1) and Regnase-1, but also by Human antigen R (HuR) mainly considered as mRNA stabilizer and translational promoting protein. However, in principle these motifs cannot be assigned to a single RNA-binding protein based on their base sequence, rather they can be potentially bound by 2 or more **(Fig. 2)**. Vice versa, the trans-acting factors may recognize and bind to more than one cis-regulatory sequences within the 3´UTR. In addition, potential seed sequences in transcripts also provide a basis for miRNA mediated gene silencing.

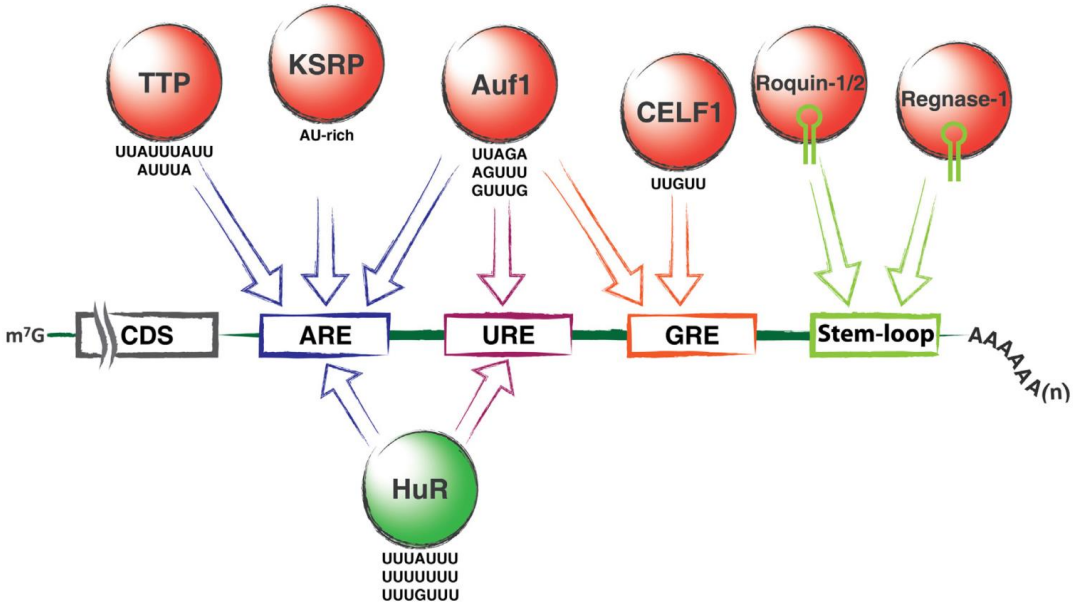

Figure 2| Overview RBPs binding to their respective regulatory sequences within cytokine transcript 3´UTR. Picture was taken from reference [10].

For instance, cooperative action in mRNA turnover has been shown for *Tnf* mRNA, as impairment of ARE mediated decay in LPS stimulated RAW 264.7 macrophages still resulted in mRNA degeneration brought about by the constitutive decay element[38]. However, this does not necessary imply redundancy, rather it may be required for a fine-tuned spatiotemporal mechanism in immunity. This is exemplified by Roquin and Regnase-1, which can target a common set of inflammatory mediators for decay due to a shared stem-loop structure[39]. Even so, Roquin acts on translationally active mRNAs at the endoplasmic reticulum with restriction to the early phase of inflammation, whereas Regnase-1 occurs at stress granules and processing bodies and tends to control late phase of inflammation. Despite negative regulation of mRNA by synergistic action of RBPs, mRNA stability control can be further regulated by proteins with opposing functions. Similarly, AT-rich interactive domain (Arid)–containing protein 5a (Arid5a) and Regnase-1 can both bind the same region within the 3´UTR of *Stat3* transcript, yet competition for binding defines weather mRNA becomes stabilized or destabilized, respectively[40]. In the same fashion iNOS expression was shown to be regulated by the contradictory action of HuR and KSRP[41].

This strongly suggests that post-transcriptional regulation on the level of mRNA decay in inflammation is highly versatile and accurately timed expression of inflammatory mediators relies on the coordinated and selective binding of different RNA-binding proteins.

1.4. Tristetraprolin (TTP)

Tristetraprolin (TTP) is encoded by the gene *Zfp36* (also known as *Gos24*, *Nup475* and *Tis11*) located on chromosome 19 in humans and 7 in mice[42]. TTP belongs to the family of Cys-Cys-Cys-His (CCCH) tandem zink (Zn)-fingers, yet is an RNA binding protein, binding mainly the consensus sequence of AREs, and not as first considered a transcription factor as most other Zn-finger proteins[43–46]. Its action as mRNA destabilizing protein upon ARE binding will be discussed below in more detail.

TTP has 3 closely related family members: Zfp36L1, Zfp36L2 and Zfp36L3[47–50]. The former two are commonly found in mammals and rodents, whereas expression of Zfp36L3 is restricted to the yolk sac of rodents. Although TTP´s paralogs are also mRNA destabilizing proteins their function is mainly restricted to an organism's development. In contrast, TTP has its major role in inflammation and immune responses. This is best highlighted by the phenotype of the TTP knockout mouse[44]. *TTP*$^{-/-}$ mice display normal embryonic

development, but suffer from severe and sometimes lethal complex inflammatory syndromes with hyper-inflammation at multiple organ sites. These include arthritis, cachexia, conjunctivitis and joint, as well as skin inflammation. Subsequently, the transcript of the pro-inflammatory mediator TNF was identified as first TTP target, as inhibition of TNF signaling by TNF neutralizing antibodies as well as deficiency of the TNFR1 ameliorated and almost completely revoked the inflammatory phenotype[44,51].

Nonetheless, the cellular and cytokine sources driving the TTP knockout phenotype still remain at least partially elusive. This is among others because the inflammatory syndrome could be transferred in bone marrow chimeras with *Rag2*$^{-/-}$ background and bone marrow transplant form *TTP*$^{-/-}$ mice[52]. Due to the absence of lymphocytes the paper suggested that myeloid cells, i.e. macrophages, may be a major cellular driver of the observed phenotype. However, reactive granulopoiesis, another hallmark of TTP knockout caused syndrome, can be copied in a non-hematopoietic manner[53]. Furthermore, the conditional knockout of TTP in the myeloid compartment yielded healthy animals, despite evoking low dose LPS hyper inflammation[54,55]. Hence, that indicates the involvement of immune as well as non-hematopoietic cells in TTP dependent systemic inflammation, with myeloid TTP suggested being important in the resolution of inflammation. Moreover, additional studies could show that the phenotype observed is not only dependent on TNF, as elimination of CCL3 and IL23 inhibits manifestation of local and system inflammatory responses, respectively[56,57].

1.4.1. ARE mediated mRNA decay by TTP

The major mechanism by which TTP promotes mRNA instability initiates with binding to AU-rich elements and ultimately ends with the decay of bound mRNA (see **figure 1**). The first incidence that AREs promote mRNA degradation was observed in the mRNA of GM-CSF, later also identified as TTP target[58,59]. In particular the consensus for TTP binding was defined in *Tnf* mRNA as a UUAUUUAUU nonamer in its 3´UTR[60,61]. This is in accordance to recent studies examining global TTP binding site, showing at least the presence of the minimal core AUUUA pentamer[62–64]. RNA binding of TTP depends on a Zn-finger RNA-binding domain with two $CX_8CX_5CX_3H$ motifs, where X indicates variable amino acids[65,66]. Interestingly, there is an indication that folding of the second Zn-finger, which changes in presence of RNA target, determines TTP activity[67].

TTP mediated target destabilization involves the participation of the decapping and deadenylation complex in the subcellular context of stress granules and processing bodies[23,68]. Interaction of TTP was shown for Dcp1 and Dcp2, as well as for Ccr4 and Not1[69–72]. Interestingly, it seems that TTP can interact with the deadenylation complex amino- as well as carboxy-terminally. This favors a model, in which upon TTP binding to its target mRNA decay is induced by the recruitment of the degeneration machinery, first electing removal of the m^7G-cap and poly-A tail with subsequent 5´-3´and 3´-5´degeneration **(Fig. 3)**.

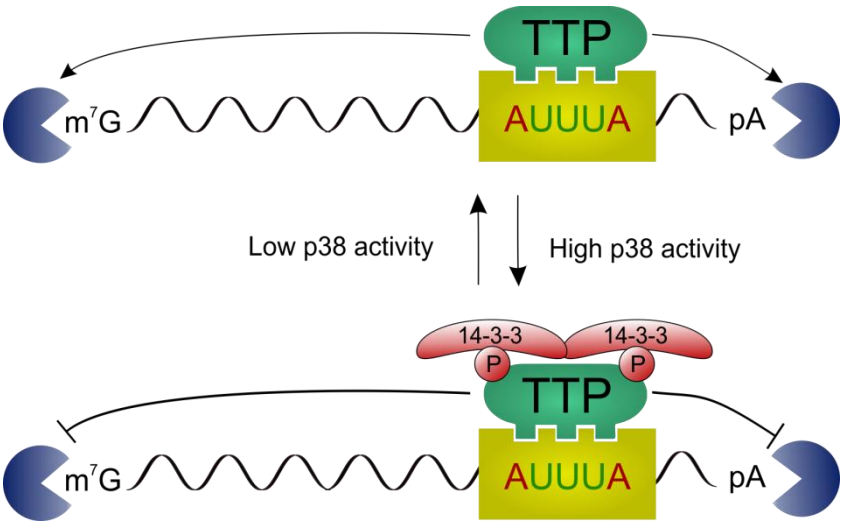

Figure 3| Function and Regulation of TTP activity during inflammation. Top panel: Upon binding to AU-rich elements (yellow box) unphosphorylated TTP can recruit the Ccr4/Caf1/Not deadenylation machinery and the Dcp1/Dcp2 decapping complex. Decapping renders the target mRNA susceptible for Xrn1 mediated 5´-3´exonucleolytic decay (left packman) and deadenylation primes mRNA for further 3´-5´exosome degradation (right packman). Bottom panel: Phosphorylation of TTP at Ser52 and Ser178 induces the binding of 14-3-3 adapter proteins. This prevents TTP mediated mRNA degradation by inhibiting the recruitment of the decay machinery to its mRNA targets.

The biological relevance of this process is given by the high selectivity of ARE mediated mRNA decay by TTP towards cytokines and chemokines[45]. These include besides the already mentioned TNF and GM-CSF transcripts i.a., mRNA of chemokines, i.e. *Cxcl1, Cxcl2, Ccl2, Ccl3* and interleukins, i.e. *Il1b, Il6, Il10,* and *Il23*. Moreover, TTP limits its own expression by an auto-inhibitory feedback loop, adding another layer to TTP function in resolving the inflammatory response[73]. In that regard, TTP itself numbers among the early inflammation phase genes, absent under homeostatic conditions, but readily induced by immunological stimuli[74]. However, the mature protein TTP can bind its own mRNA at the 3´UTR and thereby initiate its decay[73].

Besides TTP´s function in mRNA decay, the protein is also implicated in translational inhibition. Kratochvill *et al.* could show that in tumor microenvironment stability and overall mRNA expression of TTP targets where hardly affected, whereas the protein levels of respective pro-inflammatory targets were altered in a TTP dependent mechanism[75]. Similarly, it could be shown that TTP mRNA targets associated with lighter and hence less translated ribosomal fractions[76]. In accordance with that the same study could show in a luciferase reporter experiments that TTP inhibitory function on translation upon ARE binding involves its association with the general translational inhibitor RCK/p54. Furthermore, by using an artificial construct with in total 8 TTP binding motifs (i.e. ARE nonamer of *Tnf* mRNA) it was shown that TTP can interact with eIF4E2[77]. eIF4E2 inhibits proteins synthesis by preventing assembly of the translational initiation complex at the 5´cap of mRNA[78]. However, the fact that the binding affinity of eIF4E is lower than its counterpart eIF4 this points towards a TTP specific mechanism[79]. Overall, this shows that TTP can interfere with protein synthesis on the level of mRNA stability and translation, but the latter still requires further research to unfold the exact mechanisms.

1.4.2. Phosphorylation of TTP and other posttranslational modifications

In addition to autoregulation of TTP by inducing its own decay, posttranslational modifications of the trans-acting factor are largely defining TTP´s function as mRNA destabilizing protein. The best characterized is phosphorylation of the amino acid residues serine 52 and serine 178 in mouse, corresponding to S60 and S186 phosphorylation in human TTP[80]. Phosphorylation of the aforementioned residues is induced by p38 MAP kinase (MAPK) and its downstream MAP activated protein kinase 2 (MK2)[80–84]. Upon phosphorylation of TTP by the p38-MK2 pathway at S52/178 binding of the adapter proteins 14-3-3 to TTP can be observed[45,81,83,85]. 14-3-3 binding in turn negatively regulates TTP activity by prevention of association with the deadenylation components Ccr4/Not1, yet stabilizes TTP protein itself **(Fig. 3)**. This is because the unphosphylated form of TTP is rapidly targeted for proteasomal decay[84]. Furthermore, p38 induced phosphorylation was shown to alleviate binding to ARE mRNA targets[86]. Of note, dephosphorylation of TTP so far has only been shown by protein phosphatase 2A (PP2A), which is hence indicated to rescind effects brought about p38-MK2-TTP axis[85]. Albeit, the aforementioned changes in TTP function p38 MAPK is also implicated in differential localization within the cell[74].

In the starting phase of inflammation p38 is highly active, as phosphorylated by kinases of the MKK pathway[87]. However, since S58/172 phosphorylation inhibits TTP function, the equilibrium with unphosphorylated and thus active TTP has to be highly balanced, to allow efficient cytokine mRNA removal once immune response wanes upon pathogen clearance. The significance of temporal control of TTP activity by p38 MAKP was shown using time-lapse experiments[55]. LPS induced inflammation resulted initially in high p38 mediated TTP phosphorylation, but p38 activity gradually decreased over time which inversely rendered TTP less phosphorylated providing a mean to promote resolution of inflammation by mRNA decay. Contrary, the magnitude of inflammation can be altered by the mutation of both, S58/172 to nonphosphorylatable alanine in mice[88]. Although the knock-in mice, as anticipated, displayed reduced TTP levels and elevated mRNA decay, even if only monoallelic expression is given, the generated mice were otherwise healthy and the adaptive immune response in a T_H-1 governed bacterial infection model was not evidently impaired.

Besides the 2 well established S52 and S178 phosphorylation, several other post-translational modifications for TTP are described. Using RAW 264.7 with exogenous FLAG-tagged TTP expressions in a Tet-Off system, 12 additional phosphorylations have been revealed[88]. These include phosphorylation on 9 serine residues, as well as phosphorylation on 2 threonines and 1 tyrosine. Despite phosphorylation other groups have shown that TTP is substrate for ubiquitination[89,90]. However, functional annotation of these modifications is still lacking. Since the mRNA destabilizing function of TTP is highly regulated by other interacting factors with dependence on phosphorylation, further research is required to fully elucidate the role of uncovered posttranslational modifications and their potential role in inflammation.

1.4.3. Nuclear form of TTP

As previously mentioned TTP´s subcellular localization is connected to its p38 mediated phosphorylation, as unphosphorylated TTP was found in both nucleus and cytoplasm and phosphorylated was only in the cytoplasm[74]. This is because TTP function is not only restricted to cytoplasmic mRNA degradation, but also shows nuclear-cytoplasmic shuttling as reported independently from two individual groups[91,92]. Using pharmacological inhibition and GFP-tagged TTP mutant constructs they were able to map a leucine-rich nuclear export signal (NES) in the amino terminus of TTP and could reveal that export is mediated by the

nuclear export receptor CRM1. Furthermore, both groups revealed that the nuclear import of TTP requires the CCCH-tandem Zn-fingers independent of RNA-binding, finally defining the nuclear localization signal (NLS) to span a region from amino acid 88 to 161.

In contrast to mRNA decay function in the cytoplasm, the function of nuclear TTP is ill defined. Two studies in 2009 indicate that TTP might also function as transcriptional repressor of the $NF_{\kappa}B$ subunit p65, although the molecular mechanisms remain incompletely understood [93,94]. On the one hand, TTP is indicated to impair p65 nuclear translocation and thereby its transcriptional activity, independent of direct interaction[93]. On the other hand, TTP was shown to directly interact with p65 and histone-deacetylase, rather suggesting that the translational suppressor function involves aberrant acetylation of $NF_{\kappa}B$ promoters and p65[94]. However, the relevance of the effects of TTP on $NF_{\kappa}B$, which have been shown only in non-immune cells, is not clear and further experiments and validations are needed. In addition, it was shown that the interaction of TTP with the estrogen receptor α inhibited its transactivation by the recruitment of histone-deacetylases to steroid receptor´s promoters[95]. Further, the nuclear form of TTP was shown to act as co-repressor of transactivation for additional breast cancer relevant steroid receptors[96].

Another important feature of nuclear TTP is its frequent binding to intronic RNA regions observed in HEK cells, but also macrophages[62–64]. Intriguingly, using a nonphosphorylatable TTP intronic binding occurred to a lesser extent than S52/178 phosphorylatable TTP[63]. Furthermore, binding to introns turned out to be discriminatory from 3´UTR binding and also intronic TTP targets were highly stable[64]. Moreover, tailored analysis of *Irg1*, best intronic TTP target defined by PAR-CLIP, excluded TTP´s function in pre-mRNA processing. Taken together, this indicates that the nuclear-cytoplasmic shuttling activity might allow TTP to couple several processes of gene expression to limit inflammation at other layers than mRNA decay alone.

1.5. Human antigen R (HuR)

Another important RBP binding to AREs but also U-rich elements in mRNA 3´UTR is the trans-acting protein Human antigen R (HuR), also known as HuA and Embryonic lethal abnormal vision like 1 (ELAVL1) **(Fig. 2)**[97–99]. HuR is an ubiquitously expressed protein and belongs to the Hu protein family, comprising also three primarily neuron proteins HuB, HuC and HuD, which are the vertebrate homologs of *Drosophila* ELAV proteins[100–102]. Binding of HuR to target mRNA depends on 3 RNA recognition motifs (RRMs); RRM1 and RRM2 are considered to act together to mediated binding to mRNA targets and RRM3 is considered in stabilization of RNA-protein complex, but also in mediating protein-protein interactions[97]. Between RRM2 and RRM3 lies a hinge region which contains the HuR nucleocytoplasmic shuttling domain (HNS) that allows HuR, similar to TTP, to shuttle between the two subcellular compartments[103]. Importantly, under homeostatic conditions HuR´s distribution is primarily nuclear, but relocates to the cytoplasm upon stress, i.e. UV light, cytokines and hormones, where it can bind targets and elicit its function on target transcripts[104–107].

In contrast to TTP, the main function of HuR is to promote mRNA stability and translation of its targets which are mainly implicated in developmental processes such as apoptosis, differentiation and proliferation[97]. Functional importance of HuR in development is given by the fact that null mutations *in vivo* lead to rapid lethality due to apoptosis of bone marrow and intestinal progenitor cells, but also displayed defects in placental morphogenesis[108,109]. The biological relevance for HuR in adaptive immunity was shown by conditional HuR deletion in T- and B- cells respectively[110,111]. Ablation of HuR resulted in defective leukocyte maturation including differentiation and proliferation, which on the one hand decreased peripheral T-cell number due to aberrant selection, but on the other hand also revealed the crucial role in B-cell normal antibody response.

In principle, HuR is considered to promote inflammation as it was shown to stabilize pro-inflammatory transcripts[112]. The repertoire of stabilized mRNAs targeted largely overlaps with those from TTP including i.a. transcripts of GM-CSF, TNF, COX-2 and IL-6. Further, HuR can autoregulate its expression as it binds to its own 3´UTR. Nonetheless, contrary to TTP, where interaction partners and the overall mechanism for decay are broadly defined, the means of HuR induced enhanced mRNA stability and translation is puzzling. It has been suggested that rather than directly affecting half-life and translation it impairs the binding of

other trans-acting factors with opposing function, such as TTP or the miRNA/RISC complex **(Fig. 4)**. Contradictory to studies showing that HuR in general promotes inflammation and cancer[113], myeloid specific deletion of the *Elavl1* gene rendered mice highly susceptible for local inflammation and rapid progression to colitis-associated cancer[114]. This was accompanied by increased mRNA levels of cytokines like *Tnf, Ccr2* and *Ccl2*. This is in keeping with an earlier study showing that the macrophage induced increase in HuR suppresses inflammation[115]. Hence, HuR seems to act as a pleiotropic trans-acting factor in inflammation, which function may depend on the environmental cues and the involved cell types. Further, HuR is heavily modified on the posttranslational level and thus provides potential room for intricate regulation[97].

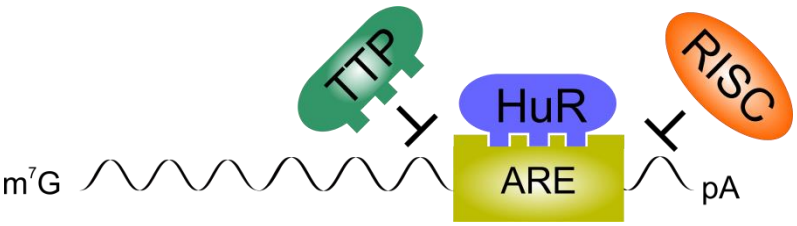

Figure 4| Model of HuR function in the regulation of mRNA stability and translation. Upon binding of HuR to its corresponding cis-elements in the 3´UTR, such as AREs, HuR may prevent binding of TTP or the binding of miRNA in association with the RISC complex to seed regions. This prevents the targeted mRNA from TTP or miRNA mediated decay, respectively. In turn mRNA half-life is increased and the thereof augmented mRNA levels allow efficient translation.

1.6. MicroRNA/RISC complex

In addition to RBPs, affecting mRNA stability and translation upon binding to transcript 3´UTRs, microRNAs (miRNAs) in association with the RNA-induced silencing complex (RISC) display another mode of posttranscriptional regulation. MicroRNAs number among the small non-coding RNAs which are endogenously expressed, with its mature form inducing translation repression or mRNA degradation of its transcript targets **(Fig. 5)**[116]. In general, microRNA generation initiates with RNA polymerase II, or III transcription of the miRNA gene yielding an approximately 60nt long primary miRNA transcript[117,118]. This precursor consists of individual hairpin structures, each of which already contains the ingrained miRNA. Similar to pre-mRNA, the primary miRNA transcript is then subjected to several other processing steps. Still within the nucleus, the primary miRNA transcript is endonucleolytically cleaved the RNase III Drosha in association with DGRC1 yielding the pre-miRNA[119–121]. Subsequently, the thereof obtained pre-miRNA becomes translocated to the cytoplasm mediated by Ras-related nuclear protein-GTP (RAN-GTP) and Exportin-5[122,123]. Within the cytoplasmic compartment the pre-miRNA readily becomes further processed by Dicer, another RNase III enzyme[124,125]. This generates an intermediate state where miRNA is still present in double stranded form with its complimentary sequence. However, only the mature single stranded miRNA, with approximately a length of 22nt, is then loaded to the Argonaut proteins in the RISC complex[126,127]. Finally, mature miRNA loaded on the RISC machinery binds to its corresponding seed sequence, often located in the 3´UTR and being at least partially complimentary[128]. This on the one hand may repress translation, involving mechanisms as inhibition of translation initiation, but also elongation. On the other hand complimentary base pairing can cause endonucleolytic cleavage of the mRNA target, brought about by its catalytic subunit Argonaute 2 (Ago2) [126,127].

So far, the involvement of miRNA induced gene silencing is poorly defined for the immune system. However, several reports implicate the role of miRNAs in regulation of host-pathogen interactions. As such interferon β treatment was found to increase the expression of numerous miRNAs with seed region in the HCV genome[129]. Hence, miRNA induce silencing may be a pivotal mechanism which directly limits viral infections. Furthermore, mimicking an inflammatory response via LPS treatment, macrophages displayed an increase in the miR-132, miR-146 and miR-155[130]. Strikingly, transcripts of the canonical $NF_{\kappa}B$ pathway, i.e. *Irak1* and *Traf6* show predicated miR-146 binding sites. This suggests that TLR signaling could be

fine-tuned on the posttranscriptional level in an auto-inhibitory manner dependent on miRNA silencing. Despite that, a lung inflammation experiment showed that several additional miRNAs become upregulated in response to LPS, which correlated with decreased expression of TNF and MIP-2131. Although computational predictions estimated no less than several hundred miRNAs encoded on the human genome[132], target site identification only could identify a few 3´UTR seed sequences in inflammatory cytokine mRNAs, e.g. *Il1a*, *Il6* and *Il10*[128]. Therefore and in accordance with studies predicting miR-146 binding sites on the transcripts of cytokine mRNA destabilizers *Zfp36* and *Auf1*, it can be assumed that miRNAs rather regulate the inflammatory gene expression indirectly[133].

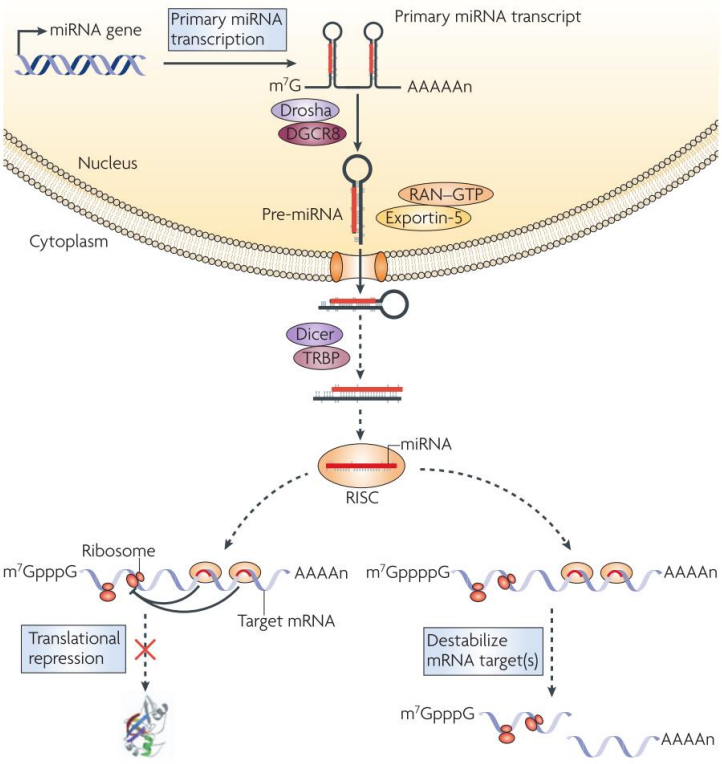

Figure 5| Pathway of miRNA biogenesis and action. Picture was taken from reference 116.

1.7. Cooperation of TTP with HuR and miRNA/RISC complex in immunity

The presence of binding sites for TTP, but also HuR and miRNAs within the 3´UTR of inflammatory mRNAs offers new perspectives for a more complex and interlinked model of post-transcriptional regulation of gene expression in inflammation. This is supported by binding site determination of TTP and HuR, which revealed an overlap between TTP and HuR binding sites of prominent inflammatory mediators, e.g. for *Tnf* and *Cxcl2* mRNA[64]. As TTP and HuR in principle display opposing functions this points towards differential regulation of mRNA stability due to competitive binding. As such Tiedje *et al*. were able to show that the p38/MK2 mediated phosphorylation provides a regulatory switch that abolishes TTP binding to the ARE site of *Tnf* mRNA, a release that in turn allowed HuR binding[86]. Hence, phosphorylation of TTP abrogated the transcript´s decay and further promoted its stabilization and translation. Similarly COX-2, a mRNA target for both TTP and HuR is highly expressed in the setting of a cancer environment based on the aberrantly shifted levels of TTP and HuR, with an increase in the later[134]. Together, this indicates that expression and posttranslational modification of the two RNA-binding proteins in a certain immuno-setting allows modulating mRNA decay as differentially bound.

In concert with that, Ago-CLIP data defined global miRNA binding in the murine macrophage transcriptome[135]. Interestingly, the comparison of WT and HuR knock out cells showed that close proximity of HuR to miRNA seed sites overall provides a mean to prevent miRNA binding to its cognate transcript. Hence, the transcript displayed increased expression. Although this mainly affected mRNA encoded by genes relevant for angiogenesis, the transcript of TTP was also found among the identified Ago targets with an adjacent HuR site. Fitting to the aforementioned statement, HuR was shown to regulate TTP expression by prevention of miR-27 binding, suggesting that miRNA mainly influence inflammation indirectly. Further, several tumor studies support the indirect role of the miRNA/RISC pathway in dictating inflammation via TTP and HuR downregulation, such as by miR-519 or miR-125a mediated reduction of HuR[136,137]. Also miR-29a, an abundantly found miRNA in breast cancer, can suppress TTP expression and hence was shown to abolish in turn TTP´s destabilizing effects on HuR mRNA[138]. Nonetheless, regulation of the TTP-HuR axis is not the sole mechanism of miRNA mediated change in inflammation. For instance, a direct and competitive action of HuR and the miR-181 family was observed for *Tnf* mRNA in immunoparalysis[139]. Using a luciferase reporter assay Dan *et al.* could demonstrate that HuR

bound to AREs in vicinity to the miR-181 seed sequences impaired the miRNA/RISC silencing pathway. Ultimately, another group proposed the essentiality for miRNA interaction with TTP for ARE mediated decay[140]. That is because miR-16 was shown to destabilize *Tnf* and *Cox2* ARE-containing reporter constructs dependent on association of TTP with subunits of the RISC machinery. Importantly, miR-16 is perfectly complimentary to the established AUUUA ARE-pentamer. Therefore, the total sequence homogeneity for binding identifies miR-16 as potential master regulator in dictating the inflammatory response in conjunction with TTP (**Fig. 4)**. However, as this study remains with follow-up works, the relevance of the miRNA-TTP interactions for immune responses still needs more validation. Taken together the studies suggest a potential role of the 3´UTR as regulatory platform, which allows cooperative interaction of TTP with HuR and the miRNA/RISC machinery in mRNA decay on several important drivers of inflammation.

2. Aims

The RNA binding protein TTP regulates the gene expression circuits of inflammation on posttranscriptional level by timed mRNA decay of inflammatory mediators instigating the resolution phase[55]. However, with the advance of global transcriptome analysis it becomes more and more evident that TTP is part of a complex network together with other factors, whose cognate interplay defines the stability of target mRNAs in time and space[62–64,135]. Further, the role of nuclear TTP remains largely undefined despite its function as co-repressor of hormone receptors in cancer cells[95,96].

High resolution mapping of TTP binding revealed hitherto two unexpected features of TTP biology. Firstly, a major fraction of TTP is bound to intronic sequences with typical tandem repeats of the AU-rich elements[64]. Strikingly, intronic binding does not induce degradation of pre-mRNA targets nor there was a relevant change in nuclear TTP protein levels throughout the LPS induced inflammatory response. Hence, we thought the intronic-bound nuclear TTP serves as a buffering system regulating the availability of bioactive (i.e., cytoplasmic) TTP during inflammation (hereafter designated as ´sponge hypothesis´). Therefore, the first aim of the study was to examine the function of nuclear TTP and elucidate if intronic binding might provide a mechanism for buffering the inflammatory response as needed.

Secondly, comparison of TTP binding sites in the 3´UTR of mRNA targets to those identified for HuR and miRNAs reveal that they are often in close proximity to each other[62,64,135]. In particular, during inflammation PAR-CLIP identified several prominent inflammatory cytokine transcripts, e.g. *Tnf* and *Cxcl2* with almost identical binding for TTP and HuR[64]. Strongly suggesting that overlapping binding sites allow co-regulation we aimed to investigate if there is cooperation of TTP with the other two trans-acting factors for synergist or antagonistic mRNA decay regulation. In addition, we wanted to investigate in detail if mutually exclusive binding provides the prime mechanism defining mRNA fate for targets with overlapping binding sites and hence enhance the current understanding of the 3´UTR as regulatory scaffold[10,15].

Finally, TTP´s function as mRNA destabilizer is largely defined by S52/178 phosphorylation[45]. However, the current model of TTP still lacks incorporation of other posttranslational modifications[88]. To that end we aimed to isolate and characterize a pure culture of RAW 264.7 macrophages expressing endogenously tagged TTP. Tagged based immunopurification in turn should allow studying posttranslational modifications under physiological relevant

conditions and enable us to examine how certain modifications impact TTP´s mode of action, subcellular localization and the partners interacting with.

3. Results

3.1. Binding of TTP to introns

3.1.1. Design of a nuclear localized RNA with an intron-binding motif

Although TTP has the capability to shuttle between the cytoplasm and nucleus[91,92] and to bind to introns, which was previously shown to constitute the majority of TTP binding site in LPS stimulated macrophages[64], its nuclear function remains rather elusive[45]. To test the ´sponge hypothesis´ and to investigate the functional impact of TTP binding to introns of mRNAs in general first a short reporter RNA (sRNA) was designed. This sRNA had to fulfill following requirements: (i) localization and maintenance within the nucleus, (ii) a TTP binding motif, resembling those of bound introns and (iii) high expression of the sRNA. As such this reporter RNA would ideally bind the vast majority of TTP within the nucleus. To that end we thought to combine a well-known TTP binding motif **(Fig. 6a, left)** found as tandem repeats of UUUAUUU at introns (TBS)[64], e.g. at *Irg1*, with the nuclear localization signal (NLS) of the lncRNA BORG (BMP-2 OP-1 responsive gene)[141] **(Fig. 6a, right)**, hereinafter designated as TBS_NLS sRNA. Among other candidate RNA known to be retrained in the nucleus, such as NEAT-1, *malat1* or CNT-RNA[142,143], lncRNA BORG was chosen because of the simplicity of its nuclear retention sequence. Mutational analysis showed that a pentamer of AGCCC with a preferential T at position -2 and retentions at -3 (G or C) and -8 (T or A) is sufficient for nuclear localization of lncRNA BORG **(Fig. 6a, right)**. Moreover, the data indicates that the pentamer not only is responsible for other RNAs nuclear localization, but also that a higher AGCCC copy number favors nuclear distribution[141]. Naturally five copies of NLS are present in the lncRNA BORG. The TBS_NLS sRNA designed consists of ten tandem repeats of TBS flanked upstream with one NLS of BORG and downstream by 3 interconnected NLS of BORG **(Fig. 6b)**, likely sufficient to retain it in the nucleus. For overexpression, the reporter RNA was put under the control of the CMV immediate-early enhancer/ promoter of a modified pEGFP_N1 plasmid **(Fig. 6b, left; Material and Methods)**, hereinafter called pTBS_NLS. Prior usage of the obtained pTBS_NLS plasmid the insert was sequence for correctness. The sequencing results match the designed sequence and are as such depicted in **Figure 6b, right.**

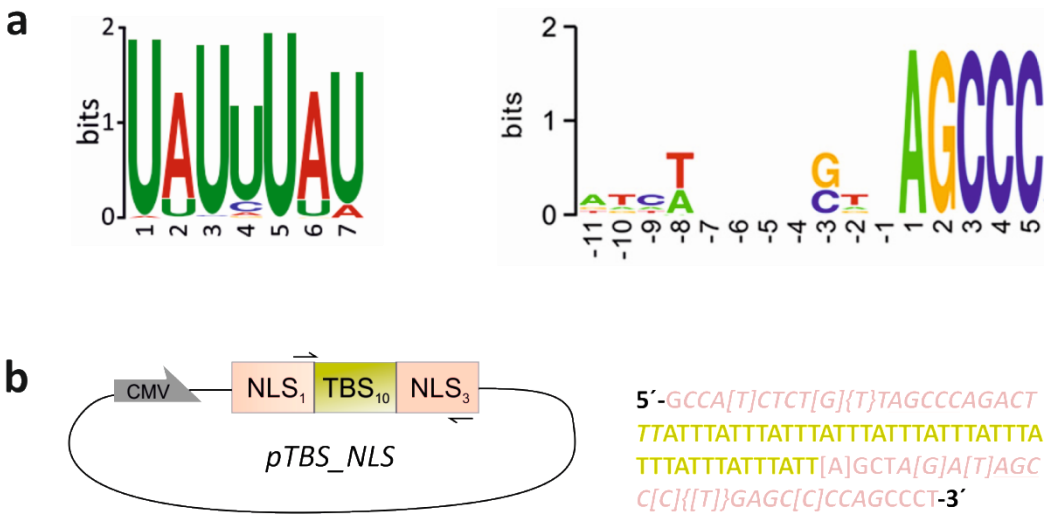

Figure 6| Design of a nuclear localized RNA with a TTP intron-binding motif. (a) Prominent TTP binding motif found in LPS stimulated macrophages (left) and the nuclear localization signal of the lncRNA BORG (right). The pictures were taken from ref. [64] and ref. [141]. **(b)** Left: Schematic of the plasmid pTBS_NLS expressing the sRNA (TBS_NLS) under the CMV immediate-early enhancer/ promoter (grey). The sRNA is constituted of four nuclear localization sequences (NLS) of BORG lnRNA (pink) and ten TTP binding sites for intons (yellow). The numbers indicate the amount of NLS and TBS copies, respectively. The arrwos indicate primer binding-sites for specific detection of the TBS_NLS sRNA. Right: Complete sequence of the TBS_NLS sRNA. The color-code matches Fig.1, right. Square brackets indicated retion positions at -3 and -8 relative to the AGCCC pentamer and curly brackets the preferential T at -2. The respective primer binding sites for TBS_NLS sRNA detection are in italics.

3.1.2. Under non-inflammatory conditions HEK293 cells highly express TBS_NLS sRNA with augmented nuclear occurrence

To test if the designed TBS_NLS sRNA is actually localized within the nucleus HEK293 T-Rex TTP wild type (WT) cells were transiently transfected with generated pTBS_NLS plasmid. HEK293 T-Rex TTP WT cells containing the Tet-On system for TTP induction were described before[144]. First, the priority was to determine if and in which amounts the designed TBS_NLS sRNA is expressed. Thus, TTP was not induced via doxycycline treatment in HEK293 T-Rex TTP WT cells, meaning the reporter RNA remains unbound of TTP upon expression. Therefore, no conclusions can be drawn concerning the immunological relevance of TTP binding to the designed sRNA. To exclude the possibility of unspecific detection of the designed sRNA the unmodified plasmid (pEGFP_N1) and the proper non-reversed transcribed samples (-RT ctrl.) were included together with water. Moreover, for efficient DNA digestion all samples were additionally treated with 2µl FastDigest SspI (Thermo Scientific, cat. no. FD00774). SspI cuts pEGFP_N1 and pTBS_NLS twice to ensure removal of any residual plasmid after RNA isolation. In accordance with our expectations qRT-PCR **(Fig. 7a)** and subsequent separation of its amplicon on an agarose gel **(Fig. 7b)** showed high

expression and specific detection of the TBS_NLS sRNA. Next, we investigated the distribution of the designed short RNA. For this the nuclear and cytoplasmic RNA fraction of HEK293 T-Rex WT cells was isolated post transfection. *Malat1* serves as control for nuclear localization[143], indicating that fractionation itself worked **(Fig. 7c, left)**. Importantly, TBS_NLS sRNA is ~2.3-fold more abundant within the nucleus when compared to the cytoplasmic fraction **(Fig. 7c, right).** Hence, the four NLS of the lncRNA BORG are sufficient to target the designed reporter RNA into the nucleus and thus provides a promising tool to study the functional impact of intron bound TTP.

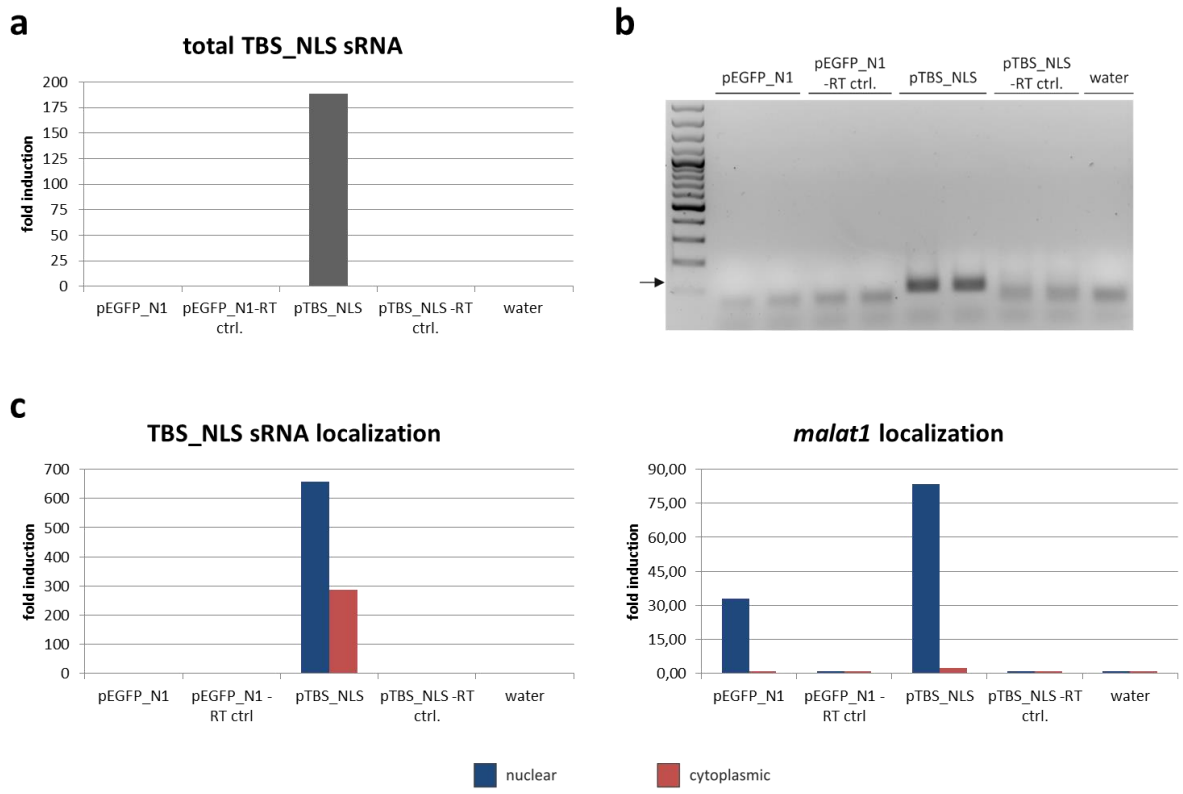

Figure 7| TBS_NLS sRNA is highly expressed and mainly localized within the nuclear compartment under non-inflammatory conditions. (a, b, c) qRT-PCR results depicting TBS_NLS sRNA expression in HEK293 T-Rex TTP WT cells. **(a)** TBS_NLS sRNA expression of total (not fractionized) RNA. **(b)** Duplicates of each amplicon received in (a) were separated on an agarose gel as indicated. Among all samples only transfection with pTBS_NLS showed the specific TBS_NLS sRNA expression with an amplicon size of 89 nucleotides (arrow). **(c)** Localization and expression level of TBS_NLS short RNA (left) and *malat1* (right) for the nuclear (blue) and cytoplasmic (red) compartment.

3.1.3. In RAW 264.7 macrophages TBS_NLS sRNA is mainly localized in the cytoplasm under inflammatory conditions

Transfection of HEK293 T-Rex TTP WT cells confirmed that flanking a TTP binding sequence for introns with 4 nuclear localization signals of BORG actually promotes nuclear localization of the thereby obtained short RNA. However, although the Tet-On system would allow TTP expression[144], HEK cells usually do not express endogenous TTP or just to a very little degree[88,145]. Thus, to mimic natural inflammation we switched to the RAW 264.7 murine macrophage-like cell line. RAW 264.7 cells express native TTP when facing bacterial products, i.e. lipopolysaccharide (LPS), as well as several prominent TTP targets[74]. In order to limit the little side effects from transfection, e.g. cytotoxicity[146], and to determine optimal transfection strategy in RAW 264.7 cell, different amounts of the pTBS_NLS plasmid were used to drive TBS_NLS sRNA transcription. Of note, viability inversely correlated with increasing amounts of the plasmid and thus transfection reagent, reaching its minimum of ~60 percent with 15µg plasmid used (data not shown).

In contrast to the approach used before, RAW 264.7 cells were treated for 3 hours with LPS. This would presumably cause endogenous TTP binding to TBS of the ectopically overexpressed reporter RNA. However, although *malat1* proofs that separation of the nuclear and cytoplasmic fractionation was successful, with at least 100-fold higher amount found within the nuclear compartment **(Fig. 8, right)** the results for the designed short RNA completely differ. First, the TBS_NLS short RNA is expressed at little levels when compared to those of HEK293 T-Rex TTP WT cells before **(Fig. 8, left)**. Second and even more relevant the artificial sRNA created is mainly found within the cytoplasm under inflammatory conditions. At best (10µg pTBS_NLS) there is half the amount of sRNA within the nuclear fraction when compart to the cytoplasmic fraction. Taken together, the data suggests that in an inflammatory environment, inducing the expression of endogenous TTP, the designed sRNA is hardly retained within the nucleus and thus renders it inappropriate for further studies on the function of intron-bound TTP within this compartment.

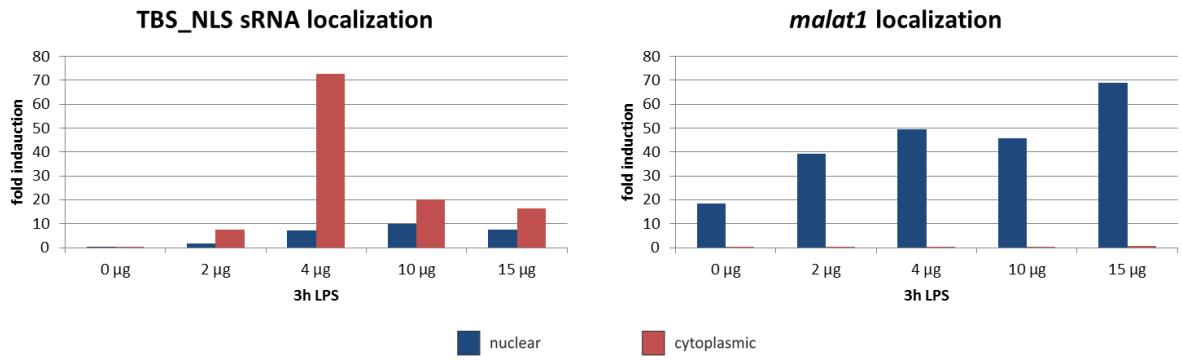

Figure 8| Under inflammatory conditions TBS_NLS sRNA is mainly localized within the cytoplasm. qRT-PCR results depicting expression of TBS_NLS sRNA and *malat1* within the nucleus (blue) and the cytoplasm (red). RAW cells were transfected with the indicated amounts of the pTBS_NLS plasmid prior LPS treatment for 3 hours promoting TTP expression. 0µg indicates cells not transfected and serves as neg. ctrl. For DNA-digestion all samples were incubated with SspI restriction enzyme as described before.

3.2. Contribution of other trans-acting factors to TTP dependent mRNA decay

3.2.1. TTP interaction with HuR requires the presence of RNA

High resolution mapping has shown that TTP and HuR share 40 common mRNA targets with almost complete overlap in the binding site[64]. Several of which are well established TTP targets, such as *Tnf, Cxcl2 and Ccl3*[44,55,57,147].Furthermore, various studies have implicated interplay between the miRNA/ RISC machinery and TTP, but also HuR[135–140,148–150]. The opposing functions of the trans-acting factors, together with the overlap in TTP and HuR binding site strongly suggest that there is co-regulation or direct competition dictating the inflammatory response[62,64].

To that extent we first aimed to determine if TTP interacts with HuR and/ or components of the miRNA/RISC machinery. Therefore a co-immunoprecipitation was done in bone marrow derived macrophages. Here, LPS stimulation and subsequent native TTP expression allows to asses if there is physiological relevant interaction at the time point assessed. In agreement with previous studies TTP can interact with HuR and 14-3-3 **(Fig. 9)**[151,152]. Of note, as macrophages specifically depleted for TTP (ΔM) also show a weak band at the height of HuR for TTP interaction it can be considered as background signal. Most importantly, TTP interacts with HuR mainly in a RNA-dependent manner but directly with 14-3-3, as shown by RNase I digestion. This suggests that mRNA targets, for which an overlapping binding motif has been identified, can be bound by both, TTP and HuR[64]. Furthermore, this supports the idea of the 3´UTR acting as their platform for post-transcriptional regulation.

In contrast, no interaction with Ago2, a component of the miRNA/ RISC machinery, could be detected neither RNA-dependent nor independently, although already described before[140]. This discrepancy could result from several effects, such as low binding affinity to TTP or that TTP interaction is more prominent at earlier phases of inflammation.

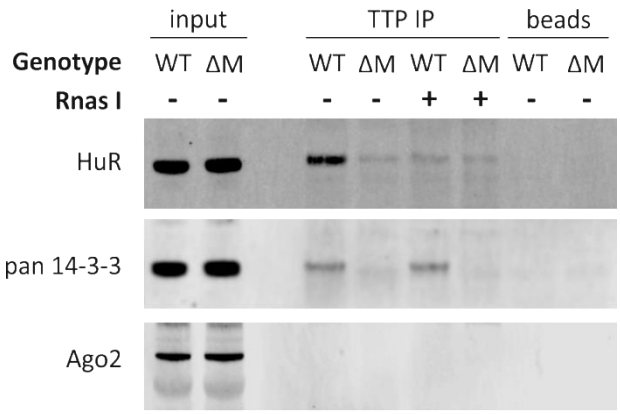

Figure 9| TTP interacts with HuR, but not Ago2 utilizing RNA as a platform. Co-immunoprecipitation of wildtype (WT) and TTP deficient bone marrow derived macrophages (ΔM) depicting HuR, pan 14-3-3 and Ago2 expression on western blot after TTP pulldown. Cells were treated for 6 hours with LPS prior lysis. Cell lysates treated with RNase I are indicated by +. Input shows the protein expression of whole cell lysates prior immunoprecipitation. Magnetic beads not coupled to TTP polyclonal K2 antibody (beads) serve as additional control to ΔM for unspecific binding. Pan 14-3-3 serves as positive control for interaction with phosphorylated TTP (see ref. [151]).

However, this does not rule out a possible co-regulation of the RNA silencing machinery with TTP or HuR, respectively. Taken into consideration that miR-16 has been shown to promote TTP mediated mRNA decay and that HuR shape the miRNA transcriptome binding in macrophages, we further aimed to investigate the functional consequences of conditional Dicer1 deletion in macrophages (ΔM^D)[135,140]. To that extent we analyzed the transcript levels decay rates of the inflammatory cytokines *Tnf* and *Cxcl2* **(Fig. 10a; Suppl. Table 1 and 2)**, as well as other TTP targets being *Il1a*, *Il1b*, *Il6* and *Il10,* and also the genes encoding TTP and HuR themselves **(Suppl. Table 1 and 2)**. Absences of Dicer1 in general promote little higher expression of the aforementioned TTP targets, including *Tnf* and *Cxcl2*. This could indicate indeed cooperation between the RNA silencing machinery and TTP. Notably TTP and HuR expression are also known to be influenced by miRNA binding in cancer[136–138,148,149]. However, knockout cells did not show relevant differences in TTP or HuR expression **(Fig. 10b)**. The subtle changes upon Dicer1 knockout, such as the half-life of *Tnf* mRNA **(Suppl. Table 1)** prompted us to validate the genotype. Unfortunately, genotyping experiments indicate that conditional targeting of Dicer1 only led to a partial knockout **(Fig. 10c)**. Since it is hardly possible to draw inferences from incomplete KO about co-regulation with TTP and HuR and also that Ago2 was not found to interact with TTP **(Fig. 9)**, we further focused on the interplay between HuR and TTP.

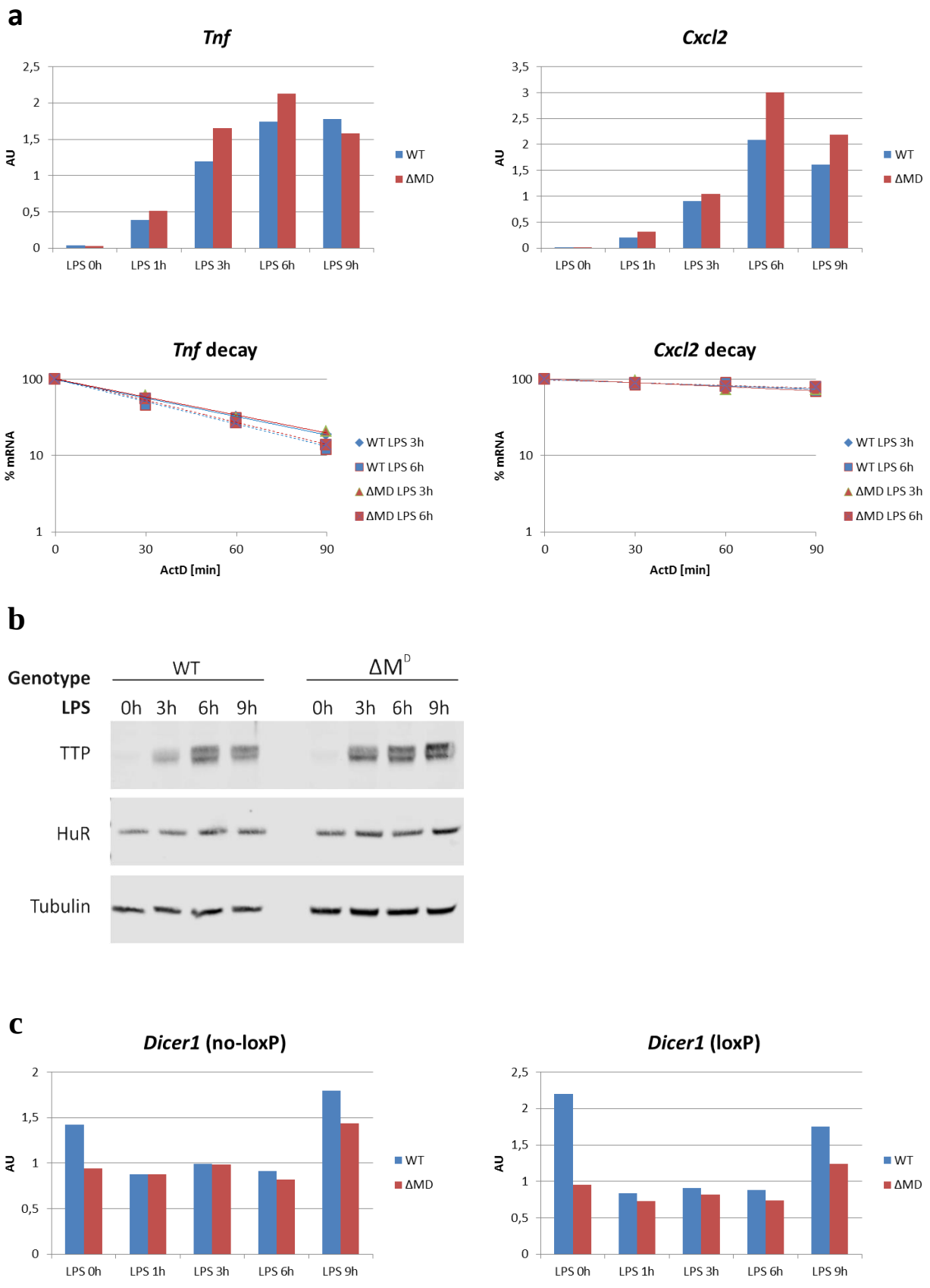

Figure 10| Incomplete Dicer1 KO prevents predictions concerning TTP-HuR-miRNA/RISC interplay.

Ad.: Figure 10| Incomplete Dicer1 KO prevents predictions concerning TTP-HuR-miRNA/RISC interplay. (a) Gene expression analysis of *Tnf* and *Cxcl2* (top lane) and the matching decay rates (bottom lane) from unstimulated (0h LPS) or 1/3/6/9h LPS stimulated bone marrow derived macrophages determined by qRT-PCR. Wild type (WT) is indicated in blue and partial conditional Dicer1 deletion in macrophages (ΔM^D) in red. Bottom lane: Decay rates are given as % of the remaining mRNA determined by Actinomycin D at the indicated time points. Solid lines represent decay after 3h LPS stimulation and dashed lines after 6h LPS stimulation. The corresponding half-lives are depicted in Suppl. Table 1 **(b)** Western blot of WT and ΔM^D bone marrow derived macrophages showing TTP, HuR and Tubulin expression after 0/3/6/9h LPS stimulation. **(c)** Gene expression analysis of *Dicer1* by qRT-PCR with primer binding upstream (no-loxP) and within (loxP) the floxed gene in the conditional KO.

Summarizing, the results obtained here add weight to the hypothesis that competitive binding may not be the main mechanism which directs RNA with mutual binding sequences towards degradation or stabilization. Rather they favor the concept of co-regulation of small fraction important inflammatory mediators by TTP and HuR[62,64].

3.2.2. TTP and HuR can bind mRNA targets with common binding sites simultaneously

TTP and HuR can interact together in a RNA-dependent way **(Fig. 9)**. That points towards the fact that during an inflammatory response early and late phase cytokine transcripts, such as *Tnf* and *Cxcl2* can be bound concomitantly by TTP and HuR[64]. Hence, simultaneous binding would rather abrogate the concept of mRNA stability dictated by mutual exclusive binding of the destabilizing TTP or the stabilizing HuR, albeit promote the hypothesis of co-regulation. To test for simultaneous binding target mRNAs must be eluted in complex with the RNA binding protein after RNA-immunoprecipitation (RNA-IP). With a second round of RNA-IP, directed against the second RNA-binding protein, mutually bound targets can be identified using qRT-PCR or RNA sequencing. Hence, two prerequisites have to be fulfilled: (i) during the whole procedure relatively mild conditions are needed to prevent RNA-digestion and (ii) after the first round of immunoprecipitation either TTP or HuR has to be demerged efficiently from the antibody used for pulldown. To test for the latter we decided to elute TTP after the first immunoprecipitation. Using standard conditions, i.e. 0.1M glycine pH=2.65, TTP could not be eluted from the immunoprecipitate **(Fig. 11)**. Nonetheless, application of the last 34 amino acids of TTP ($TTP_{c\text{-}term}$) allowed to elute TTP specifically from the bound K2 antibodies. Of note, polyclonal K2-antibodies were generated by immunization of a rabbit with a fusion of GST-$TTP_{c\text{-}term}$. Hence increasing amounts of TTP shift the binding affinity towards the $TTP_{c\text{-}term}$ and the higher the amount of the C-terminal peptide the better

the elution of TTP. Importantly, with the strategy applied here it is not possible to examine whether RNA is still bound to the eluted protein or if it has been already digested. Also, here HuR was not co-immunoprecipitated together the eluted TTP. However, due to the little amount of TTP eluted it is likely that HuR is below the detection limit, although RNA digestion would also be a feasible explanation **(**see **Fig. 9)**.

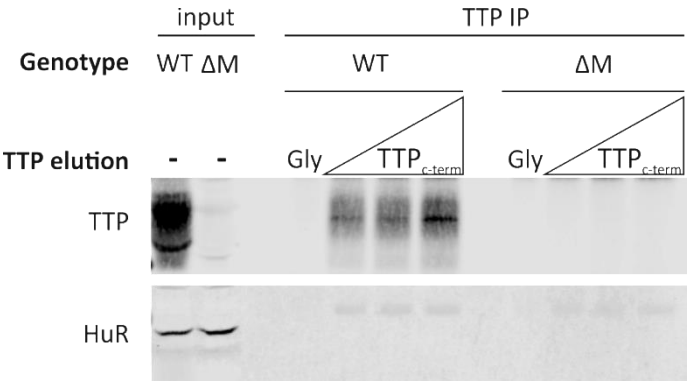

Figure 11| Immunoprecipitated TTP can be eluted with its own C-terminal peptide. Co-immunoprecipitation of wildtype (WT) and TTP deficient bone marrow derived macrophages (ΔM) depicting TTP and HuR expression on western blot after TTP elution from K2 immunoprecipitates. Cells were treated for 6 hours with LPS prior lysis. Elution was done either by 0.1M glycine pH=2.65 (Gly) or by increasing amounts of $TTP_{c\text{-}term}$ in three steps (see Materials and Methods). Input shows the protein expression of whole cell lysates prior immunoprecipitation. Immunoprecipitation in ΔM cells serve as control for unspecific binding of the K2 antibody.

To determine if there is a combinatorial effect of TTP and HuR sequential native RNA-IP was performed[1]. In short, TTP was pulled-down with K2 polyclonal TTP antibody during the first round of immunoprecipitation followed by $TTP_{c\text{-}term}$ mediated elution, using the highest amount of the C-terminal peptide described in **figure 11**. Eluted TTP complexes were then check for HuR interaction by a second round of IP against HuR. Importantly, targets containing overlapping binding sites for TTP and HuR in their 3´UTR[64] were found to be bound by both simultaneously **(Fig. 12)**. For instance the mRNAs of the pro-inflammatory cytokines *Tnf* and *Cxcl2*[64]*,* but also *Sdc4* (Syndecan 4) and *Zfp36* itself showed concomitant binding of the two RBPs. Interestingly, the proteoglycan Sdc4 is linked to TTP mediated dormant state of satellite cells, and its expression allows uptake of dead cells as well as of LDL in macrophages during inflammation[153–155]. On the contrary, RNA targets only containing HuR sites, such as *Gnb1* and *Tapbp*, and *Hprt* containing neither TTP or HuR sites have not shown concurrent binding[64].Hence, this indicates a multilayered control of a small, yet potent cohort of inflammatory mediator mRNAs in a macrophage response. In that case

[1] Method and part of the data for sequential native RNA-IP were already published in ref. [64].

posttranscriptional regulation may be defined by TTP´s and HuR´s combinatorial function on the same mRNA and not inversely by competitive binding governing mRNA fate due to their opposing functions.

3.2.3. HuR, a supporting actor in TTP´s dictated mRNA stability in inflammation

To further investigate the functional consequences of the interplay between TTP and HuR, in particular for mRNA targets with an overlapping binding site, we aimed to generate RAW 264.7 macrophages with a *Zfp36*$^{-/-}$, *Elavl1*$^{-/-}$ and *DKO* (double KO; *Zfp36*$^{-/-}$, *Elavl1*$^{-/-}$) genotype. Determination of mRNA levels and decay rates as such would allow drawing conclusions about their function during inflammation on posttranscriptional level, yet cell are easy to handle in culture. To that extent single cell derived colonies of RAW 264.7 macrophages subjected to the CRISPR/Cas9 technology were assessed for TTP and HuR protein expression, respectively. Notably, single cell clones tested already have been validated for a frameshift mutation in the exon 2 of *Zfp36*, i.e. a 1 nucleotide deletion in both alleles and another frameshift mutation in *Elavl1* exon 2, i.e. a 1 and 2 nucleotide deletion at one allele at a time, respectively (data not shown). Clone T20+/+ was subjected to CRISPR/Cas9 genome editing strategy but neither *Zfp36* nor *Elavl1* genes have been altered. Clone T20.11, T9-/- and T9.10 showed frameshift mutations in *Elavl1*, *Zfp36* or both genes, respectively. We assumed that disruption of the open reading frame at early exons would efficiently cause aberrant protein translation and thus induce a full KO. As anticipated from literature[74], TTP protein expression can only be detected in T20+/+ and T20.11 upon LPS stimulation and increases over time reaching its maximum **(Fig. 13)**. Also fitting to the sequencing results, only T9-/- and T9.10 showed HuR expression. Here, the ubiquitously expressed protein shows steady expression kinetics. Of note, in the RAW macrophages generated TTP expression does not seem to affect HuR expression or vice versa, in the time frame examined. Taken together, each RAW clone fits its genotype and for reasons of simplicity thus are referred hereafter as WT (T20+/+), TTP$^{-/-}$ (T9-/-), HuR$^{-/-}$ (T20.11) and DKO (T9.10).

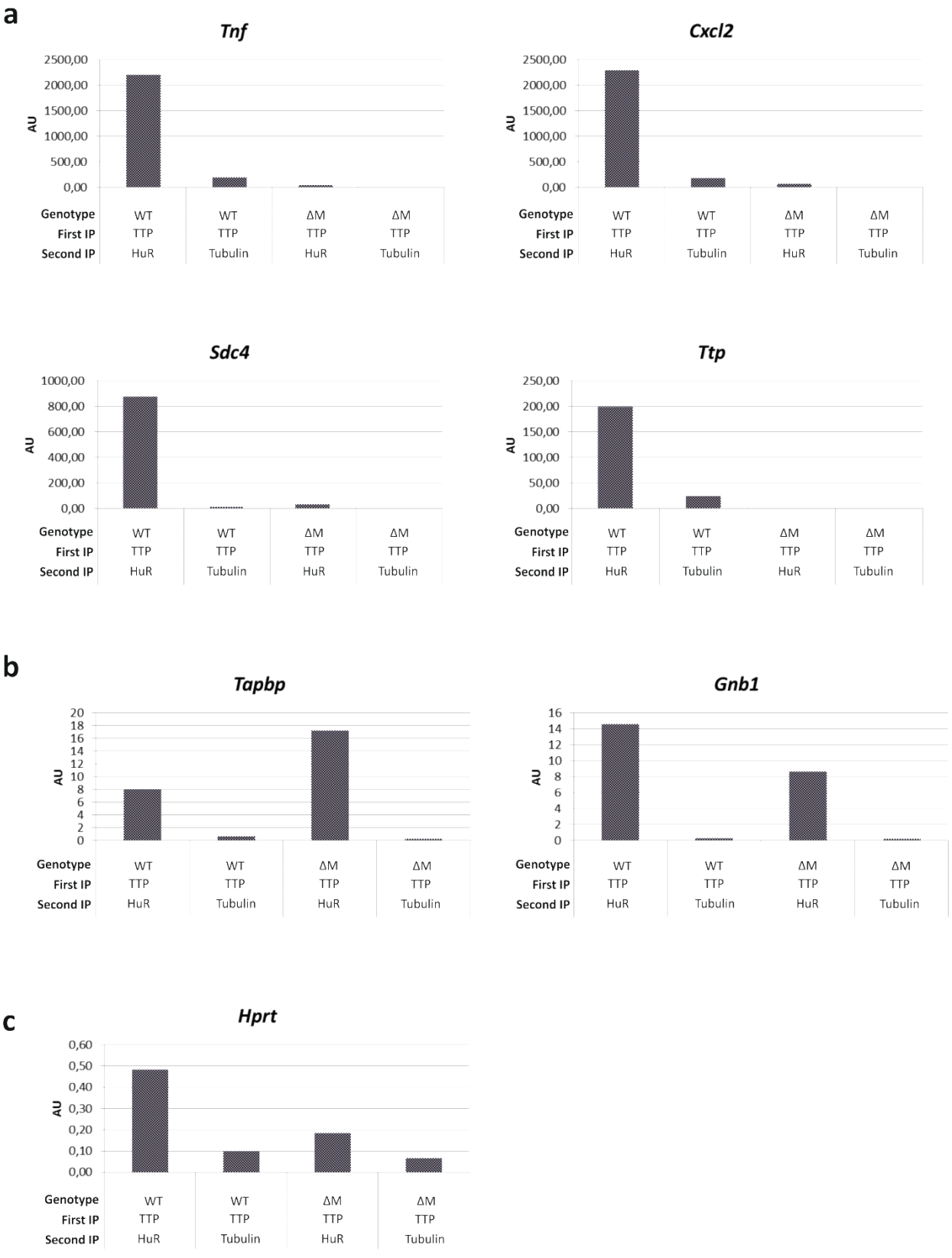

Figure 12| TTP and HuR simultaneously bind to mRNA targets with overlapping binding sites. (a,b,c) Sequential native RNA-IP followed by qRT-PCR detection for the indicated genes in WT and TTP deficient bone marrow derived macrophages (ΔM). Binding site were taken from ref. [64]. Cells were treated for 6 hours with LPS prior lysis. For the first IP K2 antibody was used, for the second IP either an anti-HuR or anti-Tubulin antibody was used. **(a)** Targets with overlapping binding sites show concomitant binding of TTP and HuR. **(b)** Targets with HuR binding site in 3´UTR only do not show simultaneous binding. **(c)** *Hprt* mRNA, in which no

significant TTP or HuR binding was detected, neither shows concomitant binding. ΔM cells and Tubulin pulldown in the second IP serve as controls for unspecific binding of the K2 and HuR antibodies, respectively.

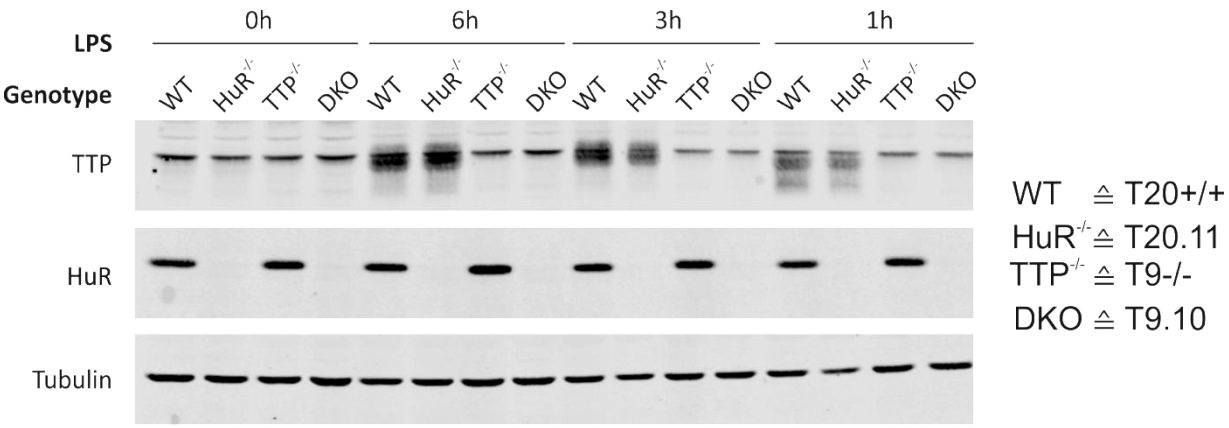

Figure 13| Confirmation of the TTP$^{-/-}$, HuR$^{-/-}$ and DKO RAW macrophage genotype generated by CRISPR/Cas9 genome editing. Single cell derived RAW colonies, i.e. T20+/+, T20.11, T9-/- and T9.10 with no mutation, 1nt deletion in *Elavl1* exon 2, 2nt deletion in *Zfp36* exon2 and both of the aforementioned were assessed for TTP and HuR expression to functionally determine their genotype by western blot. RAW 264.7 cells were untreated (0h) or treated for 1/3/6h with LPS prior cell lysis. Individual clones were named fitting to the results obtained as indicated on the right side.

Thereafter the generated cells were used to monitor mRNA expression levels and decay rates of several macrophage released pro-inflammatory and immune cell mobilizing cytokines. In particular, we focused on transcripts which showed simultaneous binding of TTP and HuR **(summarized in Suppl. Table 3 and 6)**, but also analyzed transcripts mapped for TTP and HuR binding only by PAR-CLIP[64] **(summarized in Suppl. Table 4-6)**.

Among the best studied TTP targets is *Tnf* [44,55,147]. In a LPS induced inflammatory environment *Tnf* mRNA became rapidly upregulated and mRNA stability was tightly regulated by the destabilizing TTP and to a little degree by stabilizing HuR **(Fig. 14)**. As such its mRNA levels were markedly elevated in TTP$^{-/-}$ RAW macrophages and also showed almost twice as long half-live when compared to WT. On the other hand the DKO has less Tnf expression than TTP$^{-/-}$. Together with the difference in decay data it can be assumed that HuR prevents mRNA degradation. Since, both TTP and HuR can bind *Tnf* mRNA concomitantly in BMDMs **(Fig. 12)**, this greatly supports the idea that

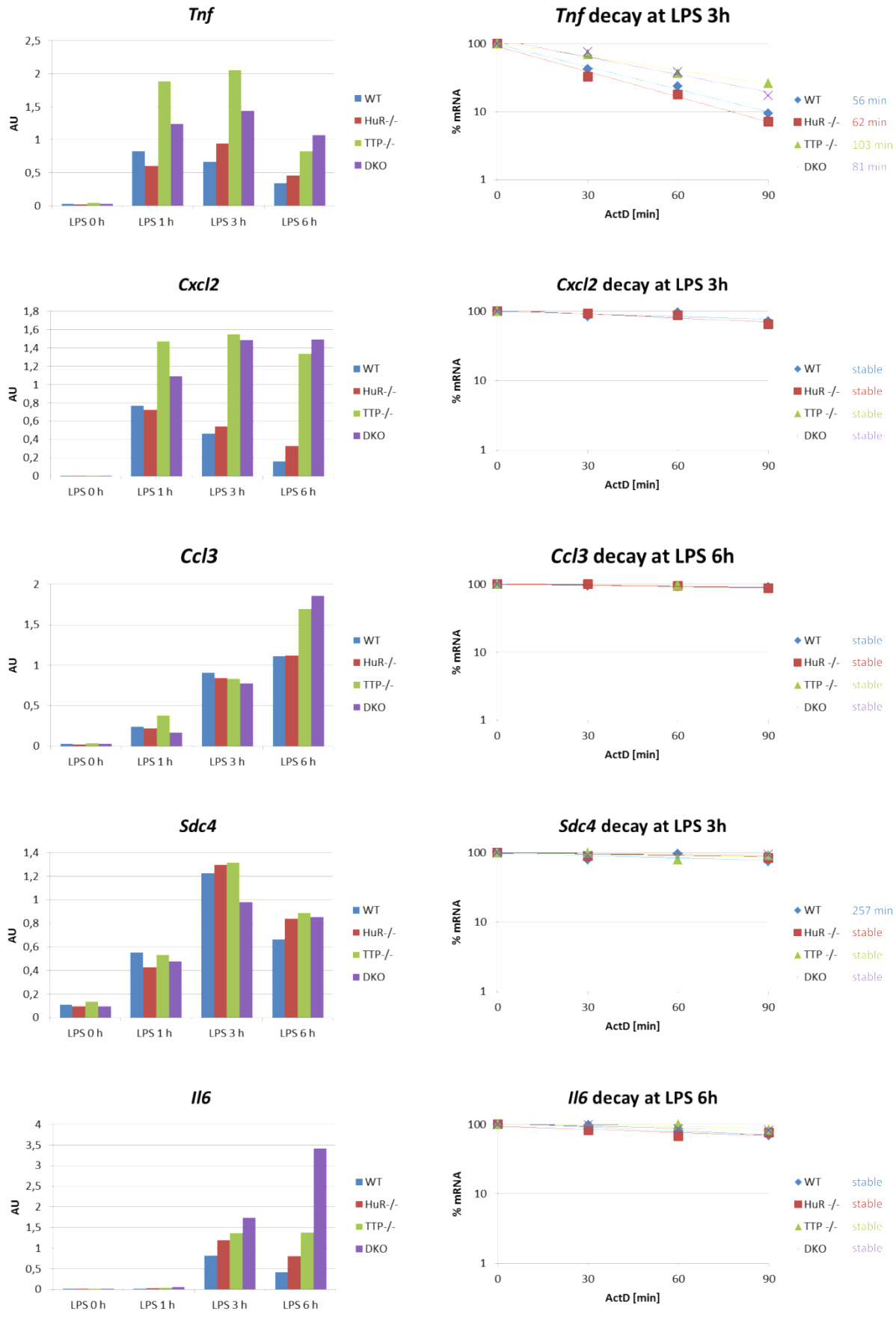

Figure 14| Versatile effects of TTP and HuR on mRNA expression and decay. Gene expression analysis (left) and decay rates (right) for the genes indicated at the top by qRT-PCR. RAW 264.7 WT (blue), HuR$^{-/-}$ (red), TTP $^{-/-}$

(green) and DKO (violet) cells were untreated (0h) or treated for 1/3/6h with LPS. Right: Decay rates are given as % of the remaining mRNA determined by Actinomycin D at the indicated time points measured after 3 or 6h LPS treatment. Decay and half-life match the color of the genotype. Half-lives are indicated next to the genotype and were considered as stable if ≥270 min.

putative competition for mRNA decay occurs independently of binding site occupation. Although this indicates that co-regulation between TTP and HuR mainly affects cytokine expression on the posttranscriptional level during inflammation, the results for *Cxcl2*, *Ccl3* and *Sdc4*, i.e. transcripts also bound simultaneously in BMDMs **(Fig. 12)**, differ. Here, transcripts in general can be considered as stable. For instance, even though *Cxcl2* and *Ccl3* can be considered here as early and late phase inflammatory cytokines based on their expression pattern over time their transcript abundance is only dependent on TTP. A HuR dependent effect on the total transcript amount can be ruled out as $TTP^{-/-}$ and DKO show almost no differences. Even more surprising, *Sdc4* mRNA is neither affected by the destabilizing capability of TTP nor of the stabilizing function of HuR. On the contrary *Il6* mRNA levels, i.e. only being mapped for TTP binding[64], interestingly is elevated in $TTP^{-/-}$ and $HuR^{-/-}$ macrophages, which peaks in the DKO genotype after three and six hour LPS treatment. This indicates that for *Il6*, not only TTP negatively affects transcription, but also HuR which synergizes when both proteins are absent. Similarly, the early phase inflammatory transcripts of *Il1a* and *Il1b* showed increased expression in absence of HuR, most relevant post three hour LPS stimulus **(Suppl. Table 4)**. Absence of HuR binding thus suggests an indirect mechanism that promotes the expression a factor, which in turn reduces *Il6* mRNA abundance. Of note, this contrast previous reports in which IL-6 release was altered by the stabilizing function of HuR on TTP, finally reducing its expression[156]. As *Il6* mRNA was described to be bound in RAW 264.7 cells[115], it is likely that here its expression is regulated differently when compared to primary macrophage cells.

Characterization of the cytokine transcription profile of the CRISPR/Cas 9 RAW KO macrophages **(Suppl. Table 3-6)** further indicates their utility for further research in posttranscriptional regulation of gene expression in the field of immunity. For instance, acute phase *Tnf* and its downstream transcriptionally induced gene *Cxcl2* have been confirmed as TTP targets **(Fig. 14)**. This also has been shown in primary macrophages before[55,147]. Therefore, *in vitro* studies in those cells may allow mechanistic annotations how TTP limits inflammation by prevention of TNF and CXCL2 synthesis. Their possible usefulness is further supported by other cytokine transcripts, such as *Ccl3*. *In vivo* knockout studies

reveal CCL3 as a major actor of TTP KO driven inflammatory syndrome[57]. On the other hand, neither in unstimulated nor in LPS treated RAW cells, *Il10* mRNA could be detected **(Suppl. Table 4),** irrespectively of the genotype. Notably, TTP was already described to bind *Il10* mRNA in murine macrophages and likely also contributes to resolution of inflammation via its reported TTP induction[157–159]. Thus, although RAW 264.7 cells would allow studying TTP and HuR mediated effects on mRNA decay in an immunological relevant context there may be limitations.

Albeit the data generated proofs that TTP interacts with HuR through RNA **(Fig. 11)** in LPS activated macrophages and that among simultaneously bound targets are well known pro-inflammatory mediators, such as *Tnf* and *Cxcl2* **(Fig. 12)**, no definitive conclusions can be drawn concerning combinatorial TTP-HuR effector function on posttranscriptional level. Except for *Tnf* mRNA HuR had in general a minor impact on mRNA stability as determined by the respective RAW knockout macrophages **(Figure 14)**. Hence, HuR acting as a stabilizing factor for commonly bound targets in inflammation may be limited to a few transcripts and co-regulation or competition between TTP and HuR might occur primarily at translational level, as already suggested elsewhere[86,115].

3.3. Tagging of TTP in its genomic locus

3.3.1. Isolation of heterozygous MYC tagged TTP RAW 264.7 cells

The versatility of TTP, such as its nuclear form, dictating mRNA decay in immunity spatiotemporally, but also reports of its involvement in translation and interaction with other trans-acting factors strongly suggest that TTP effector function involves certain posttranslational modifications[45,55,64,86,91–96]. This is exemplified by phosphorylation of murine TTP at the serine residues S52 and S178, which renders the protein more stable but prevents its degrading function[80–83]. Furthermore, p38 MAPK induced phosphorylation also was shown to alleviate TTP binding to *Tnf* mRNA and causing a shift towards translation by HuR[86]. Although this underlines the importance of posttranslational modification in TTP biology, still many observed phosphorylations at serine, threonine and tyrosine residues, but also ubiquitination remain to be fully functionally annotated[80,89,90,160,161].

To that end RAW 264.7 cells with an endogenous N-termainally MYC tagged TTP were generated using CRISPR/Cas9 genome editing in the lab, as described before[144]. In short, *Zfp36* was targeted at its genomic locus with 2 different guide RNAs aiming to repair and thus substitute the endogenous *Zfp36* sequence with the donor sequence, harboring the Myc sequence immediately downstream of the start codon of exon 1, followed by the rest of exon 1 sequence **(Fig. 15)**. Additionally, a hygromycin selection cassette was inserted in the intron between exon 1 and 2, allowing selection of positive knock-in (KI) RAW 264.7 cells.

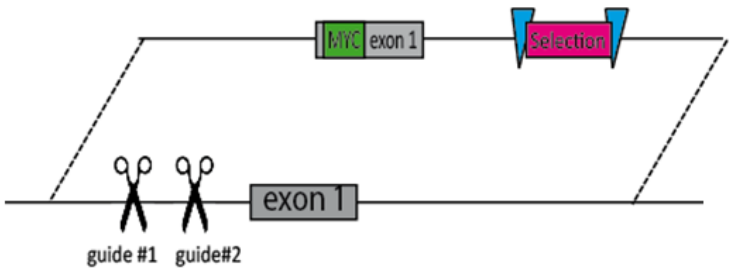

Figure 15| Design for Myc tagging endogenous TTP at its genomic locus using CRISPR/Cas9 technology. Cas9 mediated cleavage using guide #1 or #2 should ultimately allow exchange with the donor sequence upon homology directed repair (top)[162,163]. The donor sequence is expressed form the plasmid TTP-pUC57-hygromycin and consist of a MYC tag (green) sequence directly downstream of the exon 1 (grey) intrinsic AUG, which is followed by the rest of exon 1. At intron 1 there is an additional hygromycin selection (pink), flanked by loxP sites (blue), which allows negative selection. The picture was taken from ref. [144], which also provides the full description of the CRISPR/Cas9 strategy applied.

It was expected that immunopurification of TTP through its MYC tag and subsequent elution with the MYC peptide would allow to study posttranslational modifications of TTP. As RAW

macrophages endogenously express TTP when facing bacterial products[74], this system would allow mimicking the natural context without relying on overexpression or immunologically irrelevant cell lines. However, the knock-in could not be definitively confirmed nor a pure culture could be obtained[144]. Hence, colonies with the putative KI derived from single cell clones, i.e. B8, F9 and G9 were tested for protein expression of the fusion MYC-TTP. Unfortunately, Western blot analysis did not display any MYC-TTP expression, whereas TTP alone was found in all RAW cells **(Fig. 16)**. This could be explained by several possibilities. First, there is a mixture of WT and *Myc-Zfp36* RAW genotypes and the tagged protein is expressed in insufficient amounts for detection. On the other hand, it is also feasible that that the modified locus became silenced, but also that there is no KI.

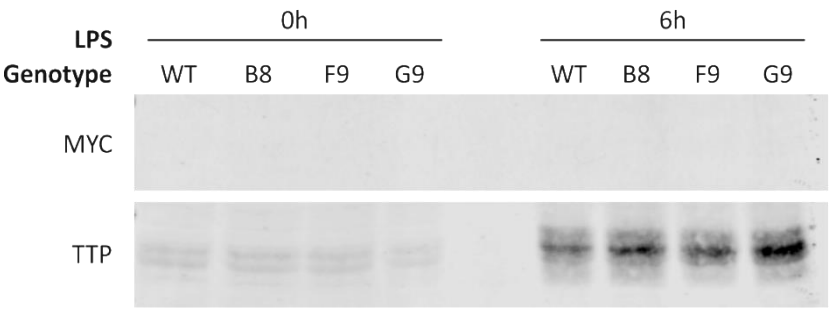

Figure 16| Absence of MYC tagged TTP expression in putative knock-in colonies. Western blot depicting protein expression of MYC, using 9B11 monoclonal antibody (mAb), and TTP, using K2 antibody. RAW WT, B8, F9, G9 cells were treated for 6h with LPS or untreated (0h) prior cell lysis. As MYC detection aims to identify MYC-TTP the same section for TTP detection, i.e. ~40-50 kDa is shown. WT serves a negative control for MYC-TTP detection.

Hence, we further generated single cell derived colonies using RAW B8. This should allow attaining a pure culture of *Myc-Zfp36* RAW 264.7 cells, on the basis that the B-8 batch really contains the KI obtained by CRISPR/Cas9. As previous genotyping PCRs only rendered inconclusive results, including the surveyor assay[144], we set out to perform dual screening of the clones. This was done on the one hand by a new genotyping PCR (i.e. ´RAW_KI_only´), designed to only detect the KI with an amplicon size of specifically 531bp, whereas primers (forward primer: RAW_KI_only FW; reverse primer: RAW_KI_only RV) should not yield a product for WT or when using the donor plasmid TTP-pUC57-hygromycin as control. This is because the forward primer binds within the 5´UTR of *Zfp36*, only present in WT and KI, and the reverse primer binds within the *Myc* sequence, not found in WT **(Fig. 17a and b)**.

Additionally, clones were examined for TTP expression on protein level with immunofluorescence using an antibody against MYC **(Fig. 17c)**.

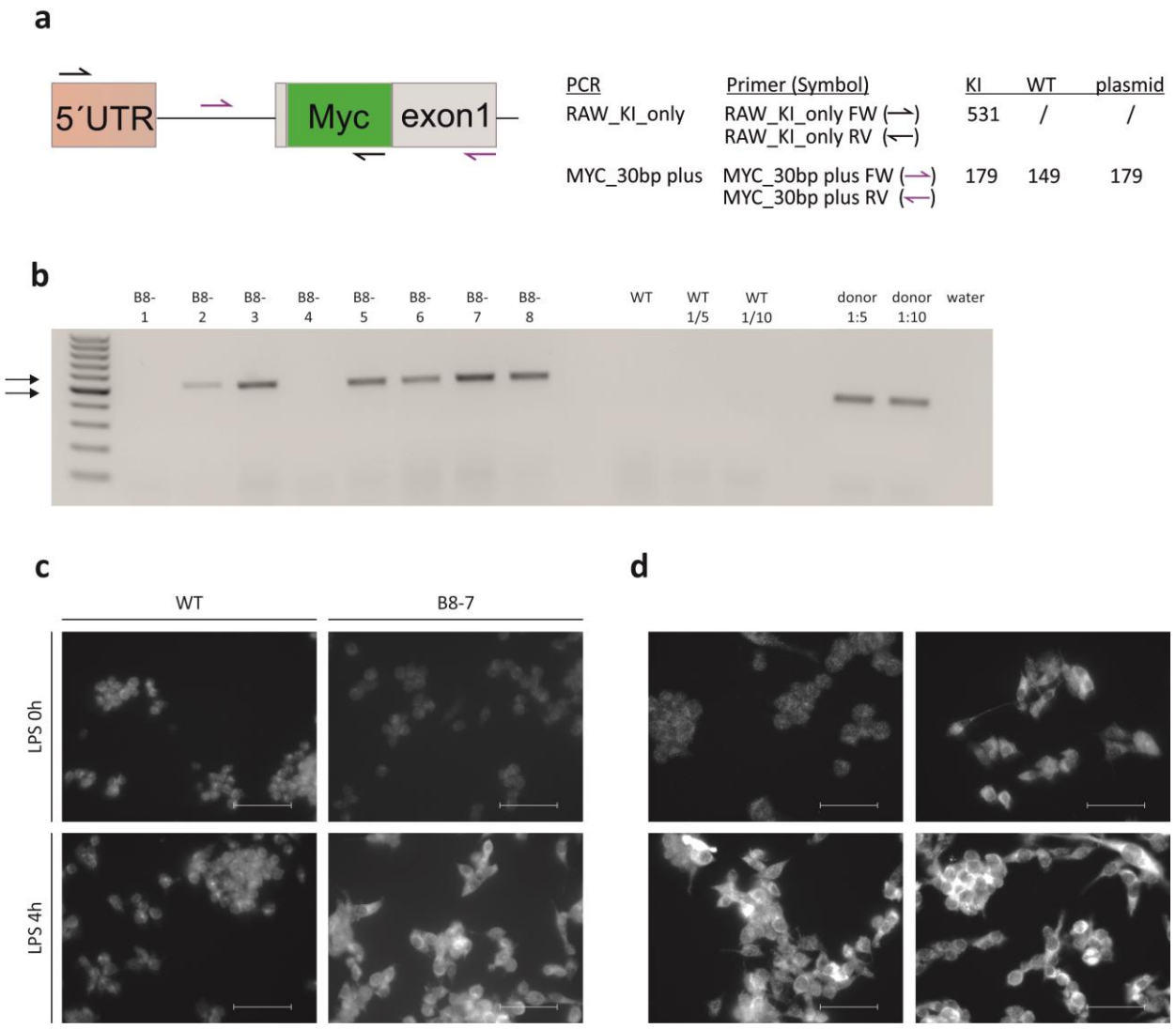

Figure 17| Narrowing of 5 clones with hetero- or homozygous *Myc-Zfp36*. (a) Schematic drawing of the 2 designed PCRs allowing to identify *Myc-Zfp36* RAW 264.7 cells and in combination to differ between heterozygous (*Zfp36*$^{WT/Myc}$) and homozygous KI (*Zfp36*$^{Myc/Myc}$). The primer binding sites for both PCR reactions are indicated on the putative KI, as well as the amplicon size [bp] for the KI, but also WT and donor plasmid control. The forward (FW) and reverse (RV) primer have the prefix of the corresponding genotyping PCR, i.e. RAW_KI_only or MYC_30bp plus (top right). **(b)** PCR products of RAW_KI_only reaction, from clone B8-1 to B8-8, as well as negative wild type (WT) and donor TTP-pUC57-hygromicin (donor), were separated on an agarose gel. For WT and donor controls the indicated 1/5 and 1/10 dilutions were included. The arrows indicate 500bp (bottom arrow) and 600bp (top arrow), respectively. **(c)** Immunofluorescence of untreated (0h) and for 4h LPS (20ng/ml) treated WT and B8-7 clone, using 9B11 mAb for MYC detection. WT serves as negative control to for MYC-TTP detection induced upon LPS stimulus. **(d)** Immunofluorescence using 9B11 mAb for MYC detection post 4h LPS (20ng/ml) treatment in B8-1 (top, left), B8-2 (top, right), B8-3 (bottom, right) and B8-5 (bottom, left) single cell derived RAW colonies. **(c, d)** Scale bars represent 50µm. WT serves a negative control for MYC-TTP detection. Pictures depict gray scale of Alexa fluor 488 measurements.

Genotyping using the ´RAW_KI_only´ PCR showed that clone B8-2, B8-3, B-5, B-6, B-7, and B-8 contain the desired KI. However, there was also amplification of the TTP-pUC57-

hygromicin donor plasmid, with an amplicon size of ~450bp. Therefore, PCR products of RAW 264.7 clones positive for the knock-in and form the donor plasmid were sent for sequencing. Sanger sequencing confirmed that in RAW cells the PCR used targeted the region designed for, and thus really identified the knock-in for N-terminally tagged TTP **(Suppl. Materials and Methods)**. The amplicon form the donor sequence was shown to be a false positive, with unspecific amplification (data not shown). To determine if clones genotyped for *Myc-Zfp36* KI actually express the fusion of MYC-TTP immunofluorescence was performed. LPS stimulation showed the specific detection of MYC tagged TTP, i.e. in B8-7, which was absent in WT and also untreated cells **(Fig. 17c)**. Moreover, single cell derived colonies of B8-2, B8-3 and B8-5 were positive for homogenous MYC-TTP expression **(Fig. 17d).** However, B8-1 **(Fig. 17, top left)**, as well as B8-6 and B8-8 (data not shown) showed the same background fluorescence as WT and unstimulated B8-7 RAW macrophages, respectively and thus were no further examined. Although this already indicates that 5 clones show the functional expression of MYC-tagged TTP, Western blot analysis could not detect the fusion proteins, opposing the previously generated results **(Fig. 18)**.

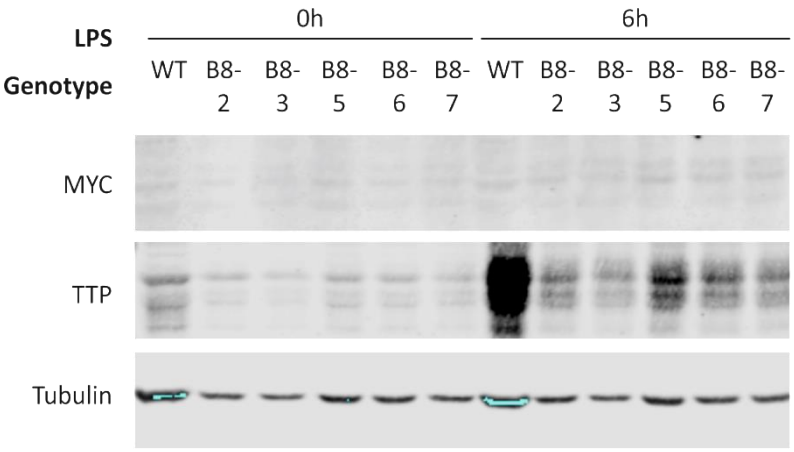

Figure 18| MYC-TTP expression cannot be determined on protein level by Western blot. Western blot depicting protein expression of MYC, TTP and Tubulin. RAW WT, B8-2, B8-3, B8-5, B-6, and B8-7 cell were untreated (0h) or treated for 6h with LPS prior cell lysis. As MYC detection aims to identify MYC-TTP the same section for TTP detection, i.e. ~40-50 kDa is shown. WT serves a negative control for MYC-TTP detection. Tubulin serves as loading control.

Although, excessive amounts of RAW 264.7 WT proteins were loaded compared to clones, it still indicates that the genome edited locus may have become silenced over time, yielding little TTP expression at all. The possibility of WT contamination is improbably since immunofluorescences showed homologous MYC detection among colonies. Summarizing,

the results obtained here do not allow to identify a definitive KI brought about by the CRISPR/Cas9 technology, nor it can be differentiated if putative knock-in cells are heterozygous (*Zfp36*$^{WT/Myc}$) or homozygous (*Zfp36*$^{Myc/Myc}$) for the N-terminal MYC tag. Since, B8-5 and B8-7, were promisingly shown to contain the knock-in of endogenous tagged *Zfp36* **(Fig. 17)** we set out to re-select those single cell derived colonies with hygromycin for 6 days. As such, negative selection would kill all cells in which hygromycin selection cassette is silenced or missing at all, i.e. RAW 264.7 cells which have been efficiently genome edited but do not express the protein and WT cells, respectively. Additionally, the design of new PCR, termed ´MYC_30bp plus´ (forward primer: MYC_30bp plus FW; reverse primer: MYC_30bp RV), allows differentiating between homozygous WT, heterozygous KI and homozygous KI based on the presence/absence of the Myc sequence **(Fig. 17a)**. Comprehensive analysis of the genotyping PCRs identified B8-5 and B8-7 hygromycin selected cells as *Zfp36*$^{WT/Myc}$. This is because, RAW_KI_only clearly shows that there is KI and MYC_30bp plus shows that one allele carries the WT and the other one the Myc tagged *Zfp36* **(Fig. 19a and b)**. Importantly, little amounts of MYC-TTP can be detected in Western blot of hygromycin selected clones **(Fig. 19c).** Of note, total TTP protein amounts are highest in wildtype RAW 264.7 cells. This might indicate that locus is not necessarily silenced, but maybe transcription of MYC-TTP is hampered by the hygromycin selection, being transcribed in opposite direction of *Myc-Zfp36*[144]. Nonetheless, the data generated here identifies the hygromycin selected single cell derived RAW 264.7 colonies B8-5 and B8-7 as heterozygous *Zfp36*$^{WT/Myc}$ which also express the protein upon inflammatory stimulus.

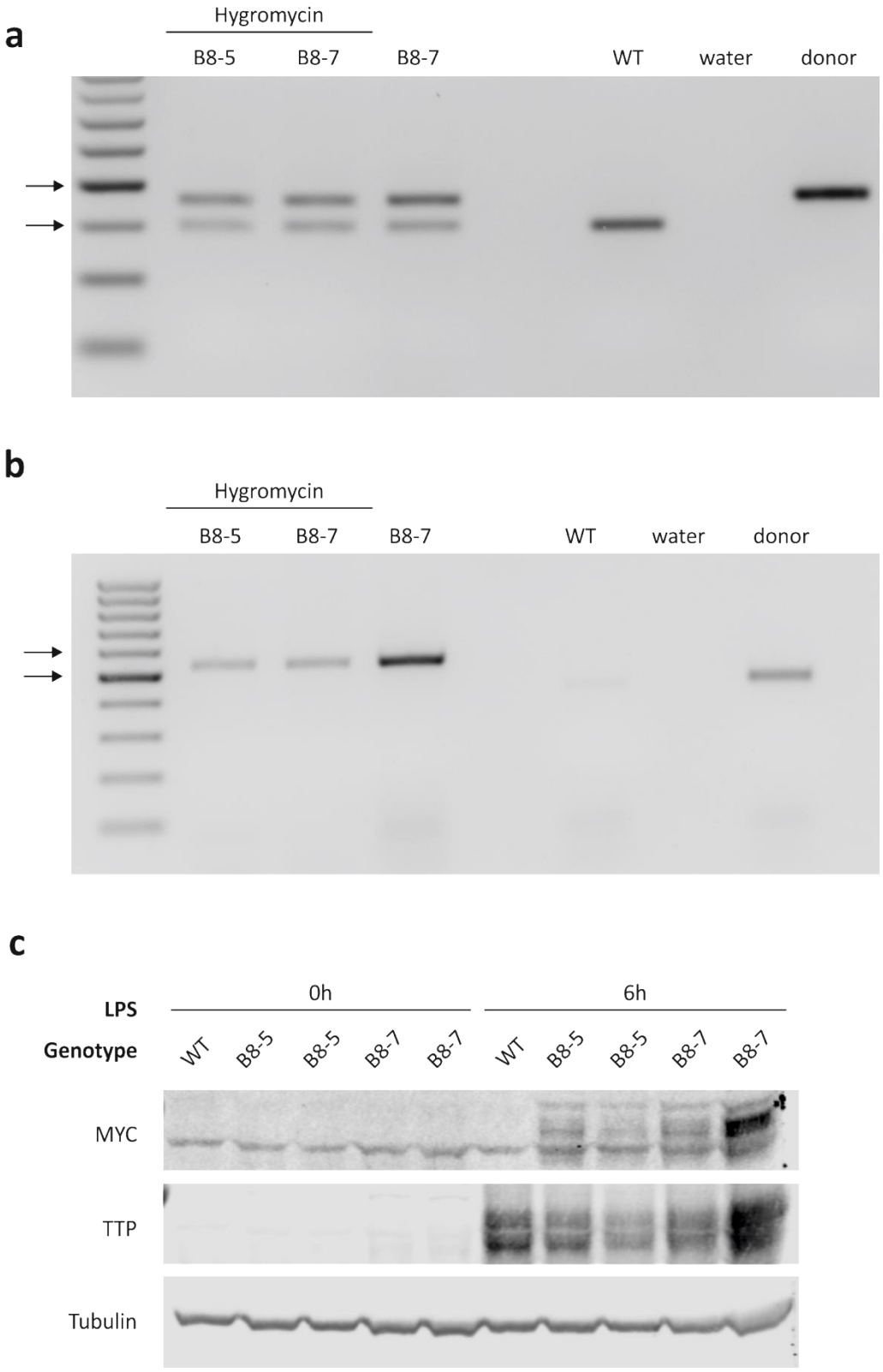

Figure 19| Identification of heterozygous *Zfp36*$^{WT/Myc}$ knock-in RAW 264.7 cells. (a, b) PCR products of MYC_30bp plus (a) and RAW_KI_only reaction (b), from clone B8-5 and B8-7 post 6 day hygromycin selection, as well as negative wild type (WT) and donor TTP-pUC57-hygromicin (donor) control, were separated on an agarose gel. As positive control gDNA from B8-7 not subjected to hygromycin selection was included. The arrows indicate 500bp (bottom arrow) and 600bp (top arrow), respectively in (b) and 100bp (bottom arrow) and 200bp (top arrow) in (a). **(c)** Western blot depicting protein expression of MYC, TTP and Tubulin. RAW WT and biological replicates of B8-5 and B8-7 post 6 day hygromycin selection were untreated (0h) or treated for

6h with LPS prior cell lysis. As MYC detection aims to identify MYC-TTP the same section for TTP detection, i.e. ~40-50 kDa is shown. WT serves a negative control for MYC-TTP detection. Tubulin serves as loading control.

3.3.2. Immunoprecipitation of N-terminally MYC tagged TTP

As RAW 264.7 cells naturally express TTP[74], the isolated heterozygous knock-in *Zfp36*$^{WT/Myc}$ cells should allow to efficiently immunopurify the trans-acting factor through its N-terminal MYC tag. By reducing sample complexity[164], this in turn should set the basis to perform mass spectrometry to identify and presumably link posttranslational modifications of endogenously expressed TTP to its function under physiological relevant conditions. This detour is necessary as previous approaches in the lab failed to get a clear signal for immunoprecipitated TTP, or just in too little amounts[144].

First, to examine how efficiently MYC tagged TTP can be immunoprecipitated tried different antibodies targeting TTP in general, i.e. rabbit K2 polyclonal antibody (pAb), or MYC, i.e. mouse 9B11 monoclonal antibody (mAb) and 9E10 mAb. Hygromycin selected B8-5 and B8-7 heterozygous KI cells both express MYC-TTP as observed in the input **(Fig. 20a).** However, immunoprecipitation of the tagged TTP is very inefficient when compared to the standard TTP K2 antibody and is restricted to covalently coupled 9E10 antibody. Furthermore, there seems to be off-target binding of 9E10 antibody as even in the WT control there is an unspecific band at the height of MYC-TTP not found when TTP alone is visualized. Additionally, elution of the precipitate also decoupled the antibodies used as observed by the heavy chain detection at the top with ~50kDa. As MYC tagged TTP was best pulled down in B8-7 we the focused on this clone for further optimization of tag based purification. To get rid of putative detergence effects disturbing IP[165], a minimal concentration Triton X-100 was compared to standard detergence amounts together with an alternative monoclonal antibody, i.e. rabbit 71D10 **(Fig. 20b).** Unfortunately, this did not entail any improvements as MYC-TTP still is only found in the 9E10-IP, independent of detergence concentration. Also the unspecific bands remain the same. Finally to determine is the MYC tag might be covered by unfavorable TTP conformation, which inhibits antibody access, low amounts of the denaturing agent SDS were added **(Fig. 20c)**.

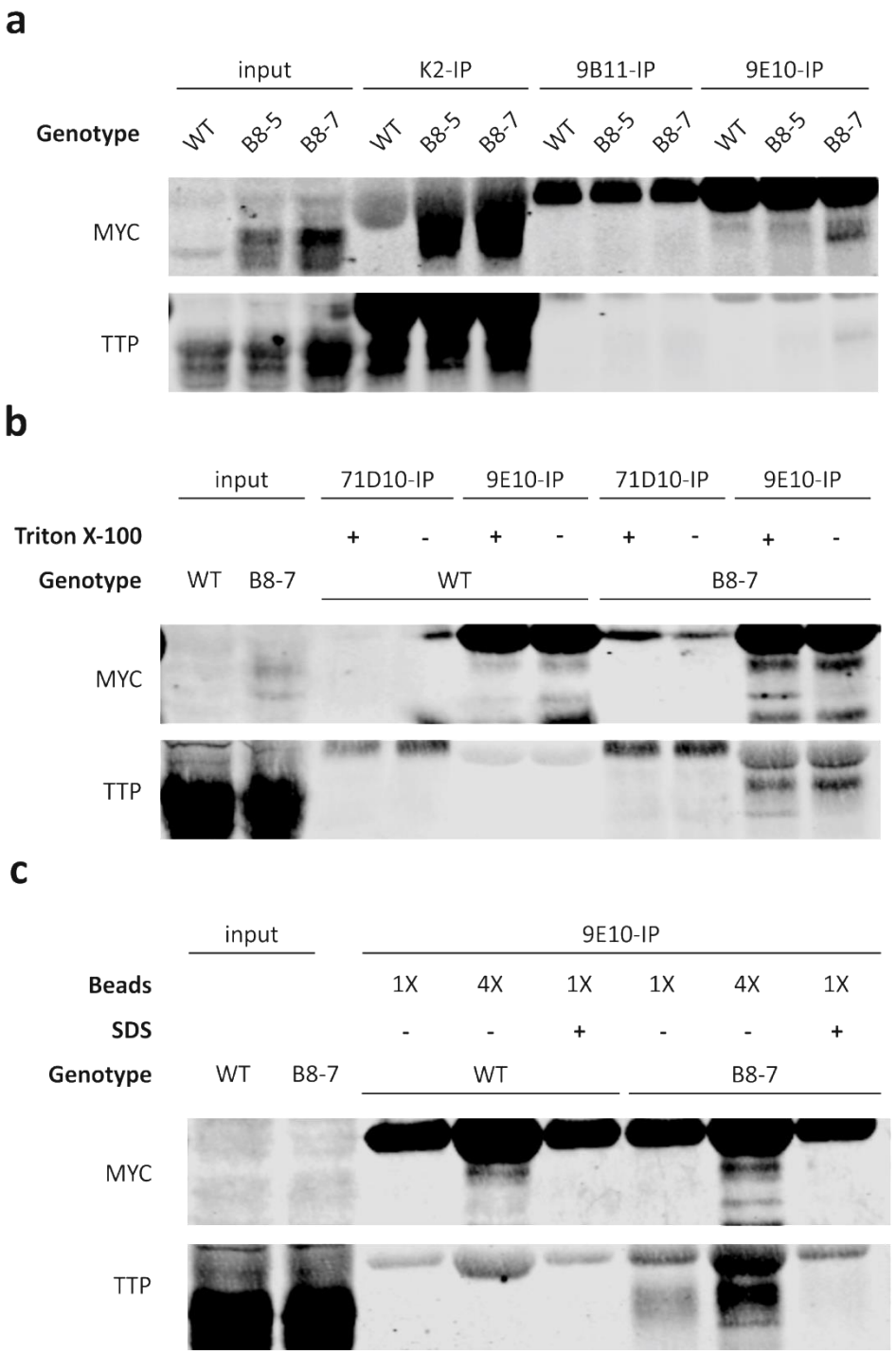

Figure 20| Different immunoprecipitation strategies to aiming to maximize the yield of MYC-TTP. (a, b, c) Immunoprecipitation of N-terminally MYC tagged TTP of RAW WT, and B8-5 and B8-7 heterozygous *Zfp36*$^{WT/Myc}$ cells after 6 hours LPS stimulation analyzed by Western blot. As MYC detection aims to identify MYC-TTP the same section for TTP detection, i.e. ~40-50 kDa is shown. WT serves a negative control for MYC-TTP detection. **(a)** Immunoprecipitation of MYC tagged TTP utilizing 9B11 mAb coupled beads and 9E10 mAb covalently coupled beads, as well as total TTP precipitation with K2 monoclonal antibody. WT serves as additional control for positive TTP-IP. **(b)** Immunoprecipitation of MYC tagged TTP utilizing 71D10 mAb coupled beads and 9E10 mAb covalently coupled beads. Alternatively from the standard IP protocol (see Materials and Methods) overnight immunoprecipitation was done in normal Frackelton buffer, with 1% Triton X-100 (+) or with 0.166% Triton X-100 (-). **(c)** Immunoprecipitation of MYC tagged TTP utilizing 9E10 mAb covalently coupled beads. Alternatively from the standard IP protocol (see Materials and Methods) overnight immunoprecipitation was either done in normal 1X Frackelton buffer (-) or supplemented with 0.2% SDS (+). Also the amount for beads covalently coupled to 9E10 mAb varied from normal (1X) to 4-fold (4X).

However, whereas additional SDS abolished MYC precipitation at all, it seems that efficiency of tag based immunopurification can be increased by increasing the amount of beads with covalently coupled 9E10 mAb. Of note, whereas MYC tagged TTP is strongly present in the heterozygous KI **(Fig. 20a)** post 6 days hygromycin of selection, the fusion proteins expression decreases over time with increasing cell passages **(Fig. 20b and c)**, as displayed by the input.

To sum up, endogenously expressed TTP can be immunoprecipitated by its MYC tag using covalently coupled 9E10 mAb. Nonetheless, compared to the standard polyclonal TTP K2 antibody, there is only little amounts bound, yet this can be increased using greater amounts of beads. Therefore, high purity and yield precipitation demands further improvements of the protocol applied here before introduction to mass spectrometry.

4. Discussion

4.1. Role of intronic TTP

The function of TTP as a cytoplasmic RNA-binding protein promoting mRNA decay of prominent cytokine transcripts is well characterized[45]. However, although studies already have established a link between posttranslational modifications, e.g. serine phosphorylation and subcellular localization the nuclear function of TTP still remains puzzling[45,74,151].

Since several PAR-CLIP studies showing that TTP binds abundantly intronic RNA sequences in HEK cells[62], but also physiologically more relevantly macrophages[63,64], we attempted to artificially tether the Zn-finger protein to an ectopically overexpressed sRNA within the nucleus. This might allow studying other potential gene regulatory mechanisms in inflammation than the function of nuclear TTP as transcriptional co-repressor previously described[93–96]. The results obtained suggest that the design of a nuclear localized short RNA conceptually works. Through flanking tandem repeats of TTP binding sites for intron with four simple nuclear localization sequences of lncRNA BORG, the reporter TBS_NLS sRNA was preferentially localized within the nuclear fraction in HEK293 T-Rex TTP WT cells **(Fig. 7)**. Nonetheless, the change from a TTP free system and environment to one where it is natively expressed, favored to the contrary cytoplasmic localization of the TBS_NLS sRNA within RAW 264.7 cells **(Fig. 7 and 8)**. This indicates that TTP binding causes the accumulation of the otherwise nuclear reporter RNA within the cytoplasm, either due to active transition or simply maintaining the sRNA within the cytoplasm upon binding. Thus, the designed RNA does not allow to asses if TTP binding to introns retrains target RNAs in the nucleus ultimately preventing their translation as provided by the ´sponge hypothesis´. However, based on the data obtained it cannot be excluded the ratio of TBS_NLS subcellular distribution simply differs based on the cell lines used.

To improve the strategy applied the usage of a different RNA design might facilitate nuclear retention. As the mechanism of nuclear retention for lncRNA BORG is unknown it would be feasible to separate the interconnected NLS, resembling those intrinsically occurring in the native transcript[141]. On the other hand a switch to *malat1*, for which structural analysis already determined the mechanisms for its stability and of binding to nuclear speckles, could foster nuclear maintenance[166,167]. Alternatively, the problem could be tackled by trying to prevent intronic TTP binding. This could be achieved via mechanical hindrance, such as by

the expression of a transcript with complimentary binding motif and subsequent formation of a double-strand RNA, or by target mutation of a binding site of individual genes.

Importantly, comprehensive analysis of the best intronic TTP target, i.e. *Irg1* and RNA sequencing data suggest that there is no participation of TTP in pre-mRNA processing[64]. Contrary, overexpressed tristetraprolin was found to interact with numerous heterogeneous nuclear ribonucleoproteins (hnRNPs)[152]. These proteins are to a large extent found in the nucleus and among other process are also involved in alternative splicing and splicing alone, as reviewed in ref. [168,169]. Furthermore, hnRNP F also participates in TTP mediated mRNA decay as direct interacting co-factor in macrophages[170]. Therefore, the possibility of the involvement intronic bound TTP in processing of pre-mRNA or mRNA degradation should not be precluded prematurely, although most likely to be fairly exceptional.

Taken together the results did not provide a conclusion concerning the TTP´s role in the nucleus bound to introns. Nonetheless, facts as the rather discriminatory 3´UTR or intron binding and that the main fraction of TTP targets bound at introns is stable in as previously shown for macrophages in the lab[64], underlines the importance to further examine the role of nuclear TTP in inflammation.

4.2. Tripartite interplay of TTP, HuR and miRNA/ RISC machinery for mRNA decay

In immunity RNA metabolism can be regulated by the joint function of different RNA-binding proteins acting on shared transcripts with common recognition sequences and structures. In T cell differentiation for instance mRNA stability of *Stat3* is regulated by competitive binding between the RNA-stabilizing Arid5a and RNA-destabilizing Regnase-1 for a mutual stem loop structure in the 3´UTR[40]. Differently, binding and function of Regnase-1 and Roquin to a common stem loop structure of shared targets can also be restricted to the cellular compartment[39].

Similarly, we aimed here to obtain insight if there is cooperation of TTP with the miRNA/RISC machinery and/or HuR regulating inflammation post-transcriptionally. Co-IP did not reveal interaction with Ago2, a component of the RISC machinery in immune stimulated BMDMs **(Fig. 9)**. Furthermore, not only the incomplete *Dicer1*$^{-/-}$, but also the deviating shift in

expression of immediate early and early cytokine for *Tnf* and *Cxcl2*[171] **(Fig. 10)**, hampered analysis concerning miRNAs putative role as agonist and/or antagonist for TTP and HuR, respectively. However, several reports indicate interplay between TTP, HuR and miRNAs during the inflammatory response. Most significantly here, Ago-CLIP in macrophages revealed a primarily antagonistic role of HuR by direct competition with miRNA binding next to their seed sites[135]. Moreover, *Tnf* mRNA stability and further expression were shown to be regulated on the one hand by the cooperative action of TTP with miR-16 inducing decay, but also by HuR preventing miRNA mediated RNA silencing[139,140]. Despite the direct effect on cytokine expression, the miRNA/RISC machinery also modulates TTP and HuR expression in macrophages[135], and thus provide means for a general impact on an immune response. Taken together, this still allows a hypothetic co-regulation of miRNAs with TTP and HuR in mRNA decay in inflammation. Hence, complete *Dicer1*$^{-/-}$ and the respective double knockouts would be required for further investigation. To that end two sgRNAs were designed, one targeting exon 3 and the other exon 4, together with primers allowing the detection of a putative Cas9 induced mutation by the so- called ´surveyor assay´[172] **(Suppl. Materials and Methods)**. Therefore, genome-editing of the already characterized RAW WT, HuR$^{-/-}$, TTP$^{-/-}$ and DKO cells provide a perfectly suited instrument for following studies on TTP-miRNA-HuR interplay.

In contrast, Co-IP in BMDMs revealed a RNA-dependent interaction of TTP and HuR **(Fig. 9)**. This was shown the first time in primary immune cells under physiological relevant conditions. Together with the simultaneous binding to mRNAs of potent pro-inflammatory mediators, such as *Tnf*, *Cxcl2* and *Ccl3* that strongly suggest that inflammation can be regulated by the combinatorial effect of TTP and HuR on the posttranscriptional level **(Fig. 12)**. Also this indicates that other mechanisms than competition for binding determines mRNA decay by TTP or stability by HuR. Unfortunately, characterization of the CRISPR/Cas9 generated RAW 264.7 knockout cells did only provide little gain of information concerning TTP and HuR function in mRNA stability and their co-regulation. First, contradictory to what is described in literature that is HuR promoting TTP expression and TTP limits its own expression in macrophages[73,135,173], protein levels for none of the two factors changed upon LPS induction **(Fig. 13)**. Second, although TTP$^{-/-}$ elevated transcript levels of pro-inflammatory cytokines, e.g. TNF, CXCL2 and CCL3 little, yet divergent effects were observed for HuR **(Fig. 14; Suppl. Table 3-6)**. Thus, with regard to co-regulation on post-

transcriptional level, *Tnf* mRNA provides the prime hint that TTP can destabilize and HuR stabilize a commonly bound transcripts on basis of the decay data. Although overall this indicates that there is co-regulation between the RNA-binding proteins, it seems rather exceptional on the stage of mRNA decay, as already proposed elswhere[64]. Therefore, a rational explanation would be that co-regulation of TTP and HuR is mediated by binding to transcripts, but mainly happens at translational level, similar to what has been described by Tiedje *et al*.[86] Additional studies implicate the importance of both trans-acting factors in translation. For instance, TTP does not only destabilize the RNA of *Tnf*, but also reduces its translation upon association with the eukaryotic initiation factor 4E2 (eIF4E2)[77]. Similarly, HuR can act as translational silencer of TNF in macrophages in cooperation with TIA-1[115]. Taken together, this favors a model in which the interplay of TTP and HuR allows to fine-tune the inflammatory response by affecting both transcript and protein abundance.

Hereof, future studies focusing on the tripartite interplay of TTP-HuR-miRNA/RISC machinery should also take the translatome into account in order to properly address a functional output. Furthermore, and also taking the subtle changes observed in RAW $HuR^{-/-}$ macrophages into account, assessment of a greater number of knockout clones would witness the cytokine profile generated and rule out possible off-target effects brought about by the CRISPR/Cas9 technology.

4.3. Immunoprecipitation

Investigation on intron-bound TTP and its interplay with other trans-acting factors performed this study underlines the importance to further expand the knowledge in TTP biology. Furthermore, additionally to its function as trans-acting factor which primes mRNAs of prominent inflammatory mediators for decay, TTP was also reported to instruct immunity on the level on transcription and translation, the latter of which tightly regulated by p38 MAPK[45,77,81–83,88,93,94,96,160]. Moreover, phosphomimetic studies on in RAW 264.7 ectopically expressed TTP conclusively link serine 52 and 178 phosphorylation to its function and stability[88]. Nonetheless, the for mass spectrometry used tagged TTP described in the study was 2-3 fold more abundantly expressed as endogenous one, yet identified tagged TTP to be heavily phosphorylated on several other amino acid residues[88]. As such this strongly suggests that the posttranslational modifications of TTP represent a means instructing subcellular localization and regulation of cytokine expression on different levels yielding a fine-tuned inflammatory response.

Nonetheless, expression of TTP upon transient transfection, even though in RAW 264.7 cells, does completely provide natural conditions[88]. Hence, we aimed to isolate endogenously expressed TTP for mass spectrometry analysis. Here we could isolate 2 pure single cell derived colonies of N-terminally MYC tagged TTP, previously generated for this purpose by CRISPR/Cas9 genome editing[144]. The idea was that MYC tagging should allow efficient immunopurification of its TTP, reducing background noise while enrichment of bait[165]. Both clones, i.e. B8-5 and B8-7, were identified as heterozygous Myc knock-in at *Zfp36* and also displayed MYC-TTP expression on protein level as determined by Western blot, immunoprecipitation and immunofluorescence **(Fig. 17-20)**. Moreover, immunofluorescence together with genotyping PCR suggests that B8-2 and B8-3 are also KI cells, but MYC-TTP expression could not be detected by Western blot **(Fig.17 and 18)**. Importantly, the very exact problem has already occurred when using another monoclonal antibody than 9B11 for MYC detection, namely the 9E10 mAb[174]. Thereof, the clones B8-2 and B8-3 may should be re-assessed for a putative knock-in.

Unfortunately, immunoprecipitation of TTP via its MYC tag only yielded very subtle amounts of the protein available and was only successful when applying covalently crossed 9E10 mAb **(Fig. 20).** Also altering the IP conditions or changing the antibody used for MYC mediated

TTP pulldown did not show improvements over the standard protocol. In contrast increasing the amounts of 9E10 covalently coupled beads applied to the cell lysate, enhanced the yield. Thus, it is feasible that changing the equilibrium of TTP available, i.e. higher cell number, and beads may improve the strategy applied. On the other hand, generation of a homozygous *Zfp36*$^{Myc/Myc}$ would also double the amount of endogenously expressed MYC-TTP. Despite that, MYC tagging is a rather scarce strategy for immunoprecipitation and substitution to a more commonly used one, such as poly-histidine tags, may facilitate immunoprecipitation[175].

Taken together, the MYC-IPs performed allow TTP purification, yet demand further optimization prior mass spectrometry analysis for identification of posttranslational modification or interacting proteins. Importantly, a prerequisite before linking posttranslational modifications to certain TTP mechanisms/interactions requires elucidating if the MYC tag may interfere with known TTP function[175]. Notably, the amino terminal GST tag of TTP did not impair TTP mRNA degrading function[88]. Due to the difficulties observed peptide mediated elution of K2 immunoprecipitated TTP done in BMDMs provides a rational alternative **(Fig. 11).** Nonetheless, heterozygous knock-in cells with MYC-TTP expression display a useful cell line to study the mechanisms of TTP in inflammation.

5. Materials and Methods

5.1. Mouse models

Mice used for experiments had a C57BL/6 background. To obtain conditional TTP deletion in myeloid cells (ΔM) mice with floxed Zfp36 alleles[55] were crossed with LysMCre mice[176], generated by Kratochvill *et al*.[55]. In addition, frozen bone marrow from mice with myeloid specific knockout for Dicer1 (ΔM^{D}), generated by crossing mice with $Dicer1^{fl/fl}$ alleles[177] to LysMCre[176], was kindly provided by Kontoyiannis D. L. For reasons of simplicity mice with the loxP-flanked gene were referred to as wild type (WT). Mice were held under pathogen-free conditions and littermates were used as controls.

5.2. Bone marrow isolation

Mice were killed by cervical dislocation and afterwards were sterilized with 70% EtOH. Tibia and femur, still joint by the knee, were isolated from the sacrificed mouse and put immediately into ice-cold 1X PBS. In cell culture the two bones were separated and cut open by scissors. Then bone marrow was isolated by flushing each bone with ~10ml pre-warmed Dulbecco´s Modified Eagle Medium (DMEM) from both sides using a G28 needle. Subsequently, cells were pelleted by 5min centrifugation at 300 rcf at room temperature. Afterwards, the supernatant was aspirated and the cell pellet was immediately used for *in vitro* differentiation generating bone marrow derived macrophages (BMDMs).

5.3. Cell culture

5.3.1. Differentiation into BMDMs

Either freshly harvested bone marrow (as described above) or frozen bone marrow was used for generation of BMDMs. 1ml of frozen bone marrow was quickly thawed by adding 9ml of pre-warmed DMEM and subsequently pelleted at 300 rcf for 5min at room temperature. Supernatant was removed and then used the same way as freshly isolated bone marrow. The cell pellet was re-suspended in 20 ml L-conditioned medium and the suspension was distributed equally to 4 uncoated 10cm square dishes in a total final volume of 15ml L-conditioned medium per dish. On day 3 post bone marrow isolation each dish was added 5ml of fresh L-conditioned medium. On day 5 cells were split depending on their confluency and earliest 2 more days later the ready BMDMs were seeded for experiments.

5.3.2. Cell lines

Besides the primary macrophages described above different genotypes of RAW 264.7 cells and HEK293 T-Rex TTP wild type (WT) cells were used in experiments. HEK293 T-Rex TTP WT cells and RAW 264.7 cells with heterozygous Myc tagged TTP (*Zfp36*$^{WT/Myc}$) were generated by Wandruszka L. as described in reference[144]. RAW 264.7 cells with WT (T20+/+), HuR$^{-/-}$ (T20.11), TTP$^{-/-}$ (T9-/-) and DKO (T9.10) genotype were made and characterized together with Ebner F. and Sedlyarov V. CRISPR/Cas9 genome editing was conducted in collaboration with the CSF Facility.

5.3.3. Growth conditions

All cells were incubated at 37°C, 95% humidity and 5% CO_2 and regularly checked for any contamination. If not stated differently cells were grown in following media. BMDMs were grown in L-conditioned medium composed of Dulbecco´s Modified Eagle Medium (DMEM) supplemented with 10% Fetal Calf Serum (FCS), 20% L929-cell derived CSF-1 and 100 U/ml penicillin and 100µg/ml streptomycin. RAW 264.7 cells, independent of the genotype, were grown in DMEM with 10% FCS, 100 U/ml penicillin and 100µg/ml streptomycin. HEK293 T-Rex TTP WT cells were kept in DMEM augmented with 10% FCS, 100 U/ml penicillin, 100µg/ml streptomycin, 200µg/ml hygromycin and 15µg/ml blasticidin. When indicated cells were exposed to LPS (10ng/ml) prior experimental usage for the indicated time.

5.3.4. Splitting cells

For splitting BMDMs first growth medium was aspirated except for ~5ml in which cells were subsequently scraped. The obtained cell suspension was either directly used or in case of low cell number and/or high cell death centrifuged for 5min at 300 rcf at room temperate prior resuspension in 5ml L-conditioned medium. For experimental usage the desired amount of cells was transferred to a cell-culture treated dish, for passaging the remained on uncoated 10cm square dishes. HEK293 cells were washed with 1X PBS after removal of the medium and then incubated for approximately 3 minutes with 1X Trypsin-EDTA (GIBCO) at 37°C. Subsequently, trypsinization was stopped by adding at least the 10-fold amount of medium. The desired number of cells was then transferred to a new cell-culture treated dish. RAW 264.7 cells were either directly scraped in the dish grown (in case of max. 80% confluency and high viability) or otherwise washed with 1X PBS prior scraping in 5ml growth

medium. The required cell number was subsequently transferred to a new cell-culture treated dish.

5.3.5. Freezing cells

After trypsinization was stopped (HEK293 T-Rex cells) or after placing cells into suspension (RAW 264.7 cells) they were centrifuged for 5 min at 300 rcf. The cell pellet was re-suspended in 1ml FCS with 10% DMSO and cells were immediately stored at -80°C. For long-term storage already frozen cells were stored in LN_2.

5.3.6. Thawing of frozen cells

1ml of frozen cells was quickly thawed and transferred to 9ml pre-warmed culture medium. The cells were centrifuged at 300 rcf for 5min. Afterwards the cell-pellet was re-suspended in 4ml or 10ml medium and then transferred to a 6cm or 10cm culture dish, respectively.

5.3.7. Single cell colonies and hygromycin selection

Colonies generated from single clones were established by seeding manually 0.5 (calculated as 1 cell every second well) RAW B8 cells (enriched culture for MYC tagged TTP) into a 96-well plate. Cells were expanded using normal culture conditions. RAW single cell derived colony B8-5 and B8-7 were selected for hygromycin (400µg/ml) for 6 days as described in results.

5.4. Plasmids

For nuclear retention experiments the plasmids pEGFP_N1 and pTBS_NLS were used **(Fig. Ia and b).** The full pEGFP_N1 sequence can be found on the Addgene Vector Database (https://www.addgene.org/vector-database/2491/). pTBS_NLS was generated by substitution of EGFP by TBS_NLS sequence for transcription of the short reporter RNA. To that end restriction digestion was done ass followed:

pEGFP_N1 digestion

pEGFP_N1	2µg
10X FastDigest Buffer (Thermo Scientific, cat. no. B64)	5µl
FastDigest NheI (Thermo Scientific, cat. no. FD0973)	2µ
FastDigest NotI (Thermo Scientific, cat. no. FD0593)	2µl
nuclease free water	to 50µl
total volume	to 50µl

For restriction digestion, to cut out EGFP, the mixture was incubated for 1h at 37°C. The cut plasmid, with sticky end overhangs, was separated on a 0.8% agarose gel. Subsequently

the plasmid was cut out from the gel and purified using the QUIAquick Gel Extraction Kit (Quiagen, cat. no.28704) according to the manufacturer's protocol. To generate the TBS_NLS insert with the right overhang **(Fig. 6c)** oligos TBS_NLS4 FW and TBS_NLS RV were ordered form Eurofin Genomics and annealed to each other as indicated below:

Oligo dimerization

10X annealing buffer	10µl
TBS_NLS4 FW (100µM)	45µl
TBS_NLS4 RV (100µM)	45µl
total volume	100µl

Dimerization program

step	cycles	temperature	time
1	1	95°C	40 sec.
2	70	95°C (-1°C/cycle)	20 sec.
3	1	4°C	∞

Ligation of the annealed TBS_NLS4 oligos to the EGFP removed pEGFP_N1 was carried out by T4 DNA Ligase for 2h at room temperature in following mixture:

Ligation

pEGFP_N1 (cut by NheI and NotI)	100ng
Annealed TBS_NLS4 oligos (1:10)	1µl
10X T4 DNA Ligase Buffer (Thermo Scientific, cat. no. B69)	2µl
50% PEG400 solution	2µl
T4 DNA Ligase (5U/µl; Thermo Scientific, cat. no. EL0011)	2µl
nuclease free water	to 20µl
total volume	20µl

This should generate the plasmid pTBS_NLS. Additionally 2 ligation controls were prepared without dimerized TBS_NLS4 oligos and one without T4 DNA ligase, respectively. This allows the assessment if the plasmid is capable to ligate back or may was not cut properly upon antibiotic selection in transformed *E. coli.*

For pTBS_NLS amplification competent DH5α *E. coli* were then transformed using the heat shock method. In short, competent DH5α cells were thawed on ice, and 50µl of bacteria were mixed with 5µl of the ligation products or controls each, and put on ice for 30 minutes. Then the bacteria were heat-shocked for 45 seconds at 42°C and put back on ice for 5 minutes. The transformed DH5α cells were subsequently plated on LB-agar dishes supplemented with 50µg/ml kanamycin and incubated on 37°C for overnight. Of note, the controls mentioned above did not display colonies. Single colonies selected for the antibiotic were then inoculated into 5ml or 250ml liquid LB-medium containing 50µg/ml kanamycin

and grown overnight. The thereby amplified plasmid was then purified using the QIAprep Spin Miniprep Kit (Quiagen, cat. no. 207104) using the spin-procedure according to the manufactures' protocol. After purification the correctness of the TBS_NLS insert was further confirmed by sequencing using the CMV FW primer.

TBS_NLS4 FW	5'-CTAGCGCCATCTCTGTTAGCCCAGACTTTATTTATTTATTTATTTA TTTATTTATTTATTTATTTATTTATTAGCTAGATAGCCCTGAGCCCCAG CCCTGC-3'
TBS_NLS4 RV	5'-GGCCGCAGGGCTGGGGCTCAGGGCTATCTAGCTAATAAATAAATAA ATAAATAAATAAATAAATAAATAAATAAATAAAGTCTGGGCTAACAGAG ATGGCG-3'
CMV FW primer	5´-CGCAAATGGGCGGTAGGCGTG-3´

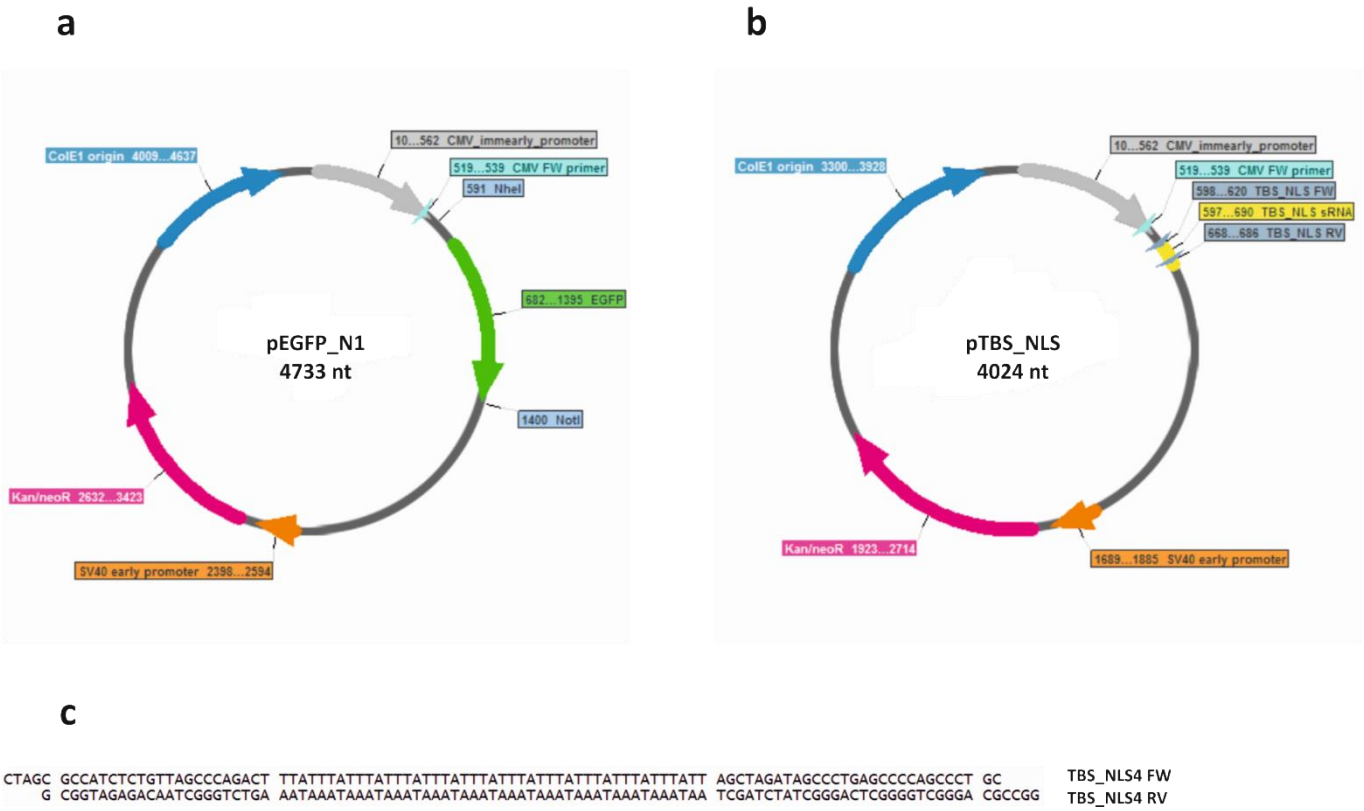

Figure I| Schematic of pEGFP_N1 and pTBS_NLS plasmid with dimerized TBS_NLS4 oligos. (a, b) Schematic picture of pEGFP_N1 and pTBS_NLS with a size of 4733 nt and 4024 nt, respectively. The most important features are color coded and their orientation is given. Numbers indicate the first and last nucleotide of the indicated feature. SV40 early promoter (orange), kanamycin resistance (pink), ColE1 origin of replication (blue), CMV immediate-early promoter (light grey), EGFP (green), CMV FW primer binding site (turquois), TBS_NLS sequence (yellow), NheI and NotI restriction sites (light blue) and TBS_NLS FW and TBS_NLS RV primer binding sites (dark grey). TBS_NLS FW and TBS_NLS RV primer allow specific detection of the short reporter RNA expression and are given in the qPCR primer list. **(c)** Schematic of dimerized TBS_NLS4 oligos (FW and RV) with stick ends required for ligation upon NheI and NotI cleavage.

5.5. Transfection

Transfection with pEGFP_N1 or pTBS_NLS of RAW 264.7 and HEK293 T-Rex TTP WT cells was done using FuGENE® HD Transfection Reagent (Promega, cat. no. E2311) in accordance to the manufacturer's protocol adjusted to 10cm dishes (http://www.promega.com/techserv/tools/FugeneHdTool/). In short, cells were seeded 1 day prior transfection in 17ml antibiotic free DMEM supplemented with 10% FCS. At the timepoint of transfection cells had a confluency of approx. 60-70%. For transfection 870µl of 0.02µg/µl plasmid solution was prepared in OptiMEM and subsequently mixed with 56µl (in case of HEK293 cell) or 65µl FuGENE HD reagent (in case of RAW cells). Of note, OptiMEM and FuGENE HD reagent must be at room temperature prior usage and the final transfection solution was quickly pipetted up and down for at least 15 times. The solution was incubated for 10min at room temperature and 850µl were directly added dropwise to the 17ml growth medium. RNA isolation was performed the next day.

5.6. Cytoplasmic and Nuclear fractionation

The protocol for separation of cytoplasmic and nuclear fractions is a modified version from Sadzak *et al* reported before[178]. Cells (approx. 90% confluency at 10cm dish) brought to suspension were centrifuged at 300 rcf for 5min at 4°C. For washing the supernatant was discarded and the cell pellet was re-suspended in 1X PBS. Cells were again spun at 300 rcf for 5min at 4°C. After aspiration of the supernatant cells were lysed in 200µl Cytoplasmic Extraction Buffer for 5min on ice. Again the solution was centrifuged for 5min at 4°C, 300 rcf. 150µl of the cytoplasmic fraction was collected and immediately filled up to 1.15ml with Isol RNA-Lysis Reagent (5 Prime, cat. no. 2302700). The rest of the cytoplasmic extract was discarded and the pellet was washed by re-suspending cells in 200µl Fractionation Wash Buffer. After final round of centrifugation at 300 rcf for 5min at 4°C, supernatant was aspirated and harvested nuclei were lysed in 1ml Isol RNA-Lysis Reagent (5 Prime, cat. no. 2302700). Nuclear and cytoplasmic RNA extracts were kept for 5-10min on ice frozen at -80°C and then processed as usual (see 5.7.1. RNA Isolation).

5.7. Gene expression analysis by qRT-PCR

Quantification of gene expression was done by qRT-PCR, which included RNA isoloation, DNA digestion, reverse transcription and final qPCR of the generated cDNA. Unless otherwise indicated $2*10^6$ BMDMs or $1.5*10^6$ RAW 264.7 cells were seeded on a 6cm dishes the day before RNA isolation.

5.7.1. RNA isolation

Prior to cell lysis with Isol RNA-Lysis Reagent (5 Prime, cat. no. 2302700) cells were washed with ice-cold 1X PBS. Usually cells grown in 6cm round dishes were lysed in 800µl and cells grown in 10cm dishes in 1ml Isol RNA-Lysis Reagent. The RNA lysate was then stored at -80°C for at least 1 day. For further processing the thawed sample was mixed in a 1:5 ratio with $CHCl_3$ (i.e. 800µl lysate with 160µl $CHCl_3$) in phase lock tubes (Phase Lock Gel Heavy 1.5 ml, cat. no. 2302810, 5 Prime)[2]. Samples were centrifuged 5-10min at 16.1 krcf at 4°C and the RNA containing aqueous phase was taken off and mixed in a 1:1 ratio with $CHCl_3$ in a new phase lock tube. After centrifugation for 5-10min at 16.1 krcf at 4°C the aqueous phase was incubated in a 1:1 ratio with 2-Propanol. For precipitation first the mixture was mixed by inverting the tube and then incubated for 10min at room temperature. In case of low cell number 1µl of GlycoBlue (Invitrogen, cat. no. AM9516) was added for better visualization of the hereinafter generated RNA pellet. Centrifugation of the RNA was done at 16.1 krcf at 4°C for at least 30min. Once the pellet became visible supernatant was decanted and the RNA pellet was as many as 3 times washed. Washing was done in 900µl ice-cold 70-75% EtOH by inversion of the tube and centrifugation for at least 3min at 16.1 krcf at 4°C and final removal of EtOH. For complete EtOH removal RNA-pellets were shortly air dried and then dissolved in 20-30µl ddH_2O, depending on the pellet size. RNA was then either directly subjected to DNA digestion or stored at -80°C.

5.7.2. DNA digestion

To remove residual DNA which might be amplified in qPCR, RNA samples were DNA digested with Recombinant DNase I (Roche, cat. no. 04716728001) for 20min at 37°C as indicated below. Nuclear and cytoplasmic RNA fractions, i.e. those transfected with pEGFP_N1 or

[2] Prior usage phase lock tubes were centrifuged at 16.1 krcf at 4°C for at least 1min. Samples were mixed by shacking tubes manually and were further processed once phase separation has started.

pTBS_NLS, were additionally digested with Fast Digest 2µl SspI (Thermo Scientific, cat. no. 7D0774) cutting both plasmids twice.

DNase I digestion

RNA	10µg
DNase I (10U/µl)	1µl
10X Incubation Buffer	5µl
RNasin Ribonuclease Inhibitor (Promega, cat. no. N2511)	1µl
nuclease free water	to 50µl
total volume	50µl

After DNA digestion the sample was added up to 200µl with nuclease free water and mixed with ice-cold mixed 1:1 with Acidid-Phenol:Chloroform, pH 4.5 (Ambion, cat. no. AM9720) in a phase lock tube. The sample was centrifuged at 16.1 krcf for 5min at 4°C. Subsequently, 200µl of $CHCl_3$ were added into the same phase lock tube and the organic phase was completely separated from the aqueous be spinning the tube at 16.1 krcf for 5min at 4°C. For overnight precipitation the aqueous phase was transferred into a new tube and mixed with 1/10 3M sodium acetate, pH 5.2 (Sigma, cat. no. S7899), 3 volumes of 96% EtOH and 1µl GlcoBlue and ultimately incubated overnight at -20°C. The next day RNA was recovered by spinning the mixture for no less than 30min at 16.1 krcf at 4°C. Once the pellet became visible supernatant was decanted and the RNA pellet was as many as 3 times washed. Washing was done in 900µl ice-cold 70-75% EtOH by inversion of the tube and centrifugation for at least 3min at 16.1 krcf at 4°C and final removal of EtOH. For complete EtOH removal RNA pellets were shortly dried at air and then eluted in 20-30µl ddH_2O, depending on the pellet size. RNA was then either directly subjected to reverse transcription or stored at -80°C.

5.7.3. Reverse transcription

cDNA generation from DNA digested RNA was carried out by using RevertAid Reverse Transcriptase (Thermo Scientific, cat. no. EP0441). For reverse transcription of nuclear and cytoplasmic RNA fractions random octamer primer were used. For other reverse transcription reactions carried out by RevertAid Reverse Transcriptase oligo$(dT)_{18}$ primer have been applied as indicated below. First, RNA was mixed with primers in total volume of 11µl and incubated at 70°C for 5min. Second, 9µl of the Master Mix were added to each sample. The solution was then incubated for 5min at 37°C followed by 1h incubation at 42°C for reverse transcription. The reaction was stopped by heat-inactivation of the reverse transcriptase at 70°C for 10min. The prepared cDNA was diluted 1:10 and either directly

used for qPCR or stored at -20°C. Double unbroken lines are indicative for first and second step of reverse transcription.

Reverse Transcription

RNA (DNA digested)	300-600ng
random octamers/ oligo $(dT)_{18}$ (100µM)	1µl
nuclease free water	to 11µl
total volume	11µl
Master Mix	9µl
total volume	20µl

Master Mix (1X)

5X Reaction Buffer	4µl
dNTPs (10mM, Thermo Scientific)	2µl
nuclease free water	2µl
RevertAid Reverse Transcriptase (200U/µl)	1µl
total volume	9

RNA of Sequential RNA-IP samples was reverse transcribed using SuperScript IV Reverse Transcriptase (Invitrogen, cat. no. 18090010) according to the manufacture's protocol with following additions/alternations. 4µl of recovered RNA were used to anneal primers, i.e. 1µl of a 1:1 mixture of random octamers/ oligo $(dT)_{18}$ (50µM each). Instead of RNaseOUT Recombinant RNase Inhibitor (Invitrogen, cat. no. 10777019), RNasin Ribonuclease Inhibitor (Promega, cat. no. N2511) was used. Reverse transcription was carried out at 55°C for 10min. After cDNA generation residual RNA was removed by digestion with 1µl *E.coli* RNase H (Invitrogen, cat. no. 18021014) for 20min at 37°C. RNA-free cDNA was eluted in total 100µl nuclease free water.

5.7.4. qPCR

Final quantification of RNA expression was done with qPCR using 5x HOT FirePol EvaGreen qPCR Supermix (Medibena, cat. no. 08-36-00001).

qPCR Master Mix (1X)

5x HOT FirePol EvaGreen qPCR Supermix	4µl
Primer FW (100µM)	0.075µl
Primer RV (100µM)	0.075µl
nuclease free water	10.85µl
total volume	15µl

15µl of the prepared qPCR Master Mix were mixed with 5µl of 1:10 diluted cDNA samples in twin-tec PCR plates (Eppendorf). For each data point examined as many as 2 technical replicates were made and in case of the reference gene 3 technical replicates.

All qPCR reactions were carried out as indicted below and fluorescence measurements were done at the end of each elongation step and during melting curve analysis.

	40 cycles				
initial denaturation	denaturation	annealing	elongation	melting curve	hold
95°C	95°C	60°C	72°C	58 - 95°C	20°C
15 sec.	15 sec.	20 sec.	20 sec.	20min	∞

Serial 1:10 dilutions until $1:10^3$ of a combination of all different cDNAs form data points assessed within one experiment were taken as standards. Normalization is done by using *Hprt* as reference gene, depicted as arbitrary units (AU). RNA levels of cytoplasmic and nuclear fractions, as well as samples from sequential RNA-IP were calculated by 2^{25-Ct} .

5.7.5. mRNA decay

Decay rate and half-life ($T_{1/2}$) of analyzed mRNA was determined by treatment with the transcriptional inhibitor actinomycin D (5µg/ml; Sigma, cat. no. A1410) for 0/30/60/90 minutes post 3h or 6h LPS stimulation. The 0min actinomycin D time point was determined exactly at 3/6h LPS stimulation and defines the point of 100% mRNA present. Assuming a stochastic decay model (see ref. [179]) the decay rate (k) can be determined by remaining mRNA at 30/60/90 minutes actinomycin D treatment, which allows to calculate the half-life of the investigated mRNA as $T_{1/2} = \ln(0.5)/k$. mRNA level determination and normalization was done by qRT-PCR as described above.

5.8. Sequential native RNA immunoprecipitation

For each approach $40*10^6$ BMDM seeded the day before on 2 separate dishes were stimulated for 6h with LPS and then lysed in ice- cold 400µl 1X Frackelton Buffer (FB)[3] after washing cells with ice-cold 1X PBS. The lysates of one approach were pooled and immediately incubated with 10µl RNasin Ribonuclease Inhibitor (Promega, cat. no. N2511) to prevent RNA digestion. Subsequently, samples were centrifuged at 16.1 krcf for 15min at 4°C. The supernatant was transferred to a new tube and mixed with 50µl (original volume) of

[3] In all IP experiments Frackelton Buffer was solely supplemented with Protease Inhibitor (cOmplete, EDTA-free Protease Inhibitor cocktail; Roche, cat. no. cat. no. 11873580001) to a final 1X concentration immediately prior usage.

Protein A/G Magnetic Beads (Thermo Scientific, cat. no. 88802) coupled in advance to K2 polyclonal antibody. Prior immobilization of the antibody to Protein A/G magnetic beads they were washed 3 times in ice-cold 900µl 1X FB. Washing steps were carried out by flipping the tube in 1X FB solution, short spinning and removal of supernatant after putting the tubes back onto magnetic rack. For K2-coupling, beads were mixed in a 1:1 ratio of original bead volume with K2 serum, together with 5µl yeast tRNA (10mg/ml; Ambion, cat. no. AM7119) and left rotating for 30min at room temperature. Then beads were then recovered in the original volume using 1X FB after 3 times washing with 1X FB. TTP-IP was done by overnight rotation at 4°C. The next day IP samples were washed 3 times with 1X FB to remove proteins not bound. Then samples were subjected to 100µl TTP elution mixture III for 30min at 37°C while shaking to elute RNA in complex with TTP. For second immunoprecipitation eluate was incubated with 25µl HuR- and Tubulin-coupled Protein A/G magnetic beads (original bead volume) prepared in advance. Bead preparation was conducted as before for K2-immobilization with the exception that original bead volume (here 25µl) was incubated with 0.5µl of HuR antibody ((Invitrogen, cat. no. 39-0600, clone 3A2) or 0.5µl Tubulin antibody (Sigma, cat. no. T9026, clone DM1A). The second IP was carried out for 20h at 4°C while rotating. Then beads were washed 3 times with ice-cold 1X FB and subsequently immunoprecipitate was eluted by addition of 50µl 1X SDS sample buffer w/o dye by incubation at 70°C for 15 minutes while shaking. Ultimately, the eluate was filled up to total 200µl with nuclease free water and RNA recovery was performed by standard phenol-chloroform and EtOH precipitation described in 5.7.1. RNA Isolation and 5.7.2. DNA-digestion, respectively.

5.9. Protein analysis

Protein analysis by Western blot included protein isolation, protein separation and final detection by Western blot. Unless otherwise indicated $2*10^6$ BMDMs or $1.5*10^6$ RAW 264.7 cells were seeded on a 6cm dishes the day before Protein isolation.

5.9.1. Protein isolation

Upon LPS stimulation (10ng/µl) for the indicated amount of time, culture dishes were put on ice and medium was discarded. After washing cells with ice-cold 1X PBS, cells were lysed in 100-120µl (depending on cell number) 1X Frackelton Buffer supplemented with 100µM Na_3VO_4, 1mM DTT and Protease Inhibitor (cOmplete, EDTA-free Protease Inhibitor cocktail;

Roche, cat. no. cat. no. 11873580001) to a final 1X concentration immediately prior usage. Cells were scraped on ice and the lysates were transferred to pre-chilled tubes. Then the lysates were centrifuged at 16.1 krcf at 4°C for 7-10min. The supernatant was collected, mixed with 5X SDS loading dye to a final 1X concentration and then were heated for 7-10min at 95°C. Finally, the lysates were either stored at -20°C or immediately used for Western blot.

5.9.2. SDS PAGE

Protein separation was usually done on by the standard SDS PAGE protocol using a 10% resolving gel and a 5% stacking Gel. 15-20µl of protein sample was loaded. As marker 8µl PageRuler Prestained Protein Ladder (Thermo Scientific, cat. no. 26616) was used. Gel electrophoresis was done at 0.2kV, 40mA/Gel (constant) in 1X Running Buffer. Co-IP samples from BMDMs shown in **Fig. 9** were separated using a NuPAGE® Novex® 4-12% Bis-Tris Protein Gel, 1.5 mm (Invitrogen, cat. no. NP0335BOX). Here, electrophoresis was done in 1X Novex® Tris-Glycine SDS Running Buffer (Novex, cat. no. LC2675) at 0.18kV, 75mA (constant). Once the bromphenol band reached the gel bottom/ dissolved in the running buffer used gel electrophoresis was stopped and protein transfer started.

5.9.3. Western blot

Protein transfer was done by Wet blot. To that end the gels with separated proteins were shortly washed with ddH_2O and then unit assembly was carried out in ice-cold 1X Wet Transfer Buffer. The unit was constituted of a nitrocellulose membrane (GE Healthcare, pore size: 0.1µm) at the top of the gel in direction of the anode, surrounded on both sides by 2 whatman paper and a sponge. Prior assembly, the membrane and whatman paper were soaked in 1X Wet transfer Buffer. For wet transfer the assembled unit was put into ice-cold 1X Wet Transfer Buffer within a Mini Trans-Blot® cell. Temperature was held constantly low by cooling 1X Transfer Buffer with an ice-block and exerting transfer in 4°C room. Wet transfer was run at 350mA (constant) for 90 minutes.

Washing, blocking and stripping of the membrane, as well as antibody incubation described below were done under constant agitation. After protein transfer the membrane was shortly rinsed with ddH_2O and successful transfer was confirmed with approx. 2-3ml Poncau S staining. Subsequently, the membrane was washed shortly with ddH_2O and 1X TBS-T. Blocking of the membrane was done 1h in 12-14% low fat milk powder (Fixmilch instant) in

1X TBST-T at room temperature. The membrane was washed at least 3 times in 1X TBS-T for 5-10 minutes and subsequently incubated with the primary antibody overnight at 4°C (antibody list, including their dilutions see below). In general, all primary antibodies used were diluted in 5% BSA in 1X TBS-T supplemented with 0.05% NaN_3. The following day the membrane was again washed at 3 times as and then incubated with the secondary antibody (LI-COR, IRDye secondary antibodies, antibody list) for 30 minutes. Prior protein detection on Odyssey CLx (LI-COR) the membrane was washed again 3 times with 1X TBS-T.

To re-probe the membrane it was shortly washed with ddH_2O, then rinsed with Stripping Buffer and incubated for additional 10min with Stripping Buffer. Subsequently, the membrane was washed 3 times with 1X TBS-T and either re-probed directly (same procedure as described above starting with membrane blocking), or stored in 1X TBS-T at 4°C.

Primary antibody	**Source**	**Dilution**	**Company, ID**
HuR/ELAVL1	mouse	$1:10^3$	Invitrogen, cat. no. 39-0600, clone 3A2
pan 14-3-3	rabbit	1:2000	CST, cat. no. 8312
Ago2	mouse	1:833	Sigma, cat. no. SAB4800048, clone 2A8
K2 (TTP)	rabbit	1:2500	Laboratory of Pavel Kovarik[55]
Tubulin	mouse	$1:2*10^4$	Sigma, cat. no. T9026, clone DM1A
9B11 (MYC)	mouse	1:000	CST, cat. no. 2276

Secondary antibody	**Source**	**Dilution**	**Company, ID**
α-Ig mouse 680 (red)	donkey	$1:10^3$	LI-COR, cat. no. 926-68073
α-Ig mouse 800 (green)	donkey	$1:10^3$	LI-COR, cat. no. 926-32212
α-Ig rabbit 680 (red)	donkey	$1:10^3$	LI-COR, cat. no. 925-68078
α-Ig rabbit 800 (green)	donkey	$1:10^3$	LI-COR, cat. no. 926-32213

5.9.4. Co-IP and TTP elution in BMDMs

As Co-IP (TTP pulldown; HuR, pan 14-3-3, Ago2 detection) and TTP elution (TTP pulldown; TTP elution) share a common experimental immunoprecipitation procedure they are described together and alternations are indicated by A (Co-IP) and B (TTP elution), respectively. For each approach $20*10^6$ BMDM seeded the day before were stimulated for

6h with LPS and then lysed in ice- cold 400µl 1X Fraceklton Buffer (FB)[4] after washing cells with ice-cold 1X PBS. 2µl RNasin Ribonuclease Inhibitor (Promega, cat. no. N2511) were immediately added to the lysates to prevent RNA digestion. A: Lysates for investigation of RNA dependent interaction were added with 5µl RNase I (100U/µl, Invitrogen, AM2294) instead of ribonuclease inhibitor and incubated 5 minutes at 37°C for RNA digestion. Subsequently, samples were centrifuged at 16.1 krcf for 15min at 4°C. The supernatant was transferred to a new tube and from each genotype 50µl of input were kept. Input samples were immediately added 5X SDS loading dye to reach a final 1X concentration and heated for 10min at 95°C. Subsequently input samples were stored at -20°C. TTP immunoprecipitation of the remaining lysate was done overnight at 4°C while rotating with 50µl (original bead volume) of K2-coupled Protein A/G magnetic beads. Bead preparation (K2 immobilization and washing) was done as described in 5.8. sequential native RNA-IP. Of note, the bead only control was prepared the same, only that instead of K2 serum 1X FB was used. The next day, IP samples were washed 3 times with 1X FB to remove proteins not bound.

A: Co-IP samples were eluted by boiling the beads at 85°C for 10min while shaking in 75µl 1X SDS loading dye. The eluate was separated from the beads on the magnetic rack and stored at -20°C. To detect TTP interaction with HuR, pan 14-3-3 and Ago2 10µl of input and 20µl of immunoprecipitated were loaded for Western blot detection (see Fig. 9).

B: For putative TTP elution 100µl of 4 different solutions were applied to the immunoprecipitated and incubated for 30min at 37°C while shaking. These were 0.1M glycine (pH 2.65), and TTP elution mixture I, II, III (with I comprising the lowest and III highest amount of C-terminal TTP peptide). The eluate was separated from the beads on the magnetic rack and mixed with 5X SDS loading dye to a final 1X conc. Samples were boiled at 85°C for 10min while shaking and then stored at -20°C. For Western blot detection 20µl of input and IP samples were loaded (see Fig. 11).

[4] In all IP experiments Frackelton Buffer was solely supplemented with Protease Inhibitor (cOmplete, EDTA-free Protease Inhibitor cocktail; Roche, cat. no. cat. no. 11873580001) to a final 1X concentration immediately prior usage.

5.10. Immunoprecipitation of MYC-TTP in RAW 264.7 *Zfp36*$^{WT/Myc}$

For each approach 10*10^6 RAW 264.7 cells seeded the day before were stimulated for 6h with LPS (10ng/ml) and then lysed in ice-cold 400µl 1X Fracekelton Buffer (FB)[5] after washing cells with ice-cold 1X PBS. Subsequently, samples were centrifuged at 16.1 krcf for 15min at 4°C. The supernatant was transferred to a new tube and from each genotype 45µl of input were kept. Input samples were immediately added 5X SDS loading dye to reach a final 1X concentration and heated for 10min at 95°C. Subsequently, input samples were stored at -20°C. MYC-TTP and TTP immunoprecipitation of the remaining lysate was done overnight at 4°C while rotating with 50µl (original bead volume) of coupled Protein A/G magnetic beads prepared in advance. Both MYC antibodies, 71D10 (CST, cat. no. 2278) and 9B11 (CST, cat. no. 2276) were coupled in a 1:100 ration to original bead volume, K2 in a 1:1 ratio and 9E10 antibodies were already provided covalently linked to magnetic beads as Pierce Anti-c-Myc Magnetic Beads (Thermo Scientific, cat. no. 88842). For washing and coupling the beads the same procedure was applied as described for sequential native RNA-IP with the exception that there was no yeast tRNA addition and that covalently linked 9E10 magnetic beads were washed 3 times with 1X FB prior usage. Alternating 1X FB buffer conditions during immunoprecipitation are described in Fig. 20 and were maintained until elution step. Elution on the next day, after 3 times washing the beads with 1X FB, was done at 85°C for 10 minutes in 60µl 1XSDS loading dye while shaking. The eluate was separated on the magnetic rack, transferred into a new tube and stored at -20°C. For MYC-TTP and TTP 20µl of input sample, as well as from eluted immunoprecipitate were loaded for Western blot detection (see Fig. 20).

5.11. Immunofluorescence for MYC detection

5*10^5 RAW 264.7 cells per approach were seed on an EtOH sterilized cover slips in 6 well plates one day prior experiment in medium without antibiotic. Before cells were fixed in 1.5% CH_2O for 5min at room temperature they were stimulated for 4h with LPS (20ng/ml). Subsequently, the cover slip was washed with 1X TBS-T 3 times and then incubated for 1minute with 1% Triton in 1X TBS-T. Afterwards blocking was done with 1% BSA in 1X TBS-T for half an hour. Fixed and permeabilized cells were then incubated overnight at 4°C with the

[5] In all IP experiments Frackelton Buffer was solely supplemented with Protease Inhibitor (cOmplete, EDTA-free Protease Inhibitor cocktail; Roche, cat. no. cat. no. 11873580001) to a final 1X concentration immediately prior usage.

primary antibody [9B11 (1:2000 dilution in 1% BSA supplemented with 0.05% NaN_3)]. The next day cover slips were washed 3 times with 1X TBS-T and then incubated with fluorophore containing secondary antibody [Alexa fluor 488 goat anti-mouse in a 1:2000 solution in 1% BSA in 1X TBS-T) for half an hour in the dark at room temperature. Unbound secondary antibody was removed by 3 times washing with 1X TBS-T and then the coverslip was inverted and put on a microscope slide using one drop of fluorescence mounting medium (Dako, cat. no. S302380). After 10min air drying MYC detection was assessed by fluorescence microscopy.

5.12. Genotyping PCRs for Myc knock-in detection

To detect a putative Myc-Zfp36 knock-in CRISPR/Cas9 genome edited RAW 264.7 cells genomic DNA was isolated from cells grown in 24 well plates with approximately 70% confluency. Therefore, cells were incubated with 100µl DirectPCR®-Cell (peqlab, cat. no. 31-302-C) supplemented with 0.4mg/ml proteinase K per well for 2.5h at 55°C. Subsequently, proteinase K was inactivated at 85°C for 45 minutes. Both, ´RAW_KI_only` and ´MYC_30bp plus` PCRs were conducted under the same conditions using Q5® High-Fidelity DNA Polymerase (NEB, cat. no. M0491S) as described below. Each clone was analyzed combining 3µl genomic DNA with 22µl Genotyping Master Mix (1X). Primer binding sites and the different amplicon sizes are given in Fig. 17a. For size analysis PCR products were separated on 1.5% (in case of RAW_KI_only) and 3% agarose gels (in case of MYC_30bp plus), prepared using 1X TAE.

Genotyping Master Mix (1X)

5X Q5 Reaction Buffer	5µl
dNTPs (10mM)	0.5µl
Primer FW (100µM)	0.075µl
Primer RV (100µM)	0.075µl
Q5 High-Fidelity DNA Polymerase	0.25µl
5X Q5 High GC Enhancer	5µl
ddH_2O	11.1µl
add genomic DNA	3µl

PCR reaction

98°C	30sec.	
98°C	10sec.	35 cycles
58°C	30sec.	
72°C	20sec.	
72°C	2min	
22°C	∞	

RAW_KI_only FW	5´- TGAATGTCTCTCACTGTCTTTGTT-3´
RAW_KI_only RV	5´- CAGATCCTCTTCAGAGATGAGTTT-3´
MYC_30bp plus FW	5´- TCCCGGAAGCTCTAGTGG-3´
MYC_30bp plus RV	5´- CTCGTAGATGGCAGAGAGAT-3´

5.13. Sequencing

For sequencing 15µl DNA (either plasmid or PCR amplicon) at a concentration of 50-100ng/µl was mixed with 2µl of the primer required (10µM). The premix of total 17µl was sent to Eurofin Genomics for Sanger sequencing.

5.14. qPCR primer List

Gene analyzed	Primer	Sequence
Human *Hprt*	hHprt FW	5´-TGTGTGCTCAAGGGGGGC-3´
	hHprt RV	5´-CGTGGGGTCCTTTTCACC-3´
Human *Malat1*	hMalat1 FW	5´-GCTCTGTGGTGTGGGATTGA-3´
	hMalat1 RV	5´-GTGGCAAAATGGCGGACTTT-3´
TBS_NLS	TBS_NLS FW	5´-CCATCTCTGTTAGCCCAGACTTT-3´
	TBS_NLS RV	5´-CTGGGGCTCAGGGCTATCT-3´
Murine *Hprt*	Hprt FW	5´- GCAGTCCCAGCGTCGTGAT-3´
	Hprt RV	5´- CGAGCAAGTCTTTCAGTCCTGTC-3´
Murine *Malat1*	Malat FW	5´-GGGGGAATGGGGGCAAAATA-3´
	Malat RV	5´-AACTACCAGCAATTCCGCCA-3´
Murine *Dicer1*	no-loxP FW	5´-CGTCCTTTCTTTGGACTGCCA-3´
	no-loxP RV	5´-GCGATGAACGTCTTCCCTGA-3´
Murine *Dicer1*	loxP FW	5´- GAAGAGGAAGGCCAAATGGGA-3´
	loxP RV	5´- TATGCTGGGGAGACAAACCG-3´
Murine *Ccl3*	Ccl3 FW	5´- TCTCCTACAGCCGGAAGATCCC-3´
	Ccl3 RV	5´- CATTCAGTTCCAGGTCAGTGATG-3´
Murine *Ccl4*	Ccl4 FW	5´- TGTTTCTCTTACACCTCCCGG-3´
	Ccl4 RV	5´- AAGAAGAGGGGCAGGAAATCTG-3´
Murine *Cflar*	QuantiTect Primer Assay	Quiagen, cat. no. QT01059016
Murine *Cxcl1*	Cxcl1 FW	5´- TGCACCCAAACCGAAGTCATAG-3´
	Cxcl1 RV	5´- TTGTATAGTGTTGTCAGAAGCCAGC-3´
Murine *Cxcl2*	Cxcl2 FW	5´- GCCCAGACAGAAGTCATAG-3´
	Cxcl2 RV	5´- GTCAGTTAGCCTTGCCTT-3´
Murine *Cxcl10*	Cxcl10 FW	5´- TCATCCACCGCTGAGAGACA-3´
	Cxcl10 RV	5´- TCGTGGCAATGATCTCAACAC-3´
Murine *Elavl1*	QuantiTect Primer Assay	Quiagen, cat. no. QT00135324
Murine *Gnb1*	Gnb1 FW	5´- GAACTAAAGCCAGGAGCAGCAG-3´
	Gnb1 RV	5´- TGTGGGTGTCCACGTTAGTATG-3´
Murine *Ier3*	Ier3 FW	5´- CGTTTGAACACTTCTCGCGG-3´
	Ier3 RV	5´- AAGATCCAGCGCATAGTCCG-3´
Murine *Il1a*	QuantiTect Primer Assay	Quiagen, cat. no. QT00113505
Murine *Il1b*	IL-1β FW	5´-AGATGAAGGGCTGCTTCCAAA-3´
	IL-1β RV	5´-AATGGGAACGTCACACACCA-3´

Murine *Il6*	IL-6 FW	5´-ATGGATGCTACCAAACTGGAT-3´
	IL-6 RV	5´-TGAAGGACTCTGGCTTTGTCT-3´
Murine *Il10*	Il10 FW	5´-GGACTTTAAGGGTTACTTGGGTTGCC-3´
	Il10 RV	5´- CATGTATGCTTCTATGCAGTTGATGA-3´
Murine *Irf1*	Irf1 FW	5´- CCGAAGACCTTATGAAGCTCTTTG-3´
	Irf1 RV	5´- GCAAGTATCCCTTGCCATCG-3´
Murine *Sdc4*	Sdc4 FW	5´- GGTCTTGGCAGCTCTGATCG-3´
	Sdc4 RV	5´- ACTCATTGGTGGGGGCTTTT-3´
Murine *Tapbp*	Tapbp FW	5´- ATACTTCAAGGTGGATGACCCG-3´
	Tapbp RV	5´- CTGCTCCGGACTCAGACTTC-3´
Murine *Tnf*	Tnf FW	5´-GATCGGTCCCCAAAGGGATG-3´
	Tnf RV	5´- CACTTGGTGGTTTGCTACGAC-3´
Murine *Zfp36*	Zfp36 FW	5´- CTCTGCCATCTACGAGAGCC-3´
	Zfp36 RV	5´- GATGGAGTCCGAGTTTATGTTCC-3´
Murine *Zfp36l1*	QuantiTect Primer Assay	Quiagen, cat. no. QT00287056
Murine *Zfp36l2*	QuantiTect Primer Assay	Quiagen, cat. no. QT00321881

5.15. Reagents

10X annealing buffer

Tris	100mM
EDTA	10mM
NaCl	500mM

adjust to pH 7.5

10X Phosphate Buffered Saline (PBS)

NaCl	1.4M
KH_2PO_4	15mM
KCl	25mM
Na_2HPO_4* $2H_2O$	81mM

Fractionation Wash Buffer

HEPES pH 7.5	10mM
KCl	60mM
EDTA pH 8-0	1mM
DTT	1mM
Protease Inhibitor (Roche, cat. no. 11873580001)	1X

Cytoplasmic Extract Buffer

Fractionation Wash Buffer supplemented with 0.1% NP-40

1X Frackelton Buffer

Tris	10mM
$Na_4P_2O_7$*$10H_2O$	30mM
NaCl	50mM
NaF	50mM
Triton X-100	1%

adjust to pH 7.1, sterile filtrated and store at 4°C

4X Frackelton Buffer

Tris	40mM
$Na_4P_2O_7$*$10H_2O$	120mM
NaCl	200mM
NaF	200mM
Triton X-100	4%

pH adjustment with HCl to pH 6 (as measured by pH indicator paper), sterile filtrated and store at 4°C

TTP elution mixture (100ml)	**I**	**II**	**II**
$TTP_{c\text{-}term}$ (0.2mM)	10µl	25µl	50µl
20X Protease Inhibitor (Roche, cat. no. 11873580001)	5µ	5µl	5µl
RNasin Ribonuclease Inhibitor (Promega, cat. no. N2511)	10µl	10µl	10µl
4X Frackelton Buffer	25µl	25µl	25µl
nuclease free water	to 100µl	to 100µl	to 100µl

C-terminal peptide of TTP ($TTP_{c\text{-}term}$) consists of the last 34 amino acids being GSDSPVFEAGVFGPPQTPAPPRRLPIFNRISVSE

1X SDS sample buffer w/o dye

Tris-HCl pH 6,5	50mM
DTT	100mM
SDS	2%

5X SDS loading dye

ß-Mercaptoethanol	5%
Bromphenol blue	0.02%
Glycerol	30%
SDS	10%
Tris-HCl pH 6.8	250mM

10% Resolution Gel

Acrylamid-Bis solution	5%
Tris pH 8.8	375mM
SDS	0.1%
TEMED	0.2%
APS	0.06%

5% Stacking Gel

Acrylamid-Bis solution	5%
Tris pH6.8	125mM
SDS	1%
TEMED	0.05%
APS	0.1%

10X Running Buffer

Tris	250mM
Glycine	1.92M
SDS	1%

adjust to pH 8.3 and store at 4°C

10X Wet Transfer Buffer[6]

Tris	250mM
Glycine	1.92M

10X TBS-T (TBS Buffer with Tween 20)

Tris	100mM
NaCl	1.5M
Tween 20	0.5%

adjust to pH 8

[6] 1X Wet Transfer Buffer dilution contains 1/10 10X Wet Transfer Buffer, 1/10 96% EtOH, 8/10 ddH_2O

Stripping Buffer

Glycine	200mM
NaCl	150mM
Tween 20	0.1%

adjust to pH 2.2 and autoclave

Ponceau S

Poncau	0.1%
Trichloracetic acid	3%
SDS	0.01%

50X TAE (1l)

Tris	242g
Sodium EDTA (0.5M)	100ml
CH_3COOH	57.1ml

add dH_2O up to 1l

6. Supplementary

6.1. Supplementary Tables

Gene analyzed	LPS 3h, WT, $T_{1/2}$ [min]	LPS 3h, ΔM^D, $T_{1/2}$ [min]	LPS 6h, WT, $T_{1/2}$ [min]	LPS 6h, ΔM^D, H $T_{1/2}$ [min]
Tnf	87	89	71	72
Cxcl2	stable	stable	stable	stable
Il1a	stable	stable	stable	stable
Il1b	stable	stable	stable	stable
Il6	stable	stable	stable	stable
Il10	161	144	133	141
Zfp36	110	77	100	77
Elavl1	stable	stable	stable	stable

Supplementary Table 1| Half-lives of WT and incomplete ΔM^D BMDM determined at 3 and 6h LPS treatment. Half-lives ($T_{1/2}$) were determined by the slope of the decay rates determined by qRT-PCR (see Materials and Methods) obtained through actinomycin D treatment. Minutes were rounded and transcripts are considered as stable when $T_{1/2} \geq 270$ minutes.

Gene analyzed	Genotype	AU at LPS 0h	AU at LPS 1h	AU at LPS 3h	AU at LPS 6h	AU at LPS 9h
Tnf	WT	nd	0.38	1.20	1.74	1.78
	ΔM^D	nd	0.52	1.65	2.13	1.58
Cxcl2	WT	nd	0.21	0.91	2.09	1.61
	ΔM^D	nd	0.31	1.05	3.01	2.18
Il1a	WT	nd	nd	0.12	1.10	2.64
	ΔM^D	nd	nd	0.26	2.45	4.66
Il1b	WT	nd	nd	0.34	1.62	2.63
	ΔM^D	nd	nd	0.48	2.47	3.23
Il6	WT	nd	nd	0.20	2.87	2.07
	ΔM^D	nd	nd	0.24	4.11	2.57
Il10	WT	0.41	0.85	1.42	1.43	1.31
	ΔM^D	0.40	0.98	1.20	1.27	0.79
Zfp36	WT	0.19	0.90	0.55	1.5	1.61
	ΔM^D	0.18	1.22	0.61	1.65	1.40
Elavl1	WT	0.73	0.50	0.67	0.67	0.96
	ΔM^D	0.69	0.80	0.84	1.07	1.22

Supplementary Table 2| mRNA levels of WT and incomplete ΔM^D BMDM determined at 0/1/3/6/9h LPS treatment. AU depicts arbitrary units (see Material and Methods). AU are rounded to 2 decimal figures and were considered as not detected (nd) if AU ≤ 0.05.

Gene analyzed	Genotype	AU at LPS 0h	AU at LPS 1h	AU at LPS 3h	AU at LPS 6h
Zfp36	WT	0.12	1.96	0.38	0.42
	HuR $^{-/-}$	0.09	1.54	0.40	0.56
	TTP $^{-/-}$	0.07	1.93	1.84	0.85
	DKO	0.07	1.99	0.41	0.84
Tnf	WT	nd	0.82	0.67	0.34
	HuR $^{-/-}$	nd	0.61	0.94	0.46
	TTP $^{-/-}$	nd	1.89	2.05	0.83
	DKO	nd	1.24	1.44	1.07
Cxcl2	WT	nd	0.77	0.47	0.16
	HuR $^{-/-}$	nd	0.73	0.55	0.33
	TTP $^{-/-}$	nd	1.48	1.55	1.34
	DKO	nd	1.10	1.49	1.49
Ccl3	WT	nd	0.24	0.91	1.11
	HuR $^{-/-}$	nd	0.22	0.84	1.12
	TTP $^{-/-}$	nd	0.38	0.84	1.70
	DKO	nd	0.17	0.78	1.86
Cflar	WT	0.25	1.29	1.08	0.60
	HuR $^{-/-}$	0.18	1.18	1.42	0.60
	TTP $^{-/-}$	0.27	1.49	1.16	0.82
	DKO	0.23	1.28	1.16	0.79
Ccl4	WT	nd	0.51	1.99	1.04
	HuR $^{-/-}$	nd	0.48	1.68	0.94
	TTP $^{-/-}$	nd	0.86	1.87	1.22
	DKO	nd	0.56	1.33	1.29
Cxcl10	WT	nd	0.78	2.52	0.34
	HuR $^{-/-}$	nd	0.65	2.47	0.25
	TTP $^{-/-}$	nd	0.65	2.30	0.25
	DKO	nd	0.88	2.47	0.20
Sdc4	WT	0.11	0.55	1.23	0.66
	HuR $^{-/-}$	0.10	0.43	1.30	0.84
	TTP $^{-/-}$	0.13	0.53	1.32	0.89
	DKO	0.10	0.48	0.98	0.86

Supplementary Table 3| mRNA levels of WT, TTP$^{-/-}$, HuR$^{-/-}$ and DKO RAW 264.7 cells after 0/1/3/6h LPS stimulation for transcripts with TTP and HuR binding site. Binding sites were taken from ref. [64]**.** AU depicts arbitrary units (see Material and Methods). AU are rounded to 2 decimal figures and were considered as not detected (nd) if AU ≤ 0.05.

Gene analyzed	Genotype	AU at LPS 0h	AU at LPS 1h	AU at LPS 3h	AU at LPS 6h
Il1b	WT	nd	0.07	0.85	0.57
	HuR $^{-/-}$	nd	0.17	1.71	0.98
	TTP $^{-/-}$	nd	0.12	0.81	1.17
	DKO	nd	0.22	2.02	2.64
Il1a	WT	nd	0.09	0.88	0.49
	HuR $^{-/-}$	nd	0.17	1.80	0.84
	TTP $^{-/-}$	nd	0.08	0.85	0.69
	DKO	nd	0.22	1.77	1.60
Il6	WT	nd	nd	0.82	0.42
	HuR $^{-/-}$	nd	nd	1.19	0.81
	TTP $^{-/-}$	nd	nd	1.36	1.38
	DKO	nd	0.05	1.74	3.42
Il10	WT	nd	nd	nd	nd
	HuR $^{-/-}$	nd	nd	nd	nd
	TTP $^{-/-}$	nd	nd	nd	nd
	DKO	nd	nd	nd	nd
Irf1	WT	0.31	0.26	1.11	2.27
	HuR $^{-/-}$	0.30	0.24	1.04	1.33
	TTP $^{-/-}$	0.35	0.25	1.50	1.81
	DKO	0.35	0.22	0.98	0.96
Cxcl1	WT	nd	nd	nd	nd
	HuR $^{-/-}$	nd	nd	nd	nd
	TTP $^{-/-}$	nd	nd	nd	nd
	DKO	nd	nd	nd	nd
Ier3	WT	0.09	3.01	0.86	1.27
	HuR $^{-/-}$	0.08	2.66	0.65	1.09
	TTP $^{-/-}$	0.08	2.33	1.30	2.56
	DKO	0.09	2.52	0.66	1.15
Zfp36l1	WT	0.83	1.07	0.51	0.49
	HuR $^{-/-}$	1.12	2.32	0.92	0.92
	TTP $^{-/-}$	1.02	1.37	0.75	0.71
	DKO	1.10	1.57	0.96	0.65
Zfp36l2	WT	1.67	1.94	0.30	0.61
	HuR $^{-/-}$	1.54	2.22	0.29	0.80
	TTP $^{-/-}$	1.59	2.13	0.35	0.61
	DKO	1.20	2.00	0.29	0.48

Supplementary Table 4| mRNA levels of WT, TTP$^{-/-}$, HuR$^{-/-}$ and DKO RAW 264.7 cells after 0/1/3/6h LPS stimulation for transcripts with TTP binding site only. Binding sites were taken from ref. [64]**.** AU depicts arbitrary units (see Material and Methods). AU are rounded to 2 decimal figures and were considered as not detected (nd) if AU ≤ 0.05.

Gene analyzed	Genotype	AU at LPS 0h	AU at LPS 1h	AU at LPS 3h	AU at LPS 6h
Elavl1	WT	0.64	0.62	0.55	0.60
	HuR $^{-/-}$	0.61	0.65	0.70	0.69
	TTP $^{-/-}$	0.61	0.76	0.77	0.73
	DKO	0.82	0.73	0.76	0.83
Tapbp	WT	0.64	0.60	1.03	1.97
	HuR $^{-/-}$	0.54	0.72	1.10	2.59
	TTP $^{-/-}$	0.57	0.63	1.02	2.46
	DKO	0.49	0.59	0.97	1.5
Gnb1	WT	1.40	1.28	1.37	1.72
	HuR $^{-/-}$	0.85	1.07	0.99	1.26
	TTP $^{-/-}$	1.03	1.32	1.34	2.01
	DKO	0.56	0.72	0.77	0.94

Supplementary Table 5| mRNA levels of WT, TTP$^{-/-}$, HuR$^{-/-}$ and DKO RAW 264.7 cells after 0/1/3/6h LPS stimulation for transcripts with HuR binding site only. Binding sites were taken from ref. [64]**.** AU depicts arbitrary units (see Material and Methods). AU are rounded to 2 decimal figures and were considered as not detected (nd) if AU ≤ 0.05.

Gene analyzed	Genotype	LPS 3h, $T_{1/2}$ [min]	LPS 6h, $T_{1/2}$ [min]
Tnf	WT	62	47
	HuR $^{-/-}$	56	54
	TTP $^{-/-}$	103	73
	DKO	81	53
Cxcl2	WT	stable	Stable
	HuR $^{-/-}$	stable	Stable
	TTP $^{-/-}$	stable	Stable
	DKO	stable	Stable
Il1a	WT	stable	144
	HuR $^{-/-}$	stable	Stable
	TTP $^{-/-}$	stable	Stable
	DKO	stable	187
Il1b	WT	stable	231
	HuR $^{-/-}$	stable	Stable
	TTP $^{-/-}$	stable	Stable
	DKO	stable	Stable
Il6	WT	stable	Stable
	HuR $^{-/-}$	stable	Stable
	TTP $^{-/-}$	stable	Stable
	DKO	stable	Stable
Ccl3	WT	stable	Stable
	HuR $^{-/-}$	stable	Stable
	TTP $^{-/-}$	stable	Stable
	DKO	stable	Stable
Sdc4	WT	stable	257
	HuR $^{-/-}$	stable	Stable
	TTP $^{-/-}$	stable	Stable

	DKO	stable	stable
Zfp36	WT	126	81
	HuR $^{-/-}$	107	88
	TTP $^{-/-}$	257	stable
	DKO	stable	182

Supplementary Table 6| Half-lives of WT, HuR $^{-/-}$, TTP$^{-/-}$ and DKO RAW 264.7 cells at 3 and 6h LPS treatment. Half-lives ($T_{1/2}$) were determined by the slope of the decay rates determined by qRT-PCR (see Materials and Methods) obtained through actinomycin D treatment. Minutes were rounded and transcripts are considered as stable when $T_{1/2} \geq 270$ minutes.

6.2. Supplementary Materials and Methods

6.3. sgRNA design for *Dicer1*

Guide RNA design aiming to create a Dicer1 knockout in murine cells by CRISPR/Cas9 mediated genome editing was done using the Broad Institute sgRNA Designer (http://portals.broadinstitute.org/gpp/public/analysis-tools/sgrna-design). Highest scoring guide RNAs were assessed for putative off-targets using the DNA2.0 tool (https://www.dna20.com/eCommerce/cas9/input) together with the CRSIPR/Cas9 tool from the laboratory of Feng Zhang (http://crispr.mit.edu/). The 2 gRNAs best suited based on these criteria are depicted below together with the surveyor primer, which would allow detection of successful mutation[172].

Guide sequence	Surveyor primer	Amplicon in WT [nt]	Amplicon in knockout [nt]
5´- CTCAGGGAAGACGTTCATCG-3´	5´-CGGGAGAAGCATACCTCGTG-3´	848	376 and 553
Targets sense strand on exon 3	5´- GTCAGTCTGCAGTCCCCAAA-3´		
5´- GAGATCCGAGTGAGTTCTGA-3´	5´- TGATGGAAGAGGACGGGGAT-3´	838	228 and 610
Targets sense strand on exon 4	5´- CCCATTGAGCTGACAGGGTT-3´		

6.4. Sanger sequencing of RAW KI_only PCR products

PCR products of ´RAW KI_only ´PCR of CRISPR/Cas9 genome edited RAW 264.7 cells were purified using the QUAIquick PCR Purification Kit (Quiagen, cat. no. 28104) according to the manufacturers protocol. For sequencing the primer RAW_KI_only FW was mixed with the PCR amplicon, which verified the correctness of the *Myc-Zfp36* knock-in. Below are given clipped sequences for B8-2, B8-3, B-5, B8-7 and B8-8. The color code of the clipped

sequences depicts Myc in green and the start codon of Zfp36 exon 1 in blue. Sanger sequencing was performed as described in 5. Materials and Methods.

B8-2:

TCTCCCCGCCCCCGTCTGTCTCACACGCACACGCCCTCAGTCTCTGCCCTTGTCAATTGTCCCTAGAGCCCTGCCCCCACTTCTGCCCCAGTT
CTCTTCCCGACTGCCTTCCACCTCTGAAAAACACTAGGACGCCCCCGCTACCATCACCTCCAGTTGGTCGTACACAACCCTCCCTACTACCC
CCCGAGAGGGGCCGGAGCTGCGGGAGGGCCAAGTTCAGGCACATTTTGCATGCTAACCAGCAGATAGGCGGAAGGGGCCTAGTACCA
GGCCGGCCGAGCTACGCCGCCCGGGCGCGTCCCGGAAGCTCTAGTGGCCACCGCCCCAGGCCGCCCCATAAAAGGAGAAAGCTCCTGC
TGCGGGCCACAGCCTGACTTCTGCGAACCGACAGTCCCTCTCTTCACCAAGGCCATTCGCGCCACCATGGAACAAAAACTCATCTCTGAA
GA

B8-3:

CCCCCGTCTGTCTCACACGCACACGCCCTCAGTCTCTGCCCTTGTCAATTGTCCCTAGAGCCCTGCCCCCACTTCTGCCCCAGTTCTCTTCCC
GACTGCCTTCCACCTCTGAAAAACACTAGGACGCCCCCGCTACCATCACCTCCAGTTGGTCGTACACAACCCTCCCTACTACCCCCCGAGA
GGGGCCGGAGCTGCGGGAGGGCCAAGTTCAGGCACATTTTGCATGCTAACCAGCAGATAGGCGGAAGGGGCCTAGTACCAGGCCGGC
CGAGCTACGCCGCCCGGGCGCGTCCCGGAAGCTCTAGTGGCCACCGCCCCAGGCCGCCCCATAAAAGGAGAAAGCTCCTGCTGCGGGC
CACAGCCTGACTTCTGCGAACCGACAGTCCCTCTCTTCACCAAGGCCATTCGCGCCACCATGGAACAAAAACTCATCTCTGA

B8-5:

CCCCCGTCTGTCTCACACGCACACGCCCTCAGTCTCTGCCCTTGTCAATTGTCCCTAGAGCCCTGCCCCCACTTCTGCCCCAGTTCTCTTCCC
GACTGCCTTCCACCTCTGAAAAACACTAGGACGCCCCCGCTACCATCACCTCCAGTTGGTCGTACACAACCCTCCCTACTACCCCCCGAGA
GGGGCCGGAGCTGCGGGAGGGCCAAGTTCAGGCACATTTTGCATGCTAACCAGCAGATAGGCGGAAGGGGCCTAGTACCAGGCCGGC
CGAGCTACGCCGCCCGGGCGCGTCCCGGAAGCTCTAGTGGCCACCGCCCCAGGCCGCCCCATAAAAGGAGAAAGCTCCTGCTGCGGGC
CACAGCCTGACTTCTGCGAACCGACAGTCCCTCTCTTCACCAAGGCCATTCGCGCCACCATGGAACAAAAACTCATCTCTG

B8-7:

CCCCGTCTGTCTCACACGCACACGCCCTCAGTCTCTGCCCTTGTCAATTGTCCCTAGAGCCCTGCCCCCACTTCTGCCCCAGTTCTCTTCCCG
ACTGCCTTCCACCTCTGAAAAACACTAGGACGCCCCCGCTACCATCACCTCCAGTTGGTCGTACACAACCCTCCCTACTACCCCCCGAGAG
GGGCCGGAGCTGCGGGAGGGCCAAGTTCAGGCACATTTTGCATGCTAACCAGCAGATAGGCGGAAGGGGCCTAGTACCAGGCCGGCC
GAGCTACGCCGCCCGGGCGCGTCCCGGAAGCTCTAGTGGCCACCGCCCCAGGCCGCCCCATAAAAGGAGAAAGCTCCTGCTGCGGGCC
ACAGCCTGACTTCTGCGAACCGACAGTCCCTCTCTTCACCAAGGCCATTCGCGCCACCATGGAACAAAAACTCATCTCT

B8-8:

CCCCGTCTGTCTCACACGCACACGCCCTCAGTCTCTGCCCTTGTCAATTGTCCCTAGAGCCCTGCCCCCACTTCTGCCCCAGTTCTCTTCCCG
ACTGCCTTCCACCTCTGAAAAACACTAGGACGCCCCCGCTACCATCACCTCCAGTTGGTCGTACACAACCCTCCCTACTACCCCCCGAGAG
GGGCCGGAGCTGCGGGAGGGCCAAGTTCAGGCACATTTTGCATGCTAACCAGCAGATAGGCGGAAGGGGCCTAGTACCAGGCCGGCC
GAGCTACGCCGCCCGGGCGCGTCCCGGAAGCTCTAGTGGCCACCGCCCCAGGCCGCCCCATAAAAGGAGAAAGCTCCTGCTGCGGGCC
ACAGCCTGACTTCTGCGAACCGACAGTCCCTCTCTTCACCAAGGCCATTCGCGCCACCATGGAACAAAAACTCATCTCTGAAG

Studies of effects of CEBPα overexpression on transdifferentiation of transformed human haploid cells into macrophage-like cells

7. Introduction and Aim

During an organisms development most cells are determined to become unipotent somatic cells. In general, cell lineage commitment is a unidirectional process in which the transcriptional program and chromatin modifications largely govern the gene expression necessary for the establishment of a certain differentiated cell-type. However, breakthroughs reflected by the somatic cell nuclear transfer[180] ,but also the generation of mouse and human induced pluripotent stem cells (iPSCs)[181–183] abrogate the concept´s irreversibility. In the latter fibroblast were reprogrammed upon induction of Oct4, Klf4, Sox2 and c-Myc (collectively referred to OKSM) and thereby regained pluripotency. Similar yet different transdifferentiation allows the conversion of one differentiated cell into another[184,185]. Conceptually there are two main types of transdifferentiation: ´direct transdifferentiation´ and ´indirect transdifferentiation´ [184].

In direct transdifferentiation (also often referred as direct cell conversion or direct reprogramming) a fully differentiated cell is converted into another without the need of to acquire a partially reprogrammed or dedifferentiated intermediate state. One of the most prominent examples of transcription factor induced direct linage conversion is the transdifferentiation of fibroblasts to muscle cells through MyoD overexpression[186]. Despite that, several other reports have shown a direct switch from one cell type into another by the application of a mixture of transcription factors. For instance, this has been shown by the generation of induced brown fat cells or cardiomyocytes, both from fibroblasts, by the developmental inducers PRDM16 and C/EBPβ or Gata4, Mef2c and Tbx5, respectively[187,188]. Hereof, the induced cardiomyocytes do not only resemble the gene expression pattern of neonatal cardiomyocytes, but also conduct spontaneous contraction[188]. Importantly, direct transdifferentiation approaches in the neurobiology have confirmed the possibility of crossing germ layers during linage conversion. Exemplarily, Vierbuchen *et al.* efficiently reprogrammed fibroblast to functional neural cells by the combinatorial expression of Ascl1, Brn2 and Myt1l[189]. Furthermore, direct transdifferentiation also enables the generation of specific cellular subtypes. As such exchange of Brn2 and Myt1l with Nurr1 and Lmx1a results in dopaminergic neurons from mouse and human fibroblast[190]. Similarly, mouse and human embryonic fibroblast can be directly converted to spinal motor neuronal by expression of a

set of seven or eight transcription factors respectively, closely resembling the phenotype of developmentally differentiated motor neurons[191].

Indirect transdifferentiation (also called cell-activation and signaling-directed transdifferentiation) on the other hand, represents a more time-consuming process[184,192]. In a two-step process terminally differentiated cells first become activated and revert back into an intermediate state. Then these partially de-differentiated cells are exposed to signals which direct the differentiation program towards another cell linage. The transitory intermediate state is in general attained by induced expression of at least one of the OKSM pluripotency factors. As such restriction of Oct4 activity to the early phase of indirect transdifferentiation while Klf4, Sox2 and Myc are constitutively expressed, converts mouse fibroblast to induced neuronal stem cells with potential to differentiate into three neural subtypes[193]. Of note, the later three are endogenously expressed in neural stem cells and thus provide the signal for linage conversion[193]. This tripartite signal also can be exchanged by a mixture of small molecules, ultimately enabling the indirect conversion of fibroblast to induced neural stem cells in the human system[194]. Inductive cell fate conversion by small molecules also was achieved by conversion of fibroblasts to endothelial cells[195]. Importantly, the generation of human induced neural stem and endothelial cells supports the idea of indirect transdifferentiation without gaining pluripotency during the process [194,195]. However, diversification into direct and indirect transdifferentiation may not represent the entire picture. Although different combinations of Ngn3, Mafa and Pdx1 allow a differentiation-switch from exocrine cells into pancreatic α-, β-, or δ-cells suggesting direct reprogramming; Ngn3 alone promotes a common endocrine state as well, indicative for indirect differentiation[196,197]. In the field of Immunobiology B cells have been highly efficiently reprogrammed into macrophages by the forced expression of the single transcription factor CCAAT Enhancer Binding Protein α (C/EBPα)[198–201], which is mainly direct and hardly involves de-differentiation[202]. The canonical form of C/EBPα is a protein of 42 kDa (C/EBPα p42) in sizes and consists of 358 amino acids containing 2 N-terminal transactivation domains (TADs) and a C-terminal basic region-leucine zipper domain (BR-LZ domain) **(Fig. 21a)**[203–207].

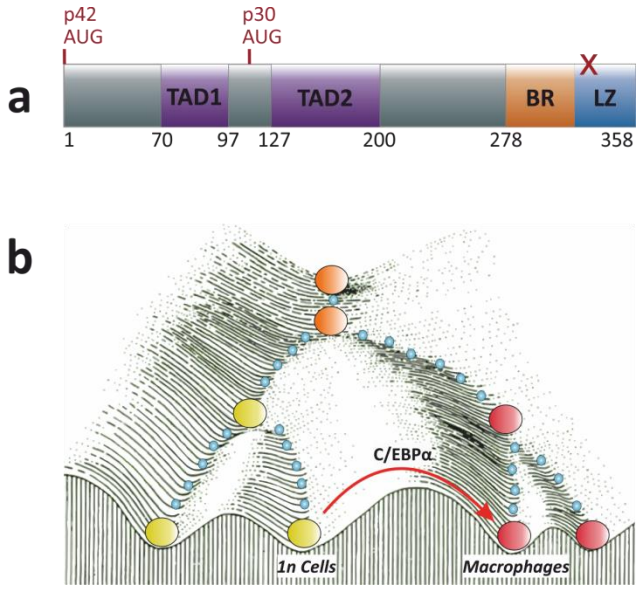

Figure 21| C/EBPα and its induced change in the Waddington's landscape in haploid cells caused by transdifferentiation. (a) Diagram of C/EBPα depicting its structure and function. The C-terminal basic region (BR)-leucine zipper (LZ) domain for homo-and hetero-dimerization is depicted in orange and blue. N-terminal trans-activation domains (TADs) are shown in violet. The canonical p42 isoform and its p30 and C/EBPαLZ alternations are indicated at the top in red. The bottom numbers refer to amino acids. The graphic was adapted from ref.[258] **(b)** Diagram showing the desired change in the Waddington's epigenetic landscape upon C/EBPα induced reprogramming. Through C/EBPα induction haploid (1n) cells should directly transdifferentiate into macrophages. The picture was adapted from ref.[202].

Upon homo- or hetero-dimerization via its LZ domain the transcriptional regulator binds to DNA with its BR and the TADs induce transcription of its target genes[204,205,207]. Importantly here, despite other functions C/EBPα is a major regulator of granulopoiesis and monopoiesis. Substantial C/EBPα levels are readily observed in the common myeloid progenitors (CMPs) and are even higher in granulocyte-monocyte progenitor (GMP) cells during hematopoiesis[208]. Therefore C/EBPα knockout inhibits the formation of both, granulocytes and monocytes[209]. However, higher levels of C/EBPα may be required for granulocyte formation than for monocyte differentiation[210]. This might be indicative for preferential heterodimer formation with the AP-1 family members c-Fos and c-Jun. Engineered LZ domains to favor C/EBPα: C/EBPα homo- or C/EBPα:AP1 hetero-dimerization showed that the hetero- , but not the homo-dimer complex directs toward monocyte fate[211]. As shown in B cell into macrophage reprogramming several macrophage specific markers become upregulated due to C/EBPα overexpression[198–202]. Furthermore, C/EBPα activates *Spi1* transcription, a crucial factor in macrophage development[212,213]. Hence, little alternations of the canonical isoform largely impact myeloid differentiation and may result in myeloid transformation. For instance, this could be due to the usage of an alternative start-codon, resulting in a truncated N-terminal 30 kDa version (C/EBPα p30) of the protein missing the first TAD[214]. C/EBPα p30 was shown to be a dominant negative form that can interfere with the transcriptional program, as it prevents DNA-binding of the p42 isoform[215].

On the other hand there are also LZ indel mutations (C/EBPαLZ), which block trans-activation, as the protein is not able to bind DNA, without prior dimerization[216]. Notably, although C/EBPα primarily acts within the nucleus as transcription factor it also has an anti-proliferative effect independent of DNA-binding[217–221].

Most reprogramming approaches focus their objective on regenerative medicine and development. In contrast, we were aiming to directly transdifferentiate the cell lines HAP1 and KBM-7 into macrophages by ectopic C/EBPα expression **(Fig. 21b)**. KBM-7 is a near human, almost haploid leukemia cell-line only disomic for chromosome 8 and a part of chromosome 15[222]. HAP1 cells were established by expression of OKSM in KBM-7 cells, which rendered them adherent and caused a loss in chromosome 8 diploidy[223]. Due to their haploid nature, these cells present powerful tools to study biological mechanisms using large scale genetic screens. Using gene-trap insertional mutagenesis several pathogen-host interaction[223–225], but also epigenetic modifiers already were uncovered[226]. Furthermore, haploid screens also identified chemical compounds and mutations relevant for cancer therapy underlining their utility[227,228].

Nevertheless, the currently available human haploid cells do not respond properly to immunological stimuli, which preclude them for studying immunological pathways. Therefore, we aimed to directly transdifferentiate the human haploid cell lines into macrophages, which set the foundation for their application in large-scale forward genetic screens in an immunological background.

8. Results

8.1. Generation of C/EBPα positive human haploid cells

In order to transdifferentiate the human haploid cell-lines HAP1 and KBM-7 into macrophages or at least macrophage-like cells, first the fusion-gene of C/EBPαER was delivered by retroviral transduction randomly into their genome, as depicted in **Figure 22**. The fusion of C/EBPα to the hormone binding domain of the estrogen receptor (ER) allows its 4-OH tamoxifen mediated induction. To ensure the correctness of the sequence of the retroviral construct it was Sanger sequenced prior usage **(Suppl. Fig. 1; Suppl. Materials and Methods)**. Due to the IRES-GFP sequence in the retroviral expression plasmid GFP detection

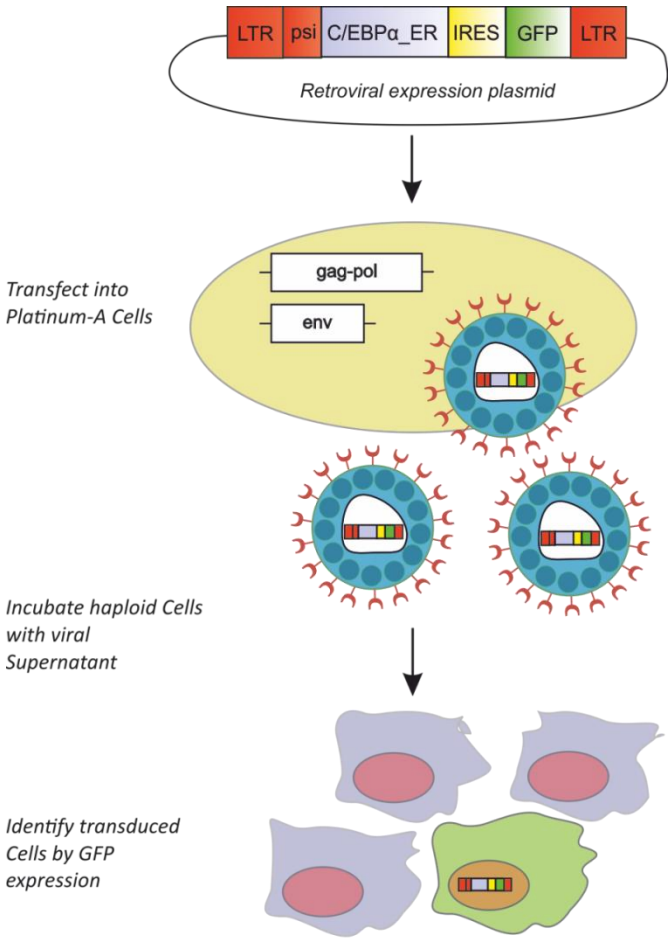

Figure 22| Approach to generate C/EBPα positive human haploid cells Platinum-A cells stably expressing gag, pol and env were transfected with the modified MSCV IRES GFP plasmid (retroviral expression plasmid) for production of the amphotrophic retrovirus. HAP1 and KBM-7 cells were incubated with the retroviral supernatant and subsequent screened for successful gene transfer of the C/EBPαER fusion by GFP detection. LTR, long terminal repeats. psi, packaging sequence.

served as steady marker for successful infection[229,230,198,231,232]. About 15-20% of HAP1 cells (white arrows) incubated with the retroviral supernatant (HAP1 batch culture) and ~7.4% of

the KBM-7 batch culture were GFP positive 5 days post infection (p.i.), as assessed by fluorescence microscopy and flow cytometry, respectively **(Fig. 23a and c)**. However, the relative number of both, HAP1 and KBM-7 GFP positive cells within the batch culture decreased over the course of time (data not shown). This hypothetically could result from diverse effects, e.g. a growth advantage of WT cells over retrovirally transduced caused by the random integration of C/EBPαER adjacent to cell-cycle control genes or oncogenes subsequently resulting in altered gene expression due to silencing of the integration locus[233]. Also this could be caused by the anti-proliferative effect of C/EBPα, which was reported to be independent from its function as transcription factor [217–221,234]. Therefore, to circumvent this problem and finally obtain a pure GFP positive culture, allowing to induce C/EBPα in all cells within an experimental setup, single cells from both batch cultures were seeded into 96-well plates. GFP screening was again done by fluorescence microscopy and flow cytometry. Ultimately, eight HAP1 and nine KBM-7 clones, showing homogenous GFP intensity within the colony itself, yet varying among each other, were obtained **(Fig. 23b and c ;Suppl. Table 7)**. From each cell line three representative clones were chosen to further use for the transdifferentiation approach **(Fig. 23b and c)**. Furthermore, to determine if GFP detection actually correlates with the expression of the C/EBPαER fusion-protein and how 4-OH tamoxifen (TMX) treatment, inducing the proteins translocation from the cytoplasm into the nucleus, affects this process western blot analysis was performed. As expected, ectopically overexpressed C/EBPα could only be detected in the various HAP1 and KBM-7 clones, but no in WT (**Fig. 23d and e**). In addition, the transcription factor is constitutively expressed upon transduction independent of its TMX mediated activation. Importantly, despite minimal effects on HAP1 #9, the HAP1 clones #8 and #14 were rather unaffected by the 4-OH TMX treatment. This was completely different compared to the three KBM-7 clones analyzed. Here, prolonged 4-OH tamoxifen treatment lead to a decreased cell number and as such Tubulin could not be detected anymore upon C/EBPα induction. Notably, a decreased cell number could presumably result from the transdifferentiation process itself. Such impaired proliferative capacity of KBM-7 cells could be explained by a potential repression of genes linked to cell division while reprogramming into macrophage[202]. Taken together, clones of human haploid cells, i.e. HAP1 & KBM-7 which allow the inducible activation of C/EBPα were successfully established by retroviral transduction.

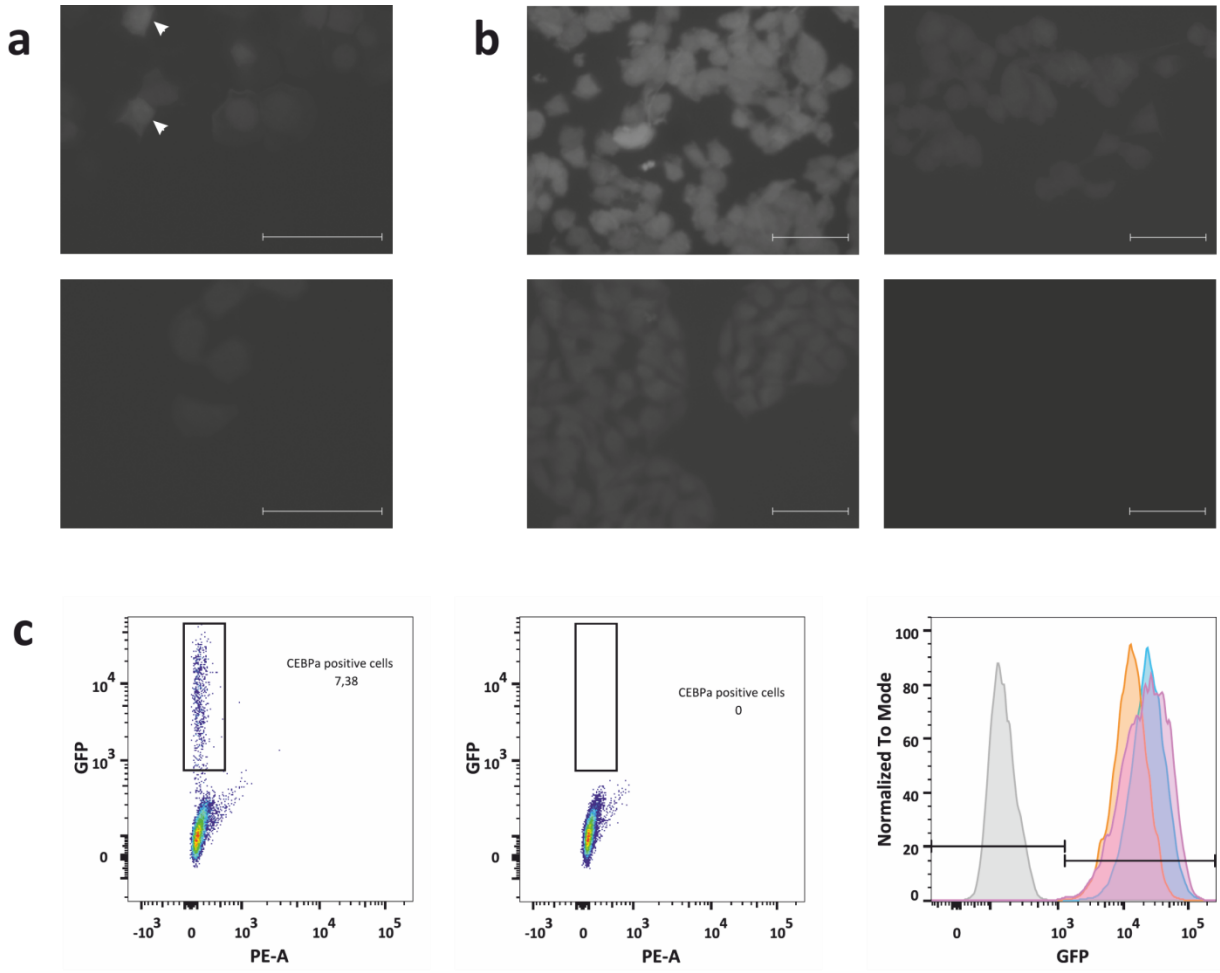

Figure 23| Generation of C/EBPα positive human haploid cells. (a,b) Fluorescence microscopy of HAP1 cells showing GFP in greyscale as indicator for successful C/EBPαER gene transfer. Scale bar represents 50µm. **(a)** Retrovirally transduced HAP1 batch culture (top) with GFP positive cells (white arrows) 5 days p.i. and HAP1 WT cells as negative control (bottom). **(b)** HAP1 batch culture clone #8 (upper left), #9 (upper right), #14 (lower left) and WT (lower right).

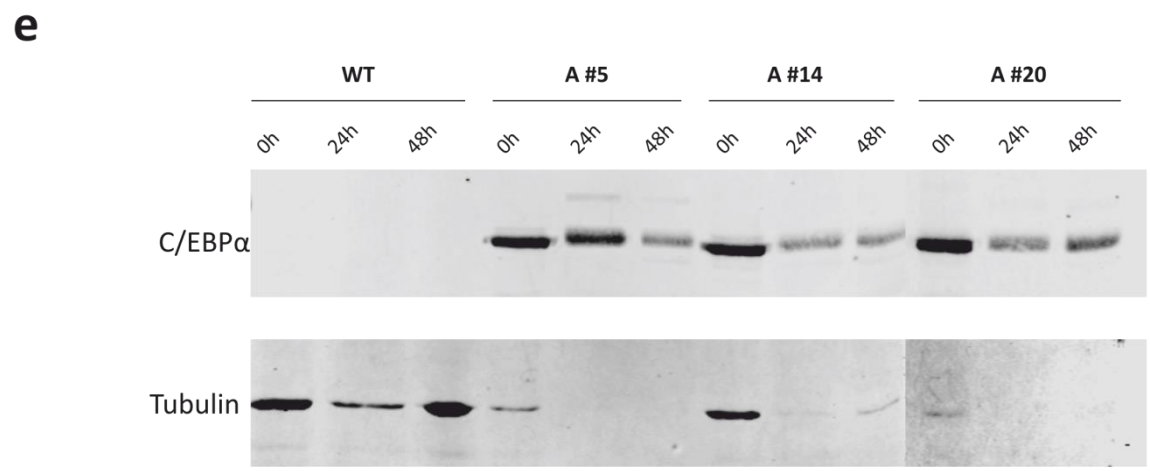

Ad.: Figure 23| Generation of C/EBPα positive human haploid cells. (c) Flow cytometry analysis of KBM-7 cells for GFP as indicator for successful C/EBPα gene transfer. PE-A represents Phycoerythrin-channel. Left, middle: Retrovirally transduced KBM-7 batch culture 5 days p.i. (left) and KBM-7 WT cells (middle) as negative control. The box encloses the percentage of C/EBPα positive cells as indicated. Right: Live (PE-A negative) KBM-7 WT in grey and batch culture clone A#5 in blue, A#14 in orange and A#20 in pink. Measurements are pre-gated for single cells.**(d, e)** Western Blot analysis for C/EBPα expression in **(d)** HAP1 WT, clone #8, #9, #14 and **(e)** KBM-7 WT, clone #5, #14 and #20 untreated (0h), treated for 24h or 48h with 4-OH tamoxifen as indicated. Tubulin serves as loading control.

8.2. Assessment of macrophage characteristic pro-inflammatory cytokines

Macrophages are potent cellular sources of pro-inflammatory cytokine secretion, such as TNF, IL-1β, IL-12 or CXCL8, when they encounter inflammatory stimuli[171,235–237]. Hence, we attempted to transdifferentiate the HAP1 and KBM-7 clones into macrophages and to subsequently test their functional response to LPS and heat-killed *Streptococcus pyogenes* (HK GAS) by determining *Tnf* and *Cxcl8* protein and mRNA levels. Hereof, re-instruction of the transcriptional program and the epigenetic modifications required for a full and stable transdifferentiation often represents a fast, yet multi-day process[188,189,198,201,202,238,239]. Therefore, cells were first treated for three days, followed by two days re-treatment with 1µM 4-OH tamoxifen prior exposure to the inflammatory stimuli. This pulsed treatment over five days probably provides enough time for the anticipated transdifferentiation into haploid macrophages.

Neither secretion of TNF, nor of CXCL8 could be detected upon 6h LPS or HK GAS stimulation post TMX-mediated C/EBPα induction by ELISA (data not shown). Likewise, qRT-PCR could not show *Tnf* transcription for the three HAP1 and KBM-7 clones characterized before (data not shown). Nonetheless, although none of the three HAP1 clones showed an increase in

Cxcl8 transcription compared to the WT, KBM-7 A #5 had highly increased *Cxcl8* mRNA levels after LPS stimulation and C/EBPα induction **(Fig. 24)**.

Thus, KBM-7 A #5, representing the most promising candidate for the applied transdifferentiation approach, was further tested for the expression of *Il1b*. Similar to *Cxcl8* the transcription *Il1b* was elevated in LPS treated cells post 4-OH tamoxifen administration for 5 days compared to the WT sample and all other treatments **(Fig. 24b, right)**. Collectively the screening data suggests that only KBM-7 A #5, from the total six haploid cell clones analyzed, possibly can be primed towards a macrophage cell upon ectopic induction of C/EBPα, based on its reactiveness to LPS. Interestingly, HK GAS stimulation in KBM-7 A #5 was insufficient to mount the aforementioned raise in *Cxcl8* or *Il1b* transcription. The sensitivity to inflammatory stimuli, by which C/EBPα drives different responses to distinct inflammatory stimuli, may be indicative of partial conversion.

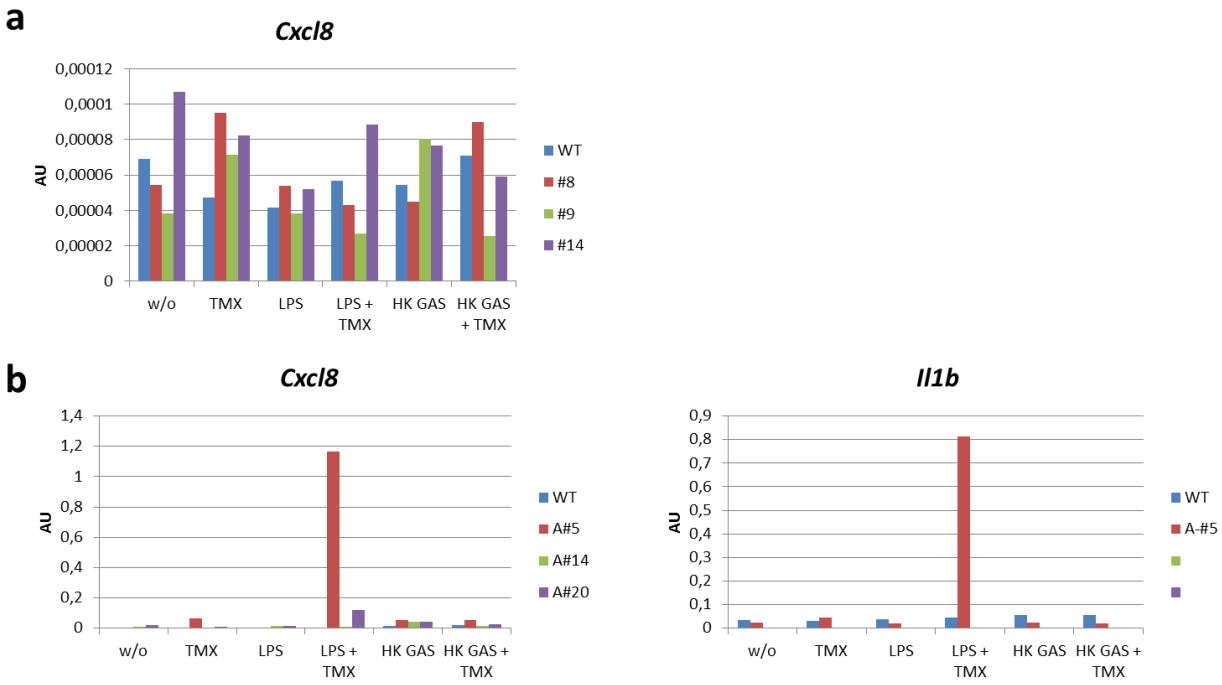

Figure 24| Assessment of macrophage characteristic pro-inflammatory cytokines indicates partial transdifferentiation. (a, b) Gene expression analysis for *Cxcl8* and *Il1b* by qRT-PCR. **(a)** HAP1 WT (blue), clone #8 (red), #9 (green) and #14 (purple) were grown 5 days (3days followed by 2 additional days) in normal (w/o) or 4-OH tamoxifen supplemented medium (TMX) followed by LPS or HK GAS treatment for 6 hours as indicated. **(b)** KBM-7 WT (blue), clone A #5 (red), A #14 (green) and A #20 (purple) were grown 5 days (3days followed by 2 additional days) in normal (w/o) or 1 µM 4-OH tamoxifen supplemented medium (TMX) followed by LPS or HK GAS treatment for 6 hours as indicated.

8.3. C/EBPα overexpression promotes the transcription of several macrophage specific markers, but this effect cannot be generalized

During the conversion process several genes expressed natively in the starter cell should become silenced, whereas those of the cell-line ought to obtain should become induce[188,190,191,196]. Previous studies from Graf and colleagues have shown that B cell to macrophage transdifferentiation, driven by the inducible expression of C/EBPα, causes the expression of macrophage characteristic antigens, e.g. CSF1R, CD14, MAC-1, FCGR1B, and MMP9 while silencing B cell specific ones, e.g. CD19[198–202]. Interestingly, this effect has been shown to be connected to the activation of de-novo and pre-existing macrophage enhancers, the latter bound by SPI1 (PU.1)[240]. Therefore, it is a plausible assumption that 4-OH tamoxifen application described before, yielding low yet detectable *Cxcl8* and *Il1b* transcription, should also trigger the expression of macrophage specific markers in KBM-7 A #5. Specifically the expression of genes encoding for macrophage surface receptors, like *Csf1r*, *Cd14* and *Itgam (Mac-1),* was assessed.

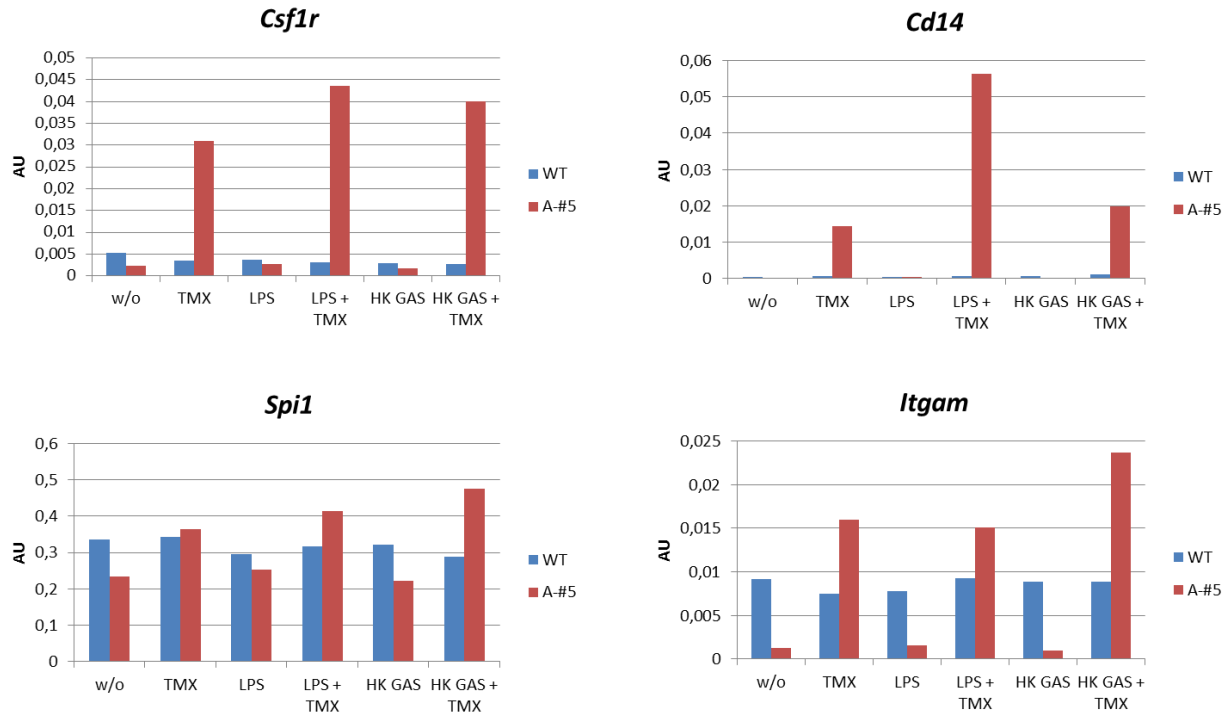

Figure 25| Ectopic overexpression of C/EBPα promotes the transcription of some macrophage specific markers. Gene expression analysis for *Csf1r, Cd14, Spi1* and *Itgam* by qRT-PCR. KBM-7 WT (blue) and clone A #5 (red) were grown 5 days (3days followed by 2 additional days) in normal (w/o) or 1µM 4-OH tamoxifen supplemented medium (TMX) followed by LPS or HK GAS treatment for 6 hours as indicated.

Among those three genes *Itgam* expression became relatively little upregulated upon C/EBPα activation compared to WT and was basically not present in absence of 4- OH tamoxifen **(Fig. 25, bottom right)**. Rather different was the expression of the 2 macrophage surface-antigens *Csf1r* and *Cd14.* Here, upregulation of *Csf1r* is completely dependent on the ectopic expression of C/EBPα but inflammatory stimuli, i.e. LPS or HK GAS did not induce its transcription alone, nor raised TMX driven transcription considerably **(Fig. 25, top left).** Similarly, yet little different *Cd14* upregulation requires C/EBPα induction, but is highest when stimulated subsequently with LPS **(Fig. 25, top right).** This profile is in accordance with those of *Cxcl8* and *Il1b* **(Fig. 24)**, implying that the approach applied caused a shift towards conversion into macrophages. In that regard it has been shown LPS is capable to increase the expression of the TLR4 co-receptor CD14 in human macrophages[237,241]. This could suggest that KBM-7 A #5 was initialized towards macrophages and thus mounted a reminiscent response. Furthermore, we tested for *Spi1* transcription, a transcription factor generally crucial in myeloid linage commitment[212,213,242,243], but also for known to be upregulated during C/EBPα mediated pre-B cell to macrophage transdifferentiation[198,201,240]. Surprisingly, none of the treatments yielded a notable change in *Spi1* mRNA levels, in fact being akin to the steady-state levels observed in the WT control. Of note, CSF1R activation und its downstream signaling impacts macrophage proliferation and drives myeloid linage commitment, but also regulate their survival and chemotaxis[244–247]. Hence, we tried to improve the transdifferentiation approach, by concomitant M-CSF administration together with 4-OH tamoxifen. Ideally this combined pulsed treatment, again for 3 days followed by 2 additional days, should trigger a monocyte/macrophage program and so boost expression of macrophage characteristic genes. However, additional M-CSF did not increase the transcription of *Cxcl8* or *Csf1r* **(Suppl. Fig. 2)**, or any other of the aforementioned genes (data not shown). Therefore, M-CSF does not facilitate transdifferentiation of KBM-7 A #5 and was no further applied.

Altogether the data shows that ectopic C/EBPα expression promotes the transcription of macrophage specific markers, which accordingly implies that KBM-7 A #5 can be partially converted into macrophages.

8.4. Prolonged C/EBPα induction is required to promote a partial macrophage-like response of KBM-7 cells

A hallmark of efficient conversion from one committed cell-line into another is the time point at which they become transgene independent and no reversion back to the initial cell-line occurs[190,197,199,239,248]. Although the gene expression profile of KBM-7 A #5 indicates partial transdifferentiation by C/EBPα induction it still remains elusive at which specific moment in time its conversion is initiated. To test this, kinetics for the gene expression of two macrophage markers, i.e. *Csf1r* and *Cd14*, as well as the kinetics for one pro-inflammatory cytokine, i.e. *Il1b*, was analyzed. *Csf1r* and *Cd14* became rapidly expressed after two to three days TMX-treatment which increased over time **(Fig. 26)**. Importantly, the elevated *Cd14* mRNA levels due to additional LPS were already evident after 3 days C/EBPα activation, a difference which was most pronounced after 5 days. As macrophages upregulate *Cd14* when exposed to certain inflammatory stimuli[237,241], this suggest that KBM-7 A #5 might have already acquired macrophage attributes three days after initiation of transdifferentiation. This is supported by the kinetics of *Il1b*, as its detection is indicative for proper macrophage response when facing antigens[236]. Here, four to five days TMX pre-treatment is crucial before LPS causes *Il1b* transcription. Based on this data it can be assumed that 72h C/EBPα activation already initiates reprogramming, yet a prolonged C/EBPα expression is required for KBM-7 cells to acquire at least some macrophage-like attributes (e.g. induction of *Cxcl8* and *Il1b* transcription).

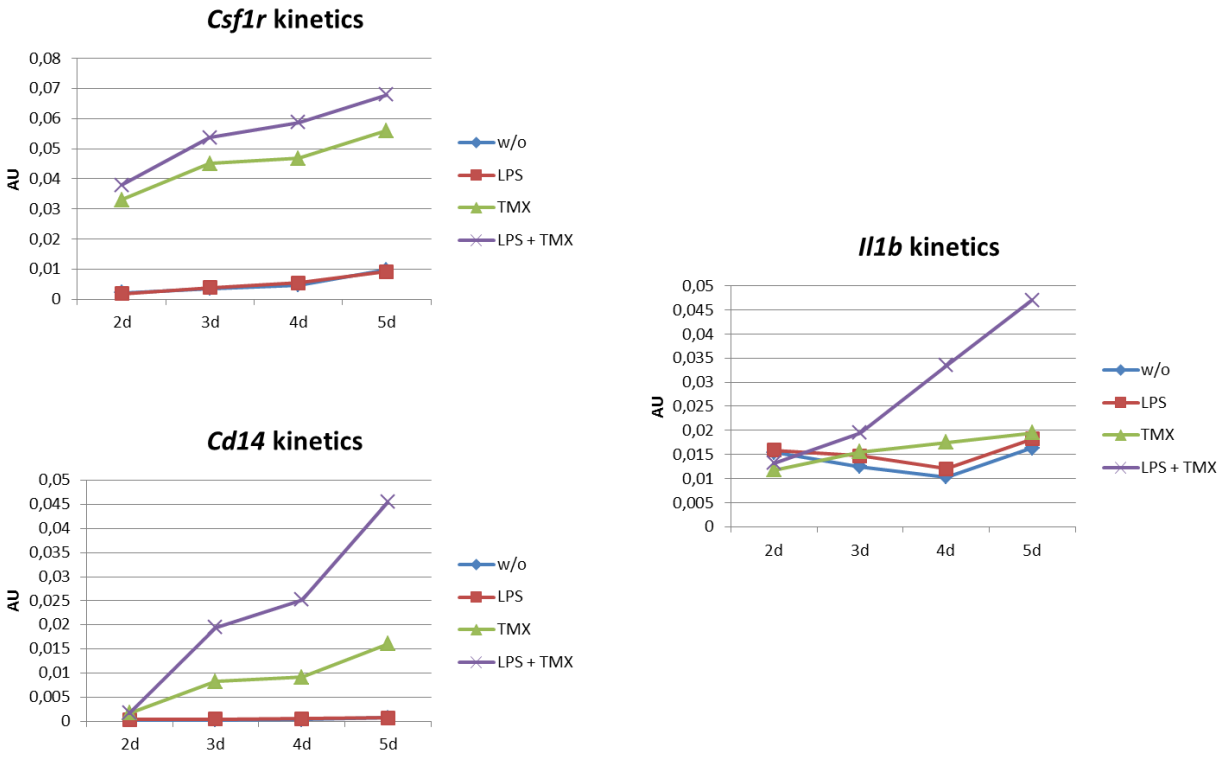

Figure 26| Prolonged C/EBPα induction is vital to promote partial transdifferentiation Gene expression analysis to determine the kinetics for *Csf1r, Cd14* and *Il1b* by qRT-PCR. KBM-7 clone A #5 was grown 2, 3, 4 and 5 days in normal (w/o) or 1 µM 4-OH tamoxifen supplemented medium (TMX) followed by LPS treatment for 6 hours as indicated.

9. Discussion

The usefulness of near haploid human cell lines for genetic screens has been addressed in a plethora of studies. Both, HAP1 and KBM-7 bear great potential to decipher disease mechanisms and uncover compounds, which ultimately holds promise for therapeutic advances[223–225,227,228]. However, their utility for studying immune responses is limited by their poor responsiveness to immunological stimuli.

Here, we aimed to circumvent this constraint by transdifferentiation of human haploid cells into macrophages by ectopic overexpression of C/EBPα. Using retroviral transduction 17 clones of haploid human cells harboring the inducible form of C/EBPα were obtained **(Fig. 23; Suppl. Table 7).** From in total six KBM-7 cell clones examined a single one showed signs of transdifferentiation as determined by its LPS response **(Fig. 24)** and the upregulation of certain macrophage specific markers **(Fig. 25)**. Surprisingly, KBM-7 A #5 displayed sensitivity to distinct inflammatory stimuli, showing no response to HK GAS treatment **(Fig. 24 and 25)**. Although promising, a greater number of macrophages should be screened for their inducible conversion into macrophages. This would exclude the possibility to misinterpret aberrant gene expression, e.g. brought about by indirect effects upon random retroviral integration, as macrophages-alike. Furthermore, it remains elusive if KBM-7 A #5 shows functional macrophage properties. To this end assays determining phagocytic capacity, adherence, staining macrophage surface-receptors, etc. might reveal whether a genuine macrophage phenotype can be established by C/EBPα induction in haploid cells, similar as described for B cell reprogramming into macrophages[198,199,201].

Of note, C/EBPα induction cause re-arraignments of histone modifications and to a little extend change in euchromatin and heterochromatin status during B cell to macrophage transition[240,249–251]. Moreover, a prerequisite for other reprogramming approaches is a combination of various transcription factors[187–191,196,197], eventually with their induction at certain time points[248]. Therefore, the usage of other additional factors may improve the transdifferentiation approach tested, though the possibility of M-CSF already can be excluded **(Suppl. Fig. 2)**. Putative enhancers may include FOSB, GFI1, RUNX1, SPI1, or SOX2 and miR-125b based on their potential to induce hematopoietic multipotent progenitors[252], or monocyte-like cells[253], respectively.

Despite that, the kinetic data suggests an early onset of partial transdifferentiation already after 72 hours which peaks at day five **(Fig. 26)**. As day 5 was the last time point measured extended - or a third pulse of TMX treatment might provide means to enhance the transdifferentiation towards macrophages. Even so, full transdifferentiation may be hampered anyhow. Leukemic cells, including KBM-7 are known to bear mutations in factors fundamental for monocyte/macrophage differentiation, e.g. endogenous C/EBPα and PU.1 [215,216,254–256]. Thus, withdrawal of TMX and consequently the prevention of ectopic C/EBPα activation might cause reversion into the original phenotype.

Summarizing, the results indicate that prolonged C/EBPα expression can promote partial transdifferentiation of KBM-7 cells into macrophages. Nonetheless, due to the subtle effects observed, the proposed changes to optimize the transdifferentiation approach used and the and the short time-window before the haploid cells regain diploidy[222], another system may be more feasible for generating human haploid macrophages, i.e. the recently described human haploid embryonic stem cells[257].

10. Methods

10.1. Cell culture

10.1.1. Growth conditions

All cells were incubated at 37°C, 95% humidity and 5% CO_2 and regularly checked for any contamination. Platinum-A (Plat-A) cells were grown in Dulbecco´s Modified Eagle Medium (DMEM) supplemented with 10% Fetal Calf Serum (FCS), 1µg/ml puromycin, 10µg/ml blasticidin. HAP1 and KBM-7 cells were grown in Iscove´s Modified Dulbecco´s Medium (IMDM) with 10% FCS, 200nM L-glutamine, 100 U/ml penicillin and 100µg/ml streptomycin if not stated differently. If indicated cells were exposed to immunological stimuli, i.e. LPS (10ng/ml) or heat killed group A streptococcus (HK GAS) ISS3348 with an MOI of 100. HK GAS was kindly provided by Marton Janos.

10.1.2. Splitting cells

Adherent Plat-A and HAP1 cells were washed with 1X PBS after removal of the medium and then incubated for approximately 3 minutes with 1X Trypsin-EDTA (GIBCO) at 37°C. Subsequently, trypsinization was stopped by adding at least the 10-fold amount of medium. The desired number of cells was then transferred to a new cell-culture treated dish. KBM-7 suspension cells were regularly passaged by transferring the desired number of cells into a new non cell-culture treated dish. Once a week KBM-7 cells were pelleted (300 rcf, 5 min) and re-suspended in medium prior passaging.

10.1.3. Freezing cells

After trypsinization was stopped (Plat-A and HAP1) or directly (KBM-7) cell were centrifuged for 5 min at 300 rcf. The cell pellet was re-suspended in in 1ml FCS with 10% DMSO and cells were immediately stored at -80°C. For long-term storage already frozen cells were stored in LN_2.

10.1.4. Thawing of frozen cells

1ml of frozen cells was quickly thawed and transferred to 9ml pre-warmed culture medium. The cells were centrifuged at 300 rcf for 5min. Afterwards the cell-pellet was re-suspended in 4ml or 10ml medium and then transferred to a 6cm or 10cm culture dish, respectively.

10.1.5. Single cell colonies

Colonies generated from single clones were established by either seeding manually 0.5 HAP1 cells per well or by sorting single GFP positive KBM-7 cells with FACS (BD FACS Aria) into a 96-well plate. FACS sorting was done in collaboration with Sauert T. form the FACS facility. Cells were expanded using normal culture conditions.

10.2. Retroviral transduction

The retrovirus, containing the C/EBPαER IRES GFP construct, was produced by transfecting Platinum-A cells with pMSCV C/EBPαER IRES GFP using FuGENE® HD Transfection Reagent (Promega, cat. no. E2311). The transfection was carried out in antibiotic-free medium and according to the manufactures' protocol. To harvest the retrovirus, Plat-A supernatant was pressed through a 0.45µm filter and immediately put on ice. To infected HAP1 and KBM-7 cells (about $3*10^4$ and $5*10^4$ cells were seeded the day before in 500µl medium, respectively) they were immediately added different amounts of viral suspension. As infection worked best with the highest volume, i.e. 500µl viral suspension, other cells incubated with 125µl, 50µl, 20µl and 5µl were discarded 3 days post infection.

10.3. Fluorescence microscopy

Retrovirally transduced HAP1 cells were steadily tested for GFP expression allowing to expand only C/EBPα positive single cell clones and also to ensure prior to each experiment that the retroviral construct was not silenced. Cells were seeded on a coverslip in 6-well plates 24h prior fixation with 1% CH_2O for 5 minutes at room temperature. Next, cells were washed 3 times with 1X TBS-T, stained with DAPI (1:3000) and again washed 3 times with 1X TBS-T before then the coverslip was put upside-down on a drop of mounting medium (Dako, fluorescence mounting medium #S302308). The microscope slide was finally dried for 10-15 min in dark and then either stored in a wet chamber at +4°C or directly used for GFP detection.

10.4. Flow cytometry

Prior each experiment C/EBPα positive KBM-7 clones were assessed for GFP expression on BD LSR Fortessa using approximately $1*10^6$ cells in 500µl normal culture medium. Cells were live/dead stained adding 1µl propidium iodide [1mg/ml] shortly before measurement and is depicted by the PE-A channel.

10.5. pMSCV C/EBPαER IRES GFP amplification and purification

5µg of the MSCV C/EBPαER IRES GFP plasmid (see ref. [198]) were kindly provided by Graf T. on a nitrocellulose membrane. 2.5µg of the plasmid were eluted by overnight incubation of the nitrocellulose in 50µl 1X TE-Buffer at room temperature. 2µl (0.1µg) of the plasmid were then transformed into competent DH5α *E. coli* using the heat shock method. In short, competent DH5α cells were thawed on ice, mixed with 0.1µg plasmid and put on ice for 30 minutes. Then the bacteria were heat-shocked for 45 seconds at 42°C and put back on ice for 5 minutes. The transformed DH5α cells were subsequently plated on LB-agar dishes supplemented with 100µg/ml ampicillin and incubated on 37°C for one day. Single colonies selected for the antibiotic were then inoculated into 4ml or 250ml liquid LB-medium containing 100µg/ml ampicillin, grown overnight. The thereby amplified plasmid was then purified using the QIAprep Spin Miniprep Kit (Quiagen, cat. no. 207104) or EndoFree Plasmid Maxi Kit (Quiagen, cat. no. 12362), respectively, using the spin-procedure according to the manufactures' protocol.

10.6. ELISA

After the pulsed transdifferentiation approach for 5 days (dual 1µM TMX treatment for three and two days, respectively), the culture medium was completely replaced by new one. 1ml of medium from unstimulated and LPS- or HK GAS stimulated cells was taken off and immediately centrifuged at 16.1 rcf for 5 minutes at 4°C. The supernatant was transferred into a new tube and stored at -80°C. Prior usage samples were slowly thawed on ice and applied undiluted or as 1:2, 1:4 and 1:8 dilutions for cytokine detection. TNF and CXCL8 secretion were determined using Cxcl8 ELISA (R&D Systems, DuoSet® ELISA, cat. no. DY208-05) and TNF ELISA (R&D Systems, DuoSet® ELISA, cat. no. DY210-05) according to the manufactures´ protocol.

10.7. Other methods

All other methods used, i.e. sequencing, protein isolation, SDS PAGE, Western blot, RNA isolation, DNA digestion, reverse transcription and gene expression analysis by qPCR were carried out as described in the section before (see 5. Materials and Methods) with following additions:

- For each experiment $5*10^5$ HAP1 or KBM-7 were seeded initially and as well as before 2nd TMX treatment in pulsed C/EBPα induction experiments
- KBM-7 cells were pelleted at 300 rcf for 5min at 4°C prior cell lysis with 1X Frackelton-Buffer or Isol-RNA Lysis Reagent (5 Prime, cat. no. 2302700)
- The primary antibody for C/EBPα detection in western blot was used in a 1:800 dilution (Santa Cruz Biotechnology, Inc., C/EBP α (14AA): sc-61)
- SDS PAGE was done by using a 8% resolution gel for protein separation
- Primer used for gene expression analysis are indicated below
  - Arbitrary Units (A.U.) were calculated by normalization to human *Hprt* expression as followed: A.U.= $2^{20\text{-Ct of gene of interest}} / 2^{20\text{-Ct of human } Hprt}$

Gene analyzed	Primer used	Primer sequence
Hprt	hHPRT_fwd	5´-TGTGTGCTCAAGGGGGGC-3´
	hHPRT_rev	5´-CGTGGGGTCCTTTTCACC-3´
Tnf	hTNF_fwd1	5´-GTGCTTGTTCCTCAGCCT-3´
	hTNF_rev1	5´-GGGTTTGCTACAACATGG-3´
Cxcl8	hCXCL8_fwd2	5´-ACCTCCAAACCTTTCCACCCC-3´
	hCXCL8_rev2	5´-CTCAGCCCTCTTCAAAAACTTCT-3´
Il-1b	hIL-1b_fwd	5'-ACTGCACGCTCCGGGACTCA-3’
	hIl-1b_rev	5'-GACATGGAGAACACCACTTGTTGC-3’
Cd14	CD14_FW	5´-GCCGCTGTGTAGGAAAGAAG-3´
	CD14_RV	5´-AGGTTCGGAGAAGTTGCAGA-3´
Csf1r	CSF1R_FW	5´-TCCAAAACACGGGGACCTATC-3´
	CSF1R_RV	5´-CGGGCAGGGTCTTTGACATA-3´
Itgam	Itgam_FW	5´-ACTGGTGAAGCCAATAACGCA-3´
	Itgam_RV	5´-TCCGTGATGACAACTAGGATCTT-3´
Spi1	Spi_FW	5´-AAATCAGGAACTTGTGCTGGC-3´
	Spi_RV	5´-TAATGGTCGCTATGGCTCTCC-3´

11. Supplementary

11.1. Supplementary Figures

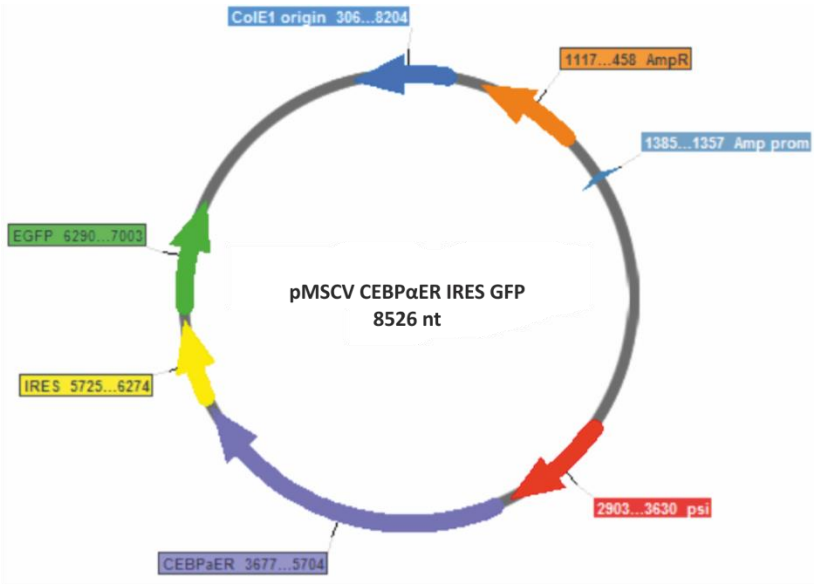

Supplementary Figure 1| Graphical map of pMSCV CEBPαER IRES GFP. Depicted is the map of the MSCV CEBPαER IRES GFP plasmid with its most important features and their orientation. Numbers indicate the first and last nucleotide of the indicated feature. Amplicinin promoter (light blue) and resistance (orange), ColE1 origin of replication (blue), psi packaging sequence (red), C/EBPαER fusion (purple), IRES (yellow) and EGFP (green).

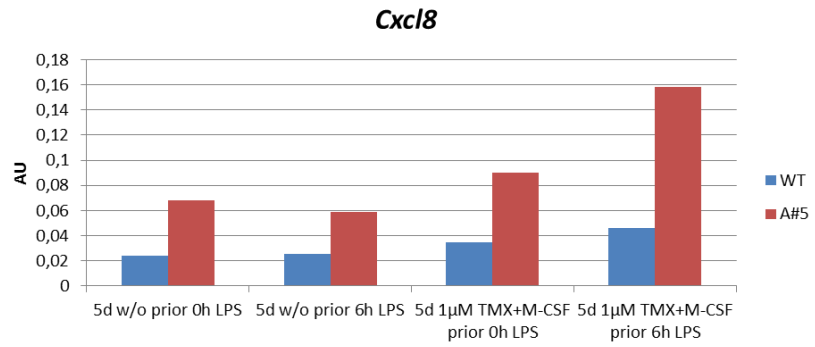

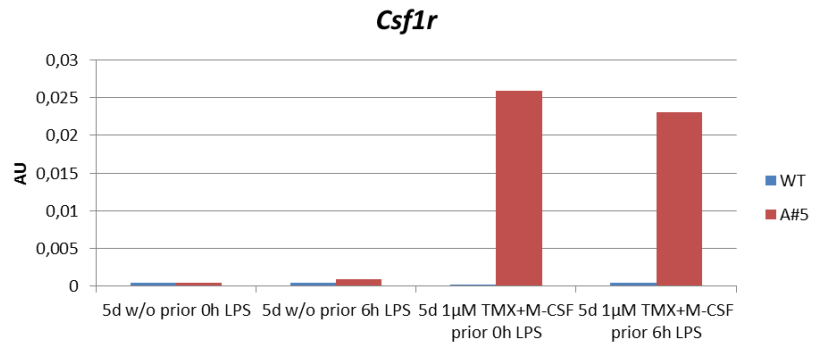

Supplementary Figure 2| Combined M-CSF and 4-OH tamoxifen treatment does not improve transdifferentiation. Gene expression analysis for *Cxcl8 and Csf1r* by qRT-PCR. KBM-7 WT (blue) and clone A #5 (red) were grown 5 days (3 days followed by 2 additional days) in normal (w/o) or M-CSF and 4-OH tamoxifen supplemented medium (TMX) followed by LPS treatment for 6 hours as indicated.

11.2. Supplementary Materials and Methods

11.2.1. Sanger sequencing of the plasmid MSCV C/EBPα IRES GFP

The pMSCV C/EBPα IRES GFP was a gift from Graf T. and has been described before[198]. After plasmid amplification in transformed DH5α *E. coli* the sequence correctness of the retroviral construct was verified using Sanger sequencing. The primers used are stated below. The obtained sequence shown matches the color-code of the MSCV C/EBPα IRES GFP plasmid **(Suppl. Fig. 1)**.

pBABE 5´	5´-CTTTATCCAGCCCTCAC-3´
pCHD-rev	5´-GCATTCCTTTGGCGAGAG-3´
FW_to CEBP	5´-GTACGAGCGCGTCGGG-3´
RV_to CEBP	5´-CAAAGGCGGCGTTGCTG-3´
FW_to ER	5´-TGATGTGGGAGAGGATGAGGA-3´
RV_to ER	5´-GTTTCCCTGCCACAGTCTGA-3´
RV_ins	5´-CTTCGCCCAGTTGATCATGTGAAC-3´
FW_ins	5´-GAACAGCTGAGCCGTGAACTG-3´
FW_gag	5´-CCTTGAACCTCCTCGTTCGAC-3´

CGTCTGTACTAGTTAGCTAACTAGCTCTGTATCTGGCGGACCCGTGGTGGAACTGACGAGTTCTGAACACCCGGCCGCAA
CCCTGGGAGACGTCCCAGGGACTTTGGGGGCCGTTTTTGTGGCCCGACCTGAGGAAGGGAGTCGATGTGGAATCCGACCC
CGTCAGGATATGTGGTTCTGGTAGGAGACGAGAACCTAAAACAGTTCCCGCCTCCGTCTGAATTTTTGCTTTCGGTTTGG
AACCGAAGCCGCGCGTCTTGTCTGCTGCAGCGCTGCAGCATCGTTCTGTGTTGTCTCTGTCTGACTGTGTTTCTGTATTT
GTCTGAAAATTAGGGCCAGACTGTTACCACTCCCTTAAGTTTGACCTTAGGTCACTGGAAAGATGTCGAGCGGATCGCTC
ACAACCAGTCGGTAGATGTCAAGAAGAGACGTTGGGTTACCTTCTGCTCTGCAGAATGGCCAACCTTTAACGTCGGATGG
CCGCGAGACGGCACCTTTAACCGAGACCTCATCACCCAGGTTAAGATCAAGGTCTTTTCACCTGGCCCGCATGGACACCC
AGACCAGGTCCCCTACATCGTGACCTGGGAAGCCTTGGCTTTTGACCCCCCTCCCTGGGTCAAGCCCTTTGTACACCCTA
AGCCTCCGCCTCCTCTTCCTCCATCCGCCCCGTCTCTCCCCCTTGAACCTCCTCGTTCGACCCCGCCTCGATCCTCCCTT
TATCCAGCCCTCACTCCTTCTCTAGGCGCCGGAATTAGATCTCTcgaggttaacatggagtcggccgacttctacgaggcg
gagccgcggcccccgatgagcagccacctccagagccccccgcacgcgcccag
caacgccgcctttggctttccccggggcgcgggccccgcgccgcccccagccccacctgccgccccggagccgctgggcg
gcatctgcgagcacgagacgtctatagacatcagcgcctacatcgacccggccgccttcaacgacgagttcctggccgac
ctcttccagcacagccggcagcaggagaaggccaaggcggcggcgggccccgcgggtggcggcggtgactttgactaccc
gggcgccccggcgggccccggcggtgcggtcatgtccgcgggggcgcacggacccccctcccggctacggctgtgcggcgg
ccggctacctggacggcaggctggagcccctgtacgagcgcgtcggggcgcccgcgctgcggccgctggtgatcaagcag
gagccccgcgaggaggacgaggcgaagcagctggcgctggccggcctcttcccctatcagcccccgccgccgccgccgcc
accgcacccgcacgcgtctcccgcgcacttggccgcccctcacttgcagttccagatcgcacactgcggccagaccacca
tgcacctgcagcctggccaccctacgccgccgccgacgcccgtgcccagccctcatcccgcgcctgcaatgggtgctgcg
ggcctgccgggccccgggggctcgctcaagggcttggctggtccgcaccccgacctccgcaccggcggcggcggcggcgg
cggggccggcgcgggcaaggccaagaagtcggtggataagaacagcaacgagtaccgggtacggcgggaacgcaacaaca
tcgcggtgcgcaagagccgagataaagccaaacagcgcaacgtggagacgcagcagaaggtgttggagttgaccagtgac
aatgaccgcctgcgcaagcgggtggaacagctgagccgtgaactggacacgctgcggggtatcttccgccagctgcctga
gagctccttggtcaaggccatgggcaactgcgcgccggatccatctgctggagacatgagagctgccaacctttggccaa
gcccgctcatgatcaaacgctctaagaagaacagcctggccttgtccctgacggccgaccagatggtcagtgccttgttg
gatgctgagccccccatactctattccgagtatgatcctaccagacccttCAGTGAAGCTTCGATGATGGGCTTACTGAC
CAACCTGGCAGACAGGGAGCTGGTTCACATGATCAACTGGGCGAAGAGGGTGCCAGGCTTTGTGGATTTGACCCTCCATG
ATCAGGTCCACCTTCTAGAATGTGCCTGGCTAGAGATCCTGATGATTGGTCTCGTCTGGCGCTCCATGGAGCACCCAGTG
AAGCTACTGTTTGCTCCTAACTTGCTCTTGGACAGGAACCAGGGAAAATGTGTAGAGGGCATGGTGGAGATCTTCGACAT

GCTGCTGGCTACATCATCTCGGTTCCGCATGATGAATCTGCAGGGAGAGGAGTTTGTGTGCCTCAAATCTATTATTTTGC
TTAATTCTGGAGTGTACACATTTCTGTCCAGCACCCTGAAGTCTCTGGAAGAGAAGGACCATATCCACCGAGTCCTGGAC
AAGATCACAGACACTTTGATCCACCTGATGGCCAAGGCAGGCCTGACCCTGCAGCAGCAGCACCAGCGGCTGGCCCAGCT
CCTCCTCATCCTCTCCCACATCAGGCACATGAGTAACAAAGGCATGGAGCATCTGTACAGCATGAAGTGCAAgaacgtgg
tgcccctctatgacctgctgctggagatgctggacgcccaccgcctacatgcgcccactagccgtggaggggcatccgtg
gaggagacggaccaaagccacttggccactgcgggctctacttcatcgcattccttgcaaaagtattacatcacgggggа
ggcagagggtttccctgccacagtctga
gagctccctggcaATTCCGCCCCCCCCCTAACGTTACTGGCCGAAGCCGCTTGGAATAAGGCCGGTGTGCGTTTGTCTATA
TGTTATTTTCCACCATATT
GCCGTCTTTTGGCAATGTGAGGGCCCGGAAACCTGGCCCTGTCTTCTTGACGAGCATTCCTAGGGGTCTTTCCCCTCTCG
CCAAAGGAATGCAAGGTCTGTTGAATGTCGTGAAGGAAGCAGTTCCTCTGGAAGCTTCTTGAAGACAAACAACGTCTGTA
GCGACCCTTTGCAGGCAGCGGAACCCCCCACCTGGCGACAGGTGCCTCTGCGGCCAAAAGCCACGTGTATAAGATACACC
TGCAAAGGCGGCACAACCCCAGTGCCACGTTGTGAGTTGGATAGTTGTGGAAAGAGTCAAATGGCTCTCCTCAAGCGTAT
TCAACAAGGGGCTGAAGGATGCCCAGAAGGTACCCCATTGTATGGGATCTGATCTGGGGCCTCGGTGCACATGCTTTACA
TGTGTTTAGTCGAGGTTAAAAAAACGTCTAGGCCCCCCGAACCACGGGGACGTGGTTTTCCTTTGAAAAACACGATAATAC
CATG GTGAGCAAGGGCGAGGAGCTGTTCACCGGGGTGGTGCCCATCCTGGTCGAGCTGGACGGCGACGTAAACGGCCACA
AGTT
CAGCGTGTCCGGCGAGGGCGAGGGCGATGCCACCTACGGCAAGCTGACCCTGAAGTTCATCTGCACCACCGGCAAGCTGC
CCGTGCCCTGGCCCACCCTCGTGACCACCCTGACCTACGGCGTGCAGTGCTTCAGCCGCTACCCCGACCACATGAAGCAG
CACGACTTCTTCAAGTCCGCCATGCCCGAAGGCTACGTCCAGGAGCGCACCATCTTCTTCAAGGACGACGGCAACTACAA
GACCCGCGCCGAGGTGAAGTTCGAGGGCGACACCCTGGTGAACCGCATCGAGCTGAAGGGCATCGACTTCAAGGAGGACG
GCAACATCCTGGGGCACAAGCTGGAGTACAACTACAACAGCCACAACGTCTATATCATGGCCGACAAGCAGAAGAACGGC
ATCAAGGTGAACTTCAAGATCCGCCACAACATCGAGGACGGCAGCGTGCAGCTCGCCGACCACTACCAGCAGAACACCCC
CATCGGCGACGGCCCCGTGCTGCTGCCCGACAACCACTACCTGAGCACCCAGTCCGCCCTGAGCAAAGACCCCAACGAGA
AGCGCGATCACATGGTCCTGCTGGAGTTCGTGACCGCCGCCGGGATCACTCTCGGCATGGACGAGCTGTACAAG

11.3. Supplementary Tables

Cell line	Clone	GFP intensity (+ to +++)
HAP1	#8	+++
	#9	+
	#14	++
	II #2	++
	II #4	+++
	II #8	+
	II #11	+++
	II #14	+
KBM-7	A #1	++
	A #5	+++
	A #9	++
	A #10	++
	A #11	+
	A #14	++
	A #19	+++
	A #20	+++
	A #22	++

Supplementary Table 7| Single cell clones of HAP1 and KBM-7 cells inducibly expressing C/EBPα. Colonies of single cells were attained by manually seeding single HAP1 cells or by FACS sorting KBM-7 cells. GFP (indicating successful retroviral infection and thus C/EBPα expression) intensity, ranging from low (+) to high (+++) was determined by fluorescence microscopy for HAP1 clones and while FACS sorting for KBM-7 clones.

12. References

1. Wu, H. J. & Wu, E. The role of gut microbiota in immune homeostasis and autoimmunity. *Gut Microbes* **3,** 4–14 (2012).
2. Chistiakov, D. A., Bobryshev, Y. V., Kozarov, E., Sobenin, I. A. & Orekhov, A. N. Intestinal mucosal tolerance and impact of gut microbiota to mucosal tolerance. *Front. Microbiol.* **6,** 1–9 (2015).
3. Abbas, A. K., Hichtman, A. H. & Pillai, S. *Cellular and molecular immunology*. *Saunders Elsevier* **6th Edition,** (2007).
4. Spits, H. & Cupedo, T. Innate Lymphoid Cells: Emerging Insights in Development, Lineage Relationships, and Function. *Annu. Rev. Immunol.* **30,** 647–675 (2012).
5. Walker, J. a, Barlow, J. L. & McKenzie, A. N. J. Innate lymphoid cells--how did we miss them? *Nat. Rev. Immunol.* **13,** 75–87 (2013).
6. Anderson, P., Phillips, K., Stoecklin, G. & Kedersha, N. Post-transcriptional regulation of proinflammatory proteins. *J. Leukoc. Biol.* **76,** 42–47 (2004).
7. Newman, R., McHugh, J. & Turner, M. RNA binding proteins as regulators of immune cell biology. *Clin. Exp. Immunol.* **183,** 37–49 (2016).
8. Lawrence, T. The nuclear factor NF-kappaB pathway in inflammation. *Cold Spring Harb. Perspect. Biol.* **1,** 1–10 (2009).
9. Müller, C. W. in *Data Mining in Structural Biology: Signal Transduction and Beyond* (eds. Schlichting, I. & Egner, U.) 143–166 (Springer Berlin Heidelberg, 2001). doi:10.1007/978-3-662-04645-6_8
10. Kovarik, P., Ebner, F. & Sedlyarov, V. Posttranscriptional regulation of cytokine expression. *Cytokine* (2015). doi:10.1016/j.cyto.2015.11.007
11. Moore, M. J. & Moore, M. J. From Birth to Death : The Complex Lives of Eukaryotic mRNAs. *Science* **1514,** 1514–1518 (2012).
12. Ganguly, K., Giddaluru, J., August, A. & Khan, N. Post-transcriptional Regulation of Immunological Responses through Riboclustering. *Front. Immunol.* **7,** 1–12 (2016).
13. Maquat, L. E. Nonsense-Mediated mRNA Decay: Splicing, Translation And mRNP Dynamics. *Nat. Rev. Mol. Cell Biol.* **5,** 89–99 (2004).
14. Mangus, D. A., Evans, M. C. & Jacobson, A. Poly(A)-binding proteins: multifunctional scaffolds for the post-transcriptional control of gene expression. *Genome Biol.* **4,** 223 (2003).
15. Carpenter, S., Ricci, E. P., Mercier, B. C., Moore, M. J. & Fitzgerald, K. a. Post-transcriptional regulation of gene expression in innate immunity. *Nat. Rev. Immunol.* **14,** 361–76 (2014).
16. Cooper, T. A., Wan, L. & Dreyfuss, G. RNA and Disease. *Cell* **136,** 777–793 (2009).
17. Kornblihtt, A. R. *et al.* Alternative splicing: a pivotal step between eukaryotic transcription and translation. *Nat. Rev. Mol. Cell Biol.* **14,** 153–65 (2013).
18. Rodrigues, R., Grosso, A. R. & Moita, L. Genome-Wide Analysis of Alternative Splicing during Dendritic Cell Response to a Bacterial Challenge. *PLoS One* **8,** (2013).
19. Sandberg, R., Neilson, J. R., Sarma, A., Sharp, P. a & Burge, C. B. Proliferating cells express mRNAs with shortened 3′ UTRs and fewer microRNA target sites. *Science (80-.).* **320,** 1643–1647 (2008).
20. Wang, I. X. *et al.* ADAR Regulates RNA Editing, Transcript Stability, and Gene Expression. *Cell Rep.* **5,** 849–860 (2013).
21. Ross, J. mRNA Stability in Mammalian Cells. **59,** 423–450 (1995).
22. Seko, Y., Cole, S., Kasprzak, W., Shapiro, B. A. & Ragheb, J. A. The role of cytokine mRNA stability in the pathogenesis of autoimmune disease. *Autoimmun. Rev.* **5,** 299–305 (2006).
23. Kedersha, N. *et al.* Stress granules and processing bodies are dynamically linked sites of mRNP remodeling. *J. Cell Biol.* **169,** 871–884 (2005).
24. Houseley, J. & Tollervey, D. The Many Pathways of RNA Degradation. *Cell* **136,** 763–776 (2009).
25. Schwede, A. *et al.* A role for Caf1 in mRNA deadenylation and decay in trypanosomes and human cells. *Nucleic Acids Res.* **36,** 3374–3388 (2008).
26. Tucker, M., Staples, R. R., Valencia-sanchez, M. a, Muhlrad, D. & Parker, R. Ccr4p is the catalytic subunit of a Ccr4p / Pop2p / Notp mRNA deadenylase complex in Saccharomyces cerevisiae. **21,** 1427–1436 (2002).
27. Kim, J. H. & Richter, J. D. Opposing Polymerase-Deadenylase Activities Regulate Cytoplasmic Polyadenylation. *Mol. Cell* **24,** 173–183 (2006).
28. Tucker, M. *et al.* The transcription factor associated Ccr4 and Caf1 proteins are components of the major cytoplasmic mRNA deadenylase in Saccharomyces cerevisiae. *Cell* **104,** 377–386 (2001).
29. Chen, J., Chiang, Y. C. & Denis, C. L. CCR4, a 3′- 5′ poly(A) RNA and ssDNA exonuclease, is the catalytic component of the cytoplasmic

deadenylase. *EMBO J.* **21,** 1414–1426 (2002).
30. Garneau, N. L., Wilusz, J. & Wilusz, C. J. The highways and byways of mRNA decay. *Nat. Rev. Mol. Cell Biol.* **8,** 113–126 (2007).
31. She, M. *et al.* Structural Basis of Dcp2 Recognition and Activation by Dcp1. *Mol. Cell* **29,** 337–349 (2008).
32. Deshmukh, M. V. *et al.* mRNA Decapping Is Promoted by an RNA-Binding Channel in Dcp2. *Mol. Cell* **29,** 324–336 (2008).
33. Eulalio, A., Behm-Ansmant, I. & Izaurralde, E. P bodies: at the crossroads of post-transcriptional pathways. *Nat. Rev. Mol. Cell Biol.* **8,** 9–22 (2007).
34. Castello, A. *et al.* Insights into RNA Biology from an Atlas of Mammalian mRNA-Binding Proteins. *Cell* **149,** 1393–1406 (2012).
35. Gerstberger, S., Hafner, M. & Tuschl, T. A census of human RNA-binding proteins. *Nat. Rev. Genet.* **15,** 829–845 (2014).
36. Eberhardt, W., Doller, A., Akool, E.-S. & Pfeilschifter, J. Modulation of mRNA stability as a novel therapeutic approach. *Pharmacol. Ther.* **114,** 56–73 (2007).
37. Hao, S. & Baltimore, D. The stability of mRNA influences the temporal order of the induction of genes encoding inflammatory molecules. *Nat. Immunol.* **10,** 281–288 (2009).
38. Stoecklin, G., Lu, M., Rattenbacher, B. & Moroni, C. A constitutive decay element promotes tumor necrosis factor alpha mRNA degradation via an AU-rich element-independent pathway. *Mol. Cell. Biol.* **23,** 3506–15 (2003).
39. Mino, T. *et al.* Regnase-1 and roquin regulate a common element in inflammatory mRNAs by spatiotemporally distinct mechanisms. *Cell* **161,** 1058–1073 (2015).
40. Masuda, K. *et al.* Arid5a regulates naive CD4 + T cell fate through selective stabilization of Stat3 mRNA. *J. Exp. Med.* **213,** 605–619 (2016).
41. Linker, K. *et al.* Involvement of KSRP in the post-transcriptional regulation of human iNOS expression-complex interplay of KSRP with TTP and HuR. *Nucleic Acids Res.* **33,** 4813–4827 (2005).
42. Taylor, G. A. *et al.* The human TTP protein: sequence, alignment with related proteins, and chromosomal localization of the mouse and human genes. *Nucleic Acids Res.* **19,** 3454 (1991).
43. Dubois, R. N. *et al.* A Growth Factor-inducible Nuclear Protein with a Novel Cysteine / Histidine Repetitive Sequence. *J. Biol. Chem.* **265,** 19185–91 (1990).
44. Taylor, G. A. *et al.* A pathogenetic role for TNFα in the syndrome of cachexia, arthritis, and autoimmunity resulting from tristetraprolin (TTP) deficiency. *Immunity* **4,** 445–454 (1996).
45. Blackshear, P. J. & Brooks, S. A. Tristetraprolin (TTP): Interactions with mRNA and proteins, and current thoughts on mechanisms of action. *Biochim. Biophys. Acta* **1829,** 666–679 (2013).
46. Matthews, J. M. & Sunde, M. Zinc Fingers — Folds for Many Occasions. *IUMB Life* **54,** 351–355 (2002).
47. Blackshear, P. J. Zfp36l3, a Rodent X Chromosome Gene Encoding a Placenta-Specific Member of the Tristetraprolin Family of CCCH Tandem Zinc Finger Proteins. *Biol. Reprod.* **73,** 297–307 (2005).
48. Stumpo, D. J. *et al.* Targeted disruption of Zfp36l2, encoding a CCCH tandem zinc finger RNA-binding protein, results in defective hematopoiesis. *Blood* **114,** 2401–2410 (2009).
49. Bell, S. E. *et al.* The RNA binding protein Zfp36l1 is required for normal vascularisation and post-transcriptionally regulates VEGF expression. *Dev. Dyn.* **235,** 3144–3155 (2006).
50. Zhang, L. *et al.* ZFP36L2 is required for self-renewal of early burst-forming unit erythroid progenitors. *Nature* **499,** 92–96 (2013).
51. Carballo, E. & Blackshear, P. J. Roles of tumor necrosis factor-α receptor subtypes in the pathogenesis of the tristetraprolin-deficiency syndrome. *Blood* **98,** 2389–2395 (2001).
52. Carballo, E. *et al.* Bone Marrow Transplantation Reproduces the Tristetraprolin-Deficiency Syndrome in Recombination Activating Gene-2 (- / -) Mice. *J. Clin. Invest* **100,** 986–995 (1997).
53. Kaplan, I. M. *et al.* Deletion of Tristetraprolin Caused Spontaneous Reactive Granulopoiesis by a Non-Cell-Autonomous Mechanism Without Disturbing Long-Term Hematopoietic Stem Cell Quiescence. *J. Immunol.* **186,** 2826–2834 (2011).
54. Qiu, L.-Q., Stumpo, D. J. & Blackshear, P. J. Myeloid-specific tristetraprolin deficiency in mice results in extreme lipopolysaccharide sensitivity in an otherwise minimal phenotype. *J. Immunol.* **188,** 5150–9 (2012).
55. Kratochvill, F. *et al.* Tristetraprolin-driven regulatory circuit controls quality and timing of mRNA decay in inflammation. *Mol. Syst. Biol.* **7,** 560 (2011).
56. Molle, C. *et al.* Tristetraprolin regulation of interleukin 23 mRNA stability prevents a spontaneous inflammatory disease. *J. Exp. Med.* **210,** 1675–84 (2013).
57. Kang, J.-G. *et al.* Zinc Finger Protein Tristetraprolin Interacts with CCL3 mRNA and Regulates Tissue Inflammation. *J. Immunol.* **187,** 2696–2701 (2011).
58. Shaw, G. & Kamen, R. A conserved adenine-uridine sequence from the 3' untranslated region of granulocyte-monocyte colony stimulating factor messenger RNA mediates selective messenger RNA degradation. *Cell* **46,**

659–668 (1986).
59. Carballo, E., Lai, W. S. & Blackshear, P. J. Evidence that tristetraprolin is a physiological regulator of granulocyte-macrophage colony-stimulating factor messenger RNA deadenylation and stability. *Blood* **95,** 1891–1899 (2000).
60. Blackshear, P. J. *et al.* Characteristics of the interaction of a synthetic human tristetraprolin tandem zinc finger peptide with AU-rich element-containing RNA substrates. *J. Biol. Chem.* **278,** 19947–19955 (2003).
61. Worthington, M. T. *et al.* RNA binding properties of the AU-rich element-binding recombinant Nup475/TIS11/tristetraprolin protein. *J. Biol. Chem.* **277,** 48558–48564 (2002).
62. Mukherjee, N. *et al.* Global target mRNA specification and regulation by the RNA-binding protein ZFP36. *Genome Biol.* **15,** R12 (2014).
63. Tiedje, C. *et al.* The RNA-binding protein TTP is a global post-transcriptional regulator of feedback control in inflammation. *Nucleic Acids Res.* **44,** 7418–7440 (2016).
64. Sedlyarov, V. *et al.* TTP binding site atlas in the macrophage transcriptome reveals a switch for inflammation resolution. *Mol. Syst. Biol.* **12,** 1–21 (2016).
65. Lai, W. S., Carballo, E., Thorn, J. M., Kennington, E. A. & Blackshear, P. J. Interactions of CCCH zinc finger proteins with mRNA. Binding of tristetraprolin-related zinc finger proteins to AU-rich elements and destabilization of mRNA. *J. Biol. Chem.* **275,** 17827–17837 (2000).
66. Morgan, B. R. & Massi, F. A computational study of RNA binding and specificity in the tandem zinc finger domain of TIS11d. *Protein Sci.* **19,** 1222–1234 (2010).
67. Deveau, L. M. & Massi, F. Three Residues Make an Evolutionary Switch for Folding and RNA-Destabilizing Activity in the TTP Family of Proteins. *ACS Chem. Biol.* **11,** 435–443 (2016).
68. Franks, T. M. & Lykke-Andersen, J. TTP and BRF proteins nucleate processing body formation to silence mRNAs with AU-rich elements. *Genes Dev.* **21,** 719–735 (2007).
69. Fenger-Grøn, M., Fillman, C., Norrild, B. & Lykke-Andersen, J. Multiple processing body factors and the ARE binding protein TTP activate mRNA decapping. *Mol. Cell* **20,** 905–915 (2005).
70. Sandler, H., Kreth, J., Timmers, H. T. M. & Stoecklin, G. Not1 mediates recruitment of the deadenylase Caf1 to mRNAs targeted for degradation by tristetraprolin. *Nucleic Acids Res.* **39,** 4373–4386 (2011).
71. Lykke-Andersen, J. & Wagner, E. Recruitment and activation of mRNA decay enzymes by two ARE-mediated decay activation domains in the proteins TTP and BRF-1. *Genes Dev.* **19,** 351–361 (2005).
72. Fabian, M. R. *et al.* Structural basis for the recruitment of the human CCR4-NOT deadenylase complex by tristetraprolin. *Nat. Struct. Mol. Biol.* **20,** 735–9 (2013).
73. Tchen, C. R., Brook, M., Saklatvala, J. & Clark, A. R. The stability of tristetraprolin mRNA is regulated by mitogen-activated protein kinase p38 and by tristetraprolin itself. *J. Biol. Chem.* **279,** 32393–32400 (2004).
74. Brook, M. *et al.* Posttranslational Regulation of Tristetraprolin Subcellular Localization and Protein Stability by p38 Mitogen-Activated Protein Kinase and Extracellular Signal-Regulated Kinase Pathways. *Mol. Cell. Biol.* **26,** 2408–2418 (2006).
75. Kratochvill, F. *et al.* Tristetraprolin limits inflammatory cytokine production in tumor-associated macrophages in an mRNA decay-independent manner. *Cancer Res.* **75,** 3054–3064 (2015).
76. Qi, M.-Y. *et al.* AU-rich-element-dependent translation repression requires the cooperation of tristetraprolin and RCK/P54. *Mol. Cell. Biol.* **32,** 913–28 (2012).
77. Tao, X. & Gao, G. Tristetraprolin Recruits Eukaryotic Initiation Factor 4E2 To Repress Translation of AU-Rich Element-Containing mRNAs. *Mol. Cell. Biol.* **35,** 3921–32 (2015).
78. Ptushkina, M. *et al.* A second eIF4E protein in Schizosaccharomyces pombe has distinct eIF4G-binding properties. *Nucleic Acids Res.* **29,** 4561–4569 (2001).
79. Zuberek, J. *et al.* Weak binding affinity of human 4EHP for mRNA cap analogs. *RNA* **13,** 691–697 (2007).
80. Cao, H., Deterding, L. J. & Blackshear, P. J. Identification of a major phosphopeptide in human tristetraprolin by phosphopeptide mapping and mass spectrometry. *PLoS One* **9,** 1–13 (2014).
81. Chrestensen, C. A. *et al.* MAPKAP Kinase 2 Phosphorylates Tristetraprolin on in Vivo Sites Including Ser178, a Site Required for 14-3-3 Binding. *J. Biol. Chem.* **279,** 10176–10184 (2004).
82. Stoecklin, G. *et al.* MK2-induced tristetraprolin:14-3-3 complexes prevent stress granule association and ARE-mRNA decay. *EMBO J.* **23,** 1313–24 (2004).
83. Clement, S. L., Scheckel, C., Stoecklin, G. & Lykke-Andersen, J. Phosphorylation of tristetraprolin by MK2 impairs AU-rich element mRNA decay by preventing deadenylase recruitment. *Mol. Cell. Biol.* **31,** 256–66 (2011).
84. Hitti, E. *et al.* Mitogen-Activated Protein Kinase-Activated Protein Kinase 2 Regulates Tumor Necrosis Factor mRNA Stability and Translation Mainly by Altering Tristetraprolin Expression,

Stability, and Binding to Adenine/Uridine-Rich Element. *Mol. Cell. Biol.* **26,** 2399–2407 (2006).
85. Sun, L. *et al.* Tristetraprolin (TTP)-14-3-3 complex formation protects TTP from dephosphorylation by protein phosphatase 2a and stabilizes tumor necrosis factor-α mRNA. *J. Biol. Chem.* **282,** 3766–3777 (2007).
86. Tiedje, C. *et al.* The p38/MK2-Driven Exchange between Tristetraprolin and HuR Regulates AU-Rich Element-Dependent Translation. *PLoS Genet.* **8,** (2012).
87. Coulthard, L. R., White, D. E., Jones, D. L. & Mcdermott, M. F. p38 MAPK : stress responses from molecular mechanisms to therapeutics. *Trensds Mol Med.* **15,** 369–379 (2011).
88. Ross, E. A. *et al.* Dominant Suppression of Inflammation via Targeted Mutation of the mRNA Destabilizing Protein Tristetraprolin. *J. Immunol.* **195,** 265–276 (2015).
89. Schichl, Y. M., Resch, U., Lemberger, C. E., Stichlberger, D. & De Martin, R. Novel phosphorylation-dependent ubiquitination of tristetraprolin by mitogen-activated protein kinase/extracellular signal-regulated kinase kinase kinase 1 (MEKK1) and tumor necrosis factor receptor-associated factor 2 (TRAF2). *J. Biol. Chem.* **286,** 38466–38477 (2011).
90. Ngoc, L. V. *et al.* Rapid Proteasomal Degradation of Posttranscriptional Regulators of the TIS11/Tristetraprolin Family Is Induced by an Intrinsically Unstructured Region Independently of Ubiquitination. *Mol. Cell. Biol.* **34,** 4315–28 (2014).
91. Phillips, R. S., Ramos, S. B. V & Blackshear, P. J. Members of the tristetraprolin family of tandem CCCH zinc finger proteins exhibit CRM1-dependent nucleocytoplasmic shuttling. *J. Biol. Chem.* **277,** 11606–11613 (2002).
92. Murata, T., Yoshino, Y., Morita, N. & Kaneda, N. Identification of nuclear import and export signals within the structure of the zinc finger protein TIS11. *Biochem. Biophys. Res. Commun.* **293,** 1242–1247 (2002).
93. Liang, J. *et al.* RNA-destabilizing factor tristetraprolin negatively regulates NF-κB signaling. *J. Biol. Chem.* **284,** 29383–29390 (2009).
94. Schichl, Y. M., Resch, U., Hofer-Warbinek, R. & de Martin, R. Tristetraprolin impairs NF-κB/p65 nuclear translocation. *J. Biol. Chem.* **284,** 29571–29581 (2009).
95. Barrios-García, T. *et al.* Tristetraprolin represses estrogen receptor α transactivation in breast cancer cells. *J. Biol. Chem.* **289,** 15554–65 (2014).
96. Barrios-García, T., Gómez-Romero, V., Tecalco-Cruz, Á., Valadéz-Graham, V. & León-Del-Río, A. Nuclear tristetraprolin acts as a corepressor of multiple steroid nuclear receptors in breast cancer cells. *Mol. Genet. Metab. Reports* **7,** 20–26 (2016).
97. Grammatikakis, I., Abdelmohsen, K. & Gorospe, M. Posttranslational control of HuR function. *Wiley Interdiscip. Rev. RNA* (2016). doi:10.1002/wrna.1372
98. Mukherjee, N. *et al.* Integrative Regulatory Mapping Indicates that the RNA-Binding Protein HuR Couples Pre-mRNA Processing and mRNA Stability. *Mol. Cell* **43,** 327–339 (2011).
99. Lebedeva, S. *et al.* Transcriptome-wide Analysis of Regulatory Interactions of the RNA-Binding Protein HuR. *Mol. Cell* **43,** 340–352 (2011).
100. King, P. H., Levine, T. D., Fremeau, R. T. & Keene, J. D. Mammalian homologs of Drosophila ELAV localized to a neuronal subset can bind in vitro to the 3' UTR of mRNA encoding the Id transcriptional repressor. *J. Neurosci.* **14,** 1943–52 (1994).
101. Hinman, M. N. & Lou, H. Diverse molecular functions of Hu proteins. *Cell. Mol. Life Sci.* **65,** 3168–3181 (2008).
102. Ma, W., Cheng, S., Campbell, C., Wright, A. & Furneaux, H. Nucleic Acids , Protein Synthesis , and Molecular Genetics : Cloning and Characterization of HuR , a Ubiquitously Expressed Elav-like Protein Cloning and Characterization of HuR , a Ubiquitously Expressed Elav-like Protein *. **271,** 8144–8151 (1996).
103. Fan, C. X. & Steitz, J. A. HNS , a nuclear-cytoplasmic shuttling sequence in HuR. *Proc. Natl. Acad. Sci. USA* **95,** 15293–15298 (1998).
104. Wang, W. *et al.* HuR regulates p21 mRNA stabilization by UV light. *Mol. Cell. Biol.* **20,** 760–769 (2000).
105. Gallouzi, I. E. *et al.* HuR binding to cytoplasmic mRNA is perturbed by heat shock. 11441–11446 (2003).
106. Yaman, I. *et al.* Nutritional Control of mRNA Stability Is Mediated by a Conserved AU-rich Element That Binds the Cytoplasmic Shuttling Protein HuR. *J Biol Chem.* **277,** 41539–41546 (2002).
107. Zucal, C. *et al.* Targeting the Multifaceted HuR Protein, Benefits and Caveats. *Curr. Drug Targets* **16,** 1–17 (2015).
108. Katsanou, V. *et al.* The RNA-binding protein Elavl1/HuR is essential for placental branching morphogenesis and embryonic development. *Mol. Cell. Biol.* **29,** 2762–2776 (2009).
109. Ghosh, M. *et al.* Essential role of the RNA-binding protein HuR in progenitor cell survival in mice. *J. Clin. Invest.* **119,** 3530–3543 (2009).
110. Papadaki, O. *et al.* Control of thymic T cell maturation, deletion and egress by the RNA-binding protein HuR. *J. Immunol.* **182,** 6779–

6788 (2009).
111. Diaz-Muñoz, M. D. *et al.* The RNA-binding protein HuR is essential for the B cell antibody response. *Nat. Immunol.* **16,** 415–25 (2015).
112. Srikantan, S. & Gorospe, M. HuR function in disease. *Front. Biosci.* **17,** 189–205 (2012).
113. Govindaraju, S. & Lee, B. S. Adaptive and maladaptive expression of the mRNA regulatory protein HuR. *World J. Biol. Chem.* **4,** 111–8 (2013).
114. Yiakouvaki, A. *et al.* Myeloid cell expression of the RNA-binding protein HuR protects mice from pathologic inflammation and colorectal carcinogenesis. *J. Clin. Invest.* **122,** 48–61 (2012).
115. Katsanou, V. *et al.* HuR as a negative posttranscriptional modulator in inflammation. *Mol. Cell* **19,** 777–789 (2005).
116. Lodish, H. F., Zhou, B., Liu, G. & Chen, C.-Z. Micromanagement of the immune system by microRNAs. *Nat. Rev. Immunol.* **8,** 120–130 (2008).
117. Lee, Y. *et al.* MicroRNA genes are transcribed by RNA polymerase II. *Eur. Mol. Biol. Organ. J.* **23,** 4051–4060 (2004).
118. Borchert, G. M., Lanier, W. & Davidson, B. L. RNA polymerase III transcribes human microRNAs. *Nat. Struct. Mol. Biol.* **13,** 1097–1101 (2006).
119. Landthaler, M., Yalcin, A. & Tuschl, T. The Human DiGeorge Syndrome Critical Region Gene 8 and Its D. melanogaster Homolog Are Required for miRNA Biogenesis. *Curr. Biol.* **14,** 2162–2167 (2004).
120. Denli, A. M., Tops, B. B. J., Plasterk, R. H. a, Ketting, R. F. & Hannon, G. J. Processing of primary microRNAs by the Microprocessor complex. *Nature* **432,** 231–5 (2004).
121. Lee, Y. *et al.* The nuclear RNase III Drosha initiates microRNA processing. *Nature* **425,** 415–419 (2003).
122. Bohnsack, M. T., Czaplinski, K. & Gorlich, D. Exportin 5 is a RanGTP-dependent dsRNA-binding protein that mediates nuclear export of pre-miRNAs. *RNA* **10,** 185–91 (2004).
123. Yi, R., Qin, Y., Macara, I. G. & Cullen, B. R. Exportin-5 mediates the nuclear export of pre-microRNAs and short hairpin RNAs Exportin-5 mediates the nuclear export of pre-microRNAs and short hairpin RNAs. 3011–3016 (2003). doi:10.1101/gad.1158803
124. Bernstein, E., Caudy, a a, Hammond, S. M. & Hannon, G. J. Role for a bidentate ribonuclease in the initiation step of RNA interference. *Nature* **409,** 363–366 (2001).
125. Hammond, S. M., Bernstein, E., Beach, D. & Hannon, G. J. An RNA-directed nuclease mediates post-transcriptional gene silencing in Drosophila cells. *Nature* **404,** 293–296 (2000).
126. Lingel, A., Simon, B., Izaurralde, E. & Sattler, M. Structure and nucleic-acid binding of the Drosophila Argonaute 2 PAZ domain. *Nature* **426,** 465–9 (2003).
127. Liu, J. *et al.* Argonaute2 Is the Catalytic Engine of Mammalian RNAi. *Science (80-.).* **305,** 1437–1441 (2004).
128. Asirvatham, A. J., Magner, W. J. & Tomasi, T. B. miRNA regulation of cytokine genes. *Cytokine* **45,** 58–69 (2009).
129. Pedersen, I. M. *et al.* Interferon modulation of cellular microRNAs as an antiviral mechanism. *Nature* **449,** 919–922 (2007).
130. Taganov, K. D., Boldin, M. P., Chang, K.-J. & Baltimore, D. NF-kappaB-dependent induction of microRNA miR-146, an inhibitor targeted to signaling proteins of innate immune responses. *Proc. Natl. Acad. Sci. U. S. A.* **103,** 12481–6 (2006).
131. Moschos, S. A. *et al.* Expression profiling in vivo demonstrates rapid changes in lung microRNA levels following lipopolysaccharide-induced inflammation but not in the anti-inflammatory action of glucocorticoids. *BMC Genomics* **8,** 240 (2007).
132. Landgraf, P. *et al.* A Mammalian microRNA Expression Atlas Based on Small RNA Library Sequencing. *Cell* **129,** 1401–1414 (2007).
133. Asirvatham, A. J., Gregorie, C. J., Hu, Z., Magner, W. J. & Tomasi, T. B. MicroRNA Targets in Immune Genes and the Dicer/Argonaute and ARE Machinery Components. *Mol. Immunol.* **45,** 1995–2006 (2008).
134. Young, L. E. *et al.* The mRNA Binding Proteins HuR and Tristetraprolin Regulate Cyclooxygenase 2 Expression During Colon Carcinogenesis. *Gastroenterology* **136,** 1669–1679 (2009).
135. Lu, Y. C. *et al.* ELAVL1 Modulates Transcriptome-wide miRNA Binding in Murine Macrophages. *Cell Rep.* **9,** 2330–2343 (2014).
136. Xun, G., Yuehan, W. & S., H. R. MicroRNA-125a represses cell growth by targeting HuR in breast cancer. *RNA Bio.* **6,** 575–583 (2009).
137. Abdelmohsen, K. *et al.* miR-519 suppresses tumor growth by reducing HuR levels. *Cell Cycle* **9,** 1354–1359 (2010).
138. Al-Ahmadi, W., Al-Ghamdi, M., Al-Souhibani, N. & Khabar, K. S. A. MiR-29a inhibition normalizes HuR over-expression and aberrant AU-rich mRNA stability in invasive cancer. *J. Pathol.* **230,** 28–38 (2013).
139. Dan, C. *et al.* Modulation of TNF- α mRNA stability by human antigen R and miR181s in sepsis-induced immunoparalysis. *EMBO Mol. Med.* 1–18 (2014).
140. Jing, Q. *et al.* Involvement of MicroRNA in AU-Rich Element-Mediated mRNA Instability. *Cell*

120, 623–634 (2005).
141. Zhang, B. *et al.* A novel RNA motif mediates the strict nuclear localization of a long noncoding RNA. *Mol. Cell. Biol.* **34,** 2318–2329 (2014).
142. Prasanth, K. V. *et al.* Regulating gene expression through RNA nuclear retention. *Cell* **123,** 249–263 (2005).
143. Hutchinson, J. N. *et al.* A screen for nuclear transcripts identifies two linked noncoding RNAs associated with SC35 splicing domains. *BMC Genomics* **8,** 39 (2007).
144. Wandruszka, L. M. Regulation of TTP activity by posttranslational modification and subcellular localization. (2016).
145. Rigby, W. F. C. *et al.* Structure/Function Analysis of Tristetraprolin (TTP): p38 Stress-Activated Protein Kinase and Lipopolysaccharide Stimulation Do Not Alter TTP Function. *J. Immunol.* **174,** 7883–7893 (2005).
146. Yamano, S., Dai, J. & Moursi, A. M. Comparison of transfection efficiency of nonviral gene transfer reagents. *Mol. Biotechnol.* **46,** 287–300 (2010).
147. Sauer, I. *et al.* Interferons limit inflammatory responses by induction of tristetraprolin. *Blood* **107,** 4790–4797 (2006).
148. Sun, X. J. *et al.* MicroRNA-29a Promotes Pancreatic Cancer Growth by Inhibiting Tristetraprolin. *Cell. Physiol. Biochem.* **37,** 707–718 (2015).
149. Xu, F. *et al.* Loss of repression of HuR translation by miR-16 may be responsible for the elevation of HuR in human breast carcinoma. *J. Cell. Biochem.* **111,** 727–734 (2010).
150. Kim, H. H. *et al.* HuR recruits let-7 / RISC to repress c-Myc expression. *Genes Dev.* **23,** 1743–1748 (2009).
151. Johnson, B. A., Stehn, J. R., Yaffe, M. B. & Keith Blackwell, T. Cytoplasmic localization of tristetraprolin involves 14-3-3-dependent and -independent mechanisms. *J. Biol. Chem.* **277,** 18029–18036 (2002).
152. Rowlett, R. M. *et al.* Inhibition of tristetraprolin deadenylation by poly(A) binding protein. *Am. J. Physiol. Gastrointest. Liver Physiol.* **295,** G421-30 (2008).
153. Hausburg, M. A. *et al.* Post-transcriptional regulation of satellite cell quiescence by TTP-mediated mRNA decay. *Elife* 1–18 (2015). doi:10.7554/eLife.03390
154. Boyanovsky, B. B., Shridas, P., Simons, M., Westhuyzen, D. R. Van Der & Webb, N. R. Syndecan-4 mediates macrophage uptake of group V secretory phospholipase A 2 -modified LDL. *J. Lipid Res.* **50,** 641–650 (2009).
155. Nadella, V., Wang, Z., Johnson, T. S., Grif, M. & Devitt, A. Transglutaminase 2 interacts with syndecan-4 and CD44 at the surface of human macrophages to promote removal of apoptotic cells. **1853,** 201–212 (2015).
156. Shi, J. X., Su, X., Xu, J., Zhang, W. Y. & Shi, Y. HuR post-transcriptionally regulates TNF-α induced IL-6 expression in human pulmonary microvascular endothelial cells mainly via tristetraprolin. *Respir. Physiol. Neurobiol.* **181,** 154–161 (2012).
157. Schaljo, B. *et al.* Tristetraprolin is required for full anti-inflammatory response of murine macrophages to IL-10. *J. Immunol.* **183,** 1197–206 (2009).
158. Tudor, C. *et al.* p38 mitogen-activated protein kinase inhibits tristetraprolin- directed decay of the mRNA of the anti-inflammatory cytokine interleukin-10. *FEBS Lett.* **583,** 1933–1938 (2009).
159. Stoecklin, G. *et al.* Genome-wide analysis identifies interleukin-10 mRNA as target of tristetraprolin. *J. Biol. Chem.* **283,** 11689–11699 (2008).
160. Cao, H. *et al.* Identification of the anti-inflammatory protein tristetraprolin as a hyperphosphorylated protein by mass spectrometry and site-directed mutagenesis. *Biochem. J.* **394,** 285–97 (2006).
161. Resch, U. *et al.* Polyubiquitinated tristetraprolin protects from TNF-induced, caspase-mediated apoptosis. *J. Biol. Chem.* **289,** 25088–25100 (2014).
162. Miller, J. C. *et al.* An improved zinc-finger nuclease architecture for highly specific genome editing. *Nat. Biotechnol.* **25,** 778–85 (2007).
163. Ran, F. A. *et al.* Genome engineering using the CRISPR-Cas9 system. *Nat. Protoc.* **8,** 2281–2308 (2013).
164. Kuo, M. H. & Allis, C. D. In vivo cross-linking and immunoprecipitation for studying dynamic Protein:DNA associations in a chromatin environment. *Methods* **19,** 425–433 (1999).
165. Yang, L., Zhang, H. & Bruce, J. E. Optimizing the detergent concentration conditions for immunoprecipitation (IP) coupled with LC-MS/MS identification of interacting proteins. *Analyst* **134,** 755–762 (2009).
166. Wilusz, J. E. *et al.* A triple helix stabilizes the 3′ ends of long noncoding RNAs that lack poly(A) tails. *Genes Dev.* **26,** 2392–2407 (2012).
167. Brown, J. A. *et al.* Structural insights into the stabilization of MALAT1 noncoding RNA by a bipartite triple helix. *Nat. Struct. Mol. Biol.* **21,** 633–40 (2014).
168. Dreyfuss, G., Matunis, M. J., Pinol-Roma, S. & Burd, C. G. hnRNP Proteins and the Biogenesis of mRNA. *Annu. Rev. Biochem.* **62,** 289–321 (1993).
169. Han, S. P., Tang, Y. H. & Smith, R. Functional diversity of the hnRNPs: past, present and perspectives. *Biochem. J.* **430,** 379–392 (2010).

170. Reznik, B., Clement, S. L. & Lykke-Andersen, J. hnRNP F Complexes with tristetraprolin and stimulates ARE-mRNA decay. *PLoS One* **9,** (2014).
171. Duque, G. A. & Descoteaux, A. Macrophage cytokines: Involvement in immunity and infectious diseases. *Front. Immunol.* **5,** 1–12 (2014).
172. Guschin, D. Y. *et al.* in *Methods in Molecular Biology* **649,** 247–256 (2010).
173. Brooks, S. A., Connolly, J. E. & Rigby, W. F. C. The role of mRNA turnover in the regulation of tristetraprolin expression: evidence for an extracellular signal-regulated kinase-specific, AU-rich element-dependent, autoregulatory pathway. *J. Immunol.* **172,** 7263–7271 (2004).
174. Fan, H., Villegas, C., Chan, a K. & Wright, J. a. Myc-epitope tagged proteins detected with the 9E10 antibody in immunofluorescence and immunoprecipitation assays but not in western blot analysis. *Biochem. Cell Biol.* **76,** 125–8 (1998).
175. Terpe, K. Overview of tag protein fusions: from molecular and biochemical fundamental to commercial systems. *Appl. Microbiol. Biotechnol.* **72,** 211–222 (2006).
176. Clausen B.E, C.Burkhardt, Reith, W., Renkawitz, R. & Förster I. Conditional gene targeting in macrophage and granulocytes using LysMcre mice. *Transgenic Res.* **96,** 317–330 (2001).
177. Cobb, B. S. *et al.* T cell lineage choice and differentiation in the absence of the RNase III enzyme Dicer. *J. Exp. Med. JEM* **201,** 1367–1373 (2005).
178. Sadzak, I. *et al.* Recruitment of Stat1 to chromatin is required for interferon-induced serine phosphorylation of Stat1 transactivation domain. *Proc. Natl. Acad. Sci. U. S. A.* **105,** 8944–9 (2008).
179. Ross, J. mRNA Stability in Mammalian Cells. *Microbiol. Rev.* **59,** 423–450 (1995).
180. Gurdon, J. B., Elsdale, T. R. & Fischberg, M. Sexually mature individuals of Xenopus laevis from the transplantation of single somatic nuclei. *Nature* **182,** 64–65 (1958).
181. Takahashi, K. *et al.* Induction of Pluripotent Stem Cells from Adult Human Fibroblasts by Defined Factors. *Cell* **131,** 861–872 (2007).
182. Takahashi, K. & Yamanaka, S. Induction of Pluripotent Stem Cells from Mouse Embryonic and Adult Fibroblast Cultures by Defined Factors. *Cell* **126,** 663–676 (2006).
183. Yu, J. *et al.* Induced pluripotent stem cell lines derived from human somatic cells. *Science (80-.).* **318,** 1917–1920 (2007).
184. Firas, J., Liu, X., Lim, S. M. & Polo, J. M. Transcription factor-mediated reprogramming: epigenetics and therapeutic potential. *Immunol. Cell Biol.* **93,** 284–289 (2015).
185. Takahashi, K. & Yamanaka, S. A decade of transcription factor-mediated reprogramming to pluripotency. *Nat. Rev. Mol. Cell Biol.* **17,** 183–93 (2016).
186. Davis, R. L., Weintraub, H. & Lassar, A. B. Expression of a single transfected cDNA converts fibroblasts to myoblasts. *Cell* **51,** 987–1000 (1987).
187. Kajimura, S. *et al.* Initiation of myoblast/brown fat switch through a PRDM16-C/EBP-b transcriptional complex. *Nature* **460,** 1154–1158 (2009).
188. Ieda, M. *et al.* Direct reprogramming of fibroblasts into functional cardiomyocytes by defined factors. *Cell* **142,** 375–386 (2010).
189. Vierbuchen, T. *et al.* Direct conversion of fibroblasts to functional neurons by defined factors. *Nature* **463,** 1035–41 (2010).
190. Caiazzo, M. *et al.* Direct generation of functional dopaminergic neurons from mouse and human fibroblasts. *Nature* **476,** 224–227 (2011).
191. Son, E. Y. *et al.* Conversion of mouse and human fibroblasts into functional spinal motor neurons. *Cell Stem Cell* **9,** 205–218 (2011).
192. Yu, C., Liu, K., Tang, S. & Ding, S. Chemical approaches to cell reprogramming. *Curr. Opin. Genet. Dev.* **28,** 50–6 (2014).
193. Thier, M. *et al.* Direct conversion of fibroblasts into stably expandable neural stem cells. *Cell Stem Cell* **10,** 473–479 (2012).
194. Zhu, S. *et al.* Small molecules enable OCT4-mediated direct reprogramming into expandable human neural stem cells. *Cell Res.* **24,** 126–9 (2014).
195. Li, J. *et al.* Conversion of human fibroblasts to functional endothelial cells by defined factors. *Arterioscler. Thromb. Vasc. Biol.* **33,** 1366–1375 (2013).
196. Li, W. *et al.* In vivo reprogramming of pancreatic acinar cells to three islet endocrine subtypes. 1–20 (2014). doi:10.7554/eLife.01846
197. Zhou, Q., Brown, J., Kanarek, A., Rajagopal, J. & Melton, D. A. In vivo reprogramming of adult pancreatic exocrine cells to β-cells. *Nature* **455,** 627–632 (2008).
198. Bussmann, L. H. *et al.* A Robust and Highly Efficient Immune Cell Reprogramming System. *Cell Stem Cell* **5,** 554–566 (2009).
199. Rapino, F. *et al.* C/EBPα Induces Highly Efficient Macrophage Transdifferentiation of B Lymphoma and Leukemia Cell Lines and Impairs Their Tumorigenicity. *Cell Rep.* **3,** 1153–1163 (2013).
200. Rodriguez-Ubreva, J. *et al.* C/EBPα-mediated activation of microRNAs 34a and 223 inhibits Lef1 expression to achieve efficient reprogramming into macrophages. *Mol. Cell.*

Biol. **34,** 1145–57 (2014).
201. Xie, H., Ye, M., Feng, R. & Graf, T. Stepwise reprogramming of B cells into macrophages. *Cell* **117,** 663–676 (2004).
202. Di, A. *et al.* CCAAT/enhancer binding protein α (C/EBPα)-induced transdifferentiation of pre-B cells into macrophages involves no overt retrodifferentiation. *Proc. Natl. Acad. Sci.* **109,** 11053 (2012).
203. Landschulz, W. H., Johnson, P. F. & Mcknight, S. L. The DNA Binding Domain of the Rat Liver Nuclear Protein C/EBP Is Bipartite. *Science (80-.).* **243,** 1681–1687 (1989).
204. Miller, M., Shuman, J. D., Sebastian, T., Dauter, Z. & Johnson, P. F. Structural basis for DNA recognition by the basic region leucine zipper transcription factor CCAAT/enhancer-binding protein α. *J. Biol. Chem.* **278,** 15178–15184 (2003).
205. Hughes, H. Identification of two polypeptide segments of CCAAT/ enhancer-binding protein required for transcriptional activation fo the serum albumin gene. *Genes Dev.* **4,** 1416–1426 (1990).
206. Ossipow, V., Descombes, P. & Schibler, U. CCAAT/enhancer-binding protein mRNA is translated into multiple proteins with different transcription activation potentials. *Proc. Natl. Acad. Sci. U. S. A.* **90,** 8219–23 (1993).
207. Paz-Priel, I. & Friedman, A. D. C/EBPα Dysregulation in AML and ALL. **4,** 93–102 (2011).
208. Zhang, P. *et al.* Enhancement of hematopoietic stem cell repopulating capacity and self-renewal in the absence of the transcription factor C/EBPα. *Immunity* **21,** 853–863 (2004).
209. Heath, V. *et al.* C/EBP-alpha deficiency results in hyperproliferation of hematopoietic progenitor cells and disrupts macrophage development in vitro and in vivo. *Blood* **104,** 1639–47 (2004).
210. Ma, O., Hong, S., Guo, H., Ghiaur, G. & Friedman, A. D. Granulopoiesis requires increased C/EBPα compared to monopoiesis, correlated with elevated Cebpa in immature G-CSF receptor versus M-CSF receptor expressing cells. *PLoS One* **9,** 1–14 (2014).
211. Cai DH, Wang D, Keefer J, Yeamans C, Hensley K, F. A. C/EBPα:AP-1 Leucine Zipper Heterodimers Bind Novel DNA Elements, Activate the PU.1 Promoter, and Direct Monocyte Lineage Commitment More Potently Than C/EBPα Homodimers or AP-1. *Oncogene* **27,** 2772–2779 (2008).
212. Yeamans, C. *et al.* C/EBPα binds and activates the PU.1 distal enhancer to induce monocyte lineage commitment. *Blood* **110,** 3136–3142 (2007).
213. Kummalue, T. & Friedman, A. D. Cross-talk between regulators of myeloid development: C/EBPα binds and activates the promoter of the PU . 1 gene. **74,** (2003).
214. Lin, F. T., MacDougald, O. A., Diehl, A. M. & Lane, M. D. A 30-kDa alternative translation product of the CCAAT/enhancer binding protein alpha message: transcriptional activator lacking antimitotic activity. *Proc. Natl. Acad. Sci. U. S. A.* **90,** 9606–10 (1993).
215. Pabst, T. *et al.* Dominant-negative mutations of CEBPA, encoding CCAAT/enhancer binding protein-α (C/EBPα), in acute myeloid leukemia. *Nat. Genet.* **27,** 263–270 (2001).
216. Gombart, A. F. *et al.* Mutations in the gene encoding the transcription factor CCAAT/enhancer binding protein α in myelodysplastic syndromes and acute myeloid leukemias. *Blood* **99,** 1332–1340 (2002).
217. Wang, H. *et al.* C/EBPα arrests cell proliferation through direct inhibition of Cdk2 and Cdk4. *Mol. Cell* **8,** 817–828 (2001).
218. Wang, X., Scott, E., Sawyers, C. L. & Friedman, A. D. C/EBPα bypasses granulocyte colony-stimulating factor signals to rapidly induce PU.1 gene expression, stimulate granulocytic differentiation, and limit proliferation in 32D cl3 myeloblasts. *Blood* **94,** 560–571 (1999).
219. Wang, Q.-F., Cleaves, R., Kummalue, T., Nerlov, C. & Friedman, A. D. Cell cycle inhibition mediated by the outer surface of the C/EBPα basic region is required but not sufficient for granulopoiesis. *Oncogene* **22,** 2548–2557 (2003).
220. Porse, B. T. *et al.* E2F repression by C/EBPα is required for adipogenesis and granulopoiesis in vivo. *Cell* **107,** 247–258 (2001).
221. Zaragoza, K., Bégay, V., Schuetz, A., Heinemann, U. & Leutz, A. Repression of transcriptional activity of C/EBPα by E2F-dimerization partner complexes. *Mol. Cell. Biol.* **30,** 2293–304 (2010).
222. Kotecki, M., Reddy, P. S. & Cochran, B. H. Isolation and characterization of a near-haploid human cell line. *Exp. Cell Res.* **252,** 273–80 (1999).
223. Carette, J. E., Raaben, M. & ... Ebola virus entry requires the cholesterol transporter Niemann-Pick C1. *Nature* **477,** 340–343 (2012).
224. Carette, J. E. *et al.* Haploid genetic screens in human cells identify host factors used by pathogens. *Science* **326,** 1231–5 (2009).
225. Jae, L. T. *et al.* Virus entry. Lassa virus entry requires a trigger-induced receptor switch. *Science* **344,** 1506–10 (2014).
226. Tchasovnikarova, I. A. *et al.* Epigenetic silencing by the HUSH complex mediates position-effect variegation in human cells. *Science* **348,** 1481–5 (2015).
227. Heijink, A. M. *et al.* A haploid genetic screen identifies the G 1/S regulatory machinery as a

determinant of Wee1 inhibitor sensitivity. *Proc. Natl. Acad. Sci. U. S. A.* **112,** 15160–15165 (2015).
228. Sdelci, S. *et al.* Mapping the chemical chromatin reactivation landscape identifies BRD4-TAF1 cross-talk. *Nat. Chem. Biol.* (2016). doi:10.1038/nchembio.2080
229. Levenson, V. V, Transue, E. D. E. & Roninson, I. B. Internal ribosomal entry site-containing retroviral vectors with green fluorescent protein and drug resistance markers. *Hum. Gene Ther.* **9,** 1233–1236 (1998).
230. Bhattacharya, D., Logue, E. C., Bakkour, S., DeGregori, J. & Sha, W. C. Identification of gene function by cyclical packaging rescue of retroviral cDNA libraries. *Proc. Natl. Acad. Sci. U. S. A.* **99,** 8838–43 (2002).
231. Feng, R. *et al.* PU.1 and C/EBPα/β convert fibroblasts into macrophage-like cells. *Proc. Natl. Acad. Sci. U. S. A.* **105,** 6057–6062 (2008).
232. Laiosa, C. V., Stadtfeld, M., Xie, H., de Andres-Aguayo, L. & Graf, T. Reprogramming of Committed T Cell Progenitors to Macrophages and Dendritic Cells by C/EBPα and PU.1 Transcription Factors. *Immunity* **25,** 731–744 (2006).
233. Shalginskikh, N., Poleshko, A., Skalka, A. M. & Katz, R. a. Retroviral DNA methylation and epigenetic repression are mediated by the antiviral host protein Daxx. *J. Virol.* **87,** 2137–50 (2013).
234. Halmos, B. *et al.* Down-Regulation and Antiproliferative Role of C/EBPα in Lung Cancer. 528–534 (2002).
235. Fieber, C. *et al.* Innate immune response to streptococcus pyogenes depends on the combined activation of TLR13 and TLR2. *PLoS One* **10,** 1–20 (2015).
236. Gaidt, M. M. *et al.* Human Monocytes Engage an Alternative Inflammasome Pathway. *Immunity* **44,** 833–846 (2016).
237. Landmann, R. *et al.* Human Monocyte CD14 Is Upregulated by Lipopolysaccharide. **64,** 1762–1769 (1996).
238. Nerlov, C. & Graf, T. PU.1 induces myoeloid lineage commitment in multipotent hematopoietic progenitors. *Genes Dev.* **12,** 2403–2412 (1998).
239. McClellan, J. S., Dove, C., Gentles, A. J., Ryan, C. E. & Majeti, R. Reprogramming of primary human Philadelphia chromosome-positive B cell acute lymphoblastic leukemia cells into nonleukemic macrophages. *Proc. Natl. Acad. Sci. U. S. A.* **112,** 4074–9 (2015).
240. Van Oevelen, C. *et al.* C/EBPα Activates Pre-existing and de Novo Macrophage Enhancers during Induced Pre-B Cell Transdifferentiation and Myelopoiesis. *Stem Cell Reports* **5,** 232–247 (2015).
241. Zamani, F., Shahneh, F. Z., Aghebati-Maleki, L. & Baradaran, B. Induction of CD14 expression and differentiation to monocytes or mature macrophages in promyelocytic cell lines: New approach. *Adv. Pharm. Bull.* **3,** 329–332 (2013).
242. DeKoter, R. P. & Singh, H. Regulation of B lymphocyte and macrophage development by graded expression of PU.1. *Science* **288,** 1439–1441 (2000).
243. Scott, E. W., Simon, M. C., Anastasi, J. & Singh, H. Requirement of Transcription Factor PU.1 in the Development of Multiple Hematopietic Lineages. *Science (80-.).* **265,** 1573–1577 (1994).
244. Rieger, M. a, Hoppe, P. S., Smejkal, B. M., Eitelhuber, A. C. & Schroeder, T. Lineage Choice. *Science (80-.).* **325,** 217–218 (2009).
245. Yu, W. *et al.* Macrophage proliferation is regulated through CSF-1 receptor tyrosines 544, 559, and 807. *J. Biol. Chem.* **287,** 13694–13704 (2012).
246. Mossadegh-Eeller, N., Sarrazin, S. & Kandalla, P. K. M-CSF instructs myeloid lineage fate in single haematopoietic stem cells. **497,** 239–243 (2013).
247. Munugalavadla, V., Borneo, J., Ingram, D. A. & Kapur, R. p85α subunit of class IA PI-3 kinase is crucial for macrophage growth and migration. *Blood* **106,** 103–109 (2005).
248. Di Stefano, B. *et al.* C/EBPα poises B cells for rapid reprogramming into induced pluripotent stem cells. *Nature* **506,** 235–9 (2014).
249. Barneda-Zahonero, B. *et al.* HDAC7 Is a Repressor of Myeloid Genes Whose Downregulation Is Required for Transdifferentiation of Pre-B Cells into Macrophages. *PLoS Genet.* **9,** (2013).
250. Rodríguez-Ubreva, J. *et al.* Pre-B cell to macrophage transdifferentiation without significant promoter DNA methylation changes. *Nucleic Acids Res.* **40,** 1954–1968 (2012).
251. Kallin, E. M. *et al.* Tet2 facilitates the derepression of myeloid target genes during CEBPα-Induced transdifferentiation of Pre-B cells. *Mol. Cell* **48,** 266–276 (2012).
252. Sandler, V. M. *et al.* Reprogramming human endothelial cells to haematopoietic cells requires vascular induction. *Nature* **511,** 312–8 (2014).
253. Studies, B., Jolla, L., Division, T. & Energ, I. Conversion of Human Fibroblasts into Monocyte-Like Progenitor Cells - Pulecio - STEM CELLS - Wiley Online Library. 2923–2938 (2014).
254. Mueller, B. U. *et al.* Heterozygous PU.1 mutations are associated with acute myeloid leukemia. *Blood* **100,** 998–1007 (2002).
255. Shih, L.-Y. *et al.* Heterogeneous Patterns of CEBPα Mutation Status in the Progression of Myelodysplastic Syndrome and Chronic

Myelomonocytic Leukemia to Acute Myelogenous Leukemia. *Clin. Cancer Res.* **11,** 1821–1826 (2005).
256. Bonadies, N., Pabst, T., Mueller, B. U. & Pru, D. R. U. Brief report Heterozygous deletion of the PU . 1 locus in human AML. **115,** 331–334 (2010).
257. Sagi, I. *et al.* Derivation and differentiation of haploid human embryonic stem cells. *Nature* **532,** 107–11 (2016).
258. Friedman, A. D. C/EBPα in normal and malignant myelopoiesis. *Int. J. Hematol.* **101,** 330–341 (2015).

I apologize for any relevant publication I missed to cite and if there is any breach in copyright, I kindly ask you to contact me.

13. Abstract

TTP is an mRNA-destabilizing protein that regulates in concert with other factors decay of transcripts of inflammatory mediators upon binding to the target 3´UTR. However, the regulation of TTP´s induced mRNA destabilizing activity is complex and involves many different facets including expression, cellular localization, posttranslational modifications and interaction with other trans-acting factors that bind cis-regulatory elements.

Interestingly, within the inflammatory response TTP and the mRNA-stabilizing protein HuR can bind to an overlapping repertoire of mRNA targets. For example, both proteins can bind mRNAs of important pro-inflammatory cytokines (*Tnf*, *Cxcl1*, *Cxcl2* etc.). We aimed to obtain a deeper insight into the cooperative action of TTP with other trans-acting factors, which help shaping the inflammatory response. Immunoprecipitation revealed that TTP and HuR do not interact directly, but utilize RNA as a platform. An interaction of TTP with Ago2 could not be detected. In the course of this thesis, a novel protocol for sequential RNA-IP experiments was established. This approach revealed that some mRNAs (e.g. *Tnf*, *Cxcl2*) were simultaneously bound by TTP and HuR. The functional consequences of concomitant binding of TTP and HuR to mRNA was examined using CRISPR/Cas9-genome edited RAW 264.7 cells bearing inactivation of TTP, HuR or both TTP an HuR genes. The data showed that HuR in general has a minor effect on mRNA stability of inflammatory mediators and only *Tnf* mRNA was unambiguously identified as target regulated by direct competition of TTP and HuR. To facilitate a comprehensive analysis of factors functionally interacting with TTP to regulate the immune response, RAW 264.7 macrophages expressing tagged version of TTP from the endogenous locus were attained. Since the expression of the tagged TTP is subject to normal transcriptional and posttranscriptional regulation in these cells, the system will allow various interaction and posttranslational analyses without risks associated with artifact-prone overexpression approaches. Further, we attempted to design a nuclear localized sRNA with an intronic TTP binding motif to study if TTP binding to introns represents a buffering system to lessen the availability of the bioactive, cytoplasmic form. However, as the sRNA was mainly localized within the cytoplasm in an immune-relevant context this system requires additional improvement before applicable for examination of the nuclear function of TTP.

In a second project we aimed to transdifferentiate human haploid cells (HAP1 and KBM-7) into macrophages as their haploid nature makes them the ideal tool for studying

immunological processes using forward genetics. Using retroviral transduction haploid cells were established allowing inducible ectopic expression of C/EBPα, a transcription factor pivotal for monopoiesis. Low, yet detectable transcription of macrophage markers, i.e. *Cd14* and *Csf1r*, but also of pro-inflammatory cytokines, i.e. *Cxcl8* and *Il1b* indicate that prolonged expression of the transcriptional regulator may promote partial transdifferentiation. Nonetheless, full reprogramming into haploid macrophages likely requires the combinatorial action of C/EBPα together with other factors, such as chromatin modifiers.

14. Zusammenfassung

TTP ist ein mRNS-destabilisierendes Protein, welches in Zusammenarbeit mit anderen Faktoren den Abbau von Entzündungsmediatoren, ausgehend von der Binding zur Ziel-3´UTR, hervorruft. Die Regulierung von TTP´s mRNS-destabilisierender Aktivität ist komplex und involviert verschiedenste Aspekte wie Expression, zelluläre Lokalisation, posttranslationale Modifizierungen und Interaktion mit anderen trans-agierenden Faktoren, welche cis-regulatorische Elemente binden.

Interessanterweise können TTP und das mRNS-stabilisierende Protein HuR ein überlappendes Repertoire an mRNS-Zielen während einer Entzündungsreaktion binden. Beispielsweise binden beide Proteine die mRNS von wichtigen inflammatorischen Zytokinen (*Tnf*, *Cxcl1*, *Cxcl2* etc.). Daher wollten wir einen tieferen Einblick in die kooperative Wechselwirkung von TTP mit anderen trans-agierenden Faktoren und deren Einfluss auf die Entzündungsreaktion gewinnen. Mittels Immunopräzipitation konnten wir zeigen, dass TTP und HuR nicht direkt, aber über RNS interagieren. Eine Interaktion von TTP und Ago2 konnte nicht festgestellt werden. Im Zuge dieser Arbeit wurde ein neues Protokoll für sequentielle RNS-IP etabliert. Dieser Ansatz zeigte die simultane Bindung von TTP und HuR an einige mRNS-Sequenzen (z.B. *Tnf*, *Cxcl2*). Die funktionalen Konsequenzen des gleichzeitigen Bindens von TTP und HuR an mRNS wurde mittels CRISPR/Cas-9 Genom-editierten RAW 264.7 Zellen, welche Inaktivierung von TTP, HuR oder beider Gene für TTP und HuR aufweisen, untersucht. Die Daten haben gezeigt, dass HuR nur einen geringen Einfluss auf die mRNS-Stabilität von inflammatorischen Mediatoren hat und einzig *Tnf* mRNS konnte als eindeutiges Ziel, reguliert durch direkte Konkurrenz zwischen TTP und HuR, identifiziert werden. Um eine umfassende Analyse von Faktoren, welche funktionell mit TTP interagieren um die Immunantwort zu regulieren, zu vereinfachen wurden RAW 264.7 Makrophagen, welche markiertes TTP vom endogenen Lokus exprimieren, gewonnen. Da die Expression von markiertem TTP in diesen Zellen der normalen transkriptionellen und posttranskriptionellen Regulation unterliegt, erlaubt dieses System verschiedene Interaktions- und posttranslationale Analysen, ohne die Risiken Artefakt-anfälliger Überexpression berücksichtigen zu müssen. Weiters haben wir versucht eine nukleare sRNS mit intronischem TTP-Bindungsmotif zu konstruieren, um zu untersuchen ob das Binden von TTP an Introns ein Puffer-System zur Einschränkung von verfügbarem, im Zytoplasma befindlich bioaktivem TTP darstellt. Da die sRNS in einem immun-relevanten Kontext

allerdings vorwiegend im Zytoplasma lokalisiert war, benötigt dieses System weitere Anpassung bevor es zur Untersuchung der funktionalen Rolle von nuklearem TTP herangezogen werden kann.

In einem Zweitprojekt haben wir versucht die humane haploide Zellen (HAP1 und KBM-7) in Makrophagen zu transdifferenzieren, da ihre haploide Natur sie zum idealen Werkzeug für das Studieren von immunologischen Prozessen mittels Vorwärtsgenetik macht. Durch Verwendung retroviraler Transduktion wurden haploide Zellen, welche eine induzierbare ektopische Expression von C/EBPα aufweisen, einen wichtigen Transkriptionsfaktor in der Monopoese, etabliert. Niedrige, dennoch nachweisbare Transkription von Makrophagenmarkern, z.B. *Cd14* und *Csf1r*, aber auch von pro-inflammatorischen Zytokinen, z.B. *Cxcl8* und *Il1b* impliziert, dass eine lang andauernde Expression des Transkriptions-Regulators partielle Transdifferenzierung ermöglicht. Allerdings erfordert eine vollständige Reprogrammierung zu haploiden Makrophagen wahrscheinlich das Zusammenwirken von C/EBPα und anderen Faktoren, wie Chromatin-modifizierende Proteine.